TECHNISCHE UNIVERSITÄT MÜNCHEN

Lehrstuhl und Versuchsanstalt für Wasserbau und Wasserwirtschaft

Numerical simulation of fish behavior and fish movement through passages

Shokry Mohamed Ahmed Abdelaziz

Vollständiger Abdruck der von der Ingenieurfakultät Bau Geo Umwelt (BGU) der Technischen Universität München zur Erlangung des akademischen Grades eines Doktor-Ingenieurs genehmigten Dissertation.

Vorsitzender: Univ.- Prof. Dr. rer. nat. B. Helmreich

Prüfer der Dissertation:

1. Univ.-Prof. Dr.-Ing. P. Rutschmann
2. Univ.-Prof. Dr.-Ing. Dr. h.c. F. Nestmann,
   Karlsruhe Institut für Technologie

Die Dissertation wurde am 21.03.2013 bei der Technischen Universität München eingereicht und durch die Ingenieurfakultät Bau Geo Umwelt (BGU) am 02.07.2013 angenommen.

Abstract

One approach to study the fish movement through fish passage is to track its behavior against the change of hydraulic conditions. This modeling approach may help to assess the efficiencies of fishways and will provide information about the proportions of the migrating populations that actually move upstream. Additionally, it can help us to better understand the mentality of the fish for traversing a velocity barrier. One of the most important issues for modeling development is observed data related to the fish movement by changing hydraulic conditions. Normally some video (image) processing techniques are applied to track the fish movement in a controlled test environment. In the present work, I use the technique of the motion detection through background estimation and subtraction. Furthermore, I develop a color-histogram based segmentation approach to track the identified fish over time and hence achieve robust fish tracking. Finally I apply signal processing techniques for post processing of the produced movement curves to filter out outliers. The algorithms are applied on three test datasets, one of them captured in the Laboratory of Hydraulics in Obernach of the Technical university of Munich (TUM). Results are very promising and a number of improvements are furthermore suggested. One of the main works of this study is to develop a numerical model for the fish movements' path. The model is based on the framework combining a low energy concept and random movements. The effects of turbulence and fish memory are also taken into account. The model is validated using field measurements data collected at a culvert in the Yellowstone River in Mulherin Creek (USA). The data include hydrologic and hydraulic conditions as well as the observed fish movement path. The simulated fish paths match well the measured one. The normalized error percentages (NE) are always less than 2.5 % in cases where the effect of turbulence is not appearing and 10-20 % in cases where the effect of turbulence is appearing. Based on the measured and the simulated path, the fish energy expenditures inside the culvert are also calculated. The average error in the simulated energy expenditure was less than 2.5 %. Based on this model a new method for culvert design for passage is suggested and used to calculate the actual fish anaerobic energy. For the case, when the flow direction strongly changes point by point (e.g. in a pool-and-weir fishway), the fish recognizes the direction of the fishway based on high water flow. At the same time, the fish tries to minimize the energy expenditure by travelling against the lower velocities. On the basis of these concepts, the numerical model is modified and applied to two different experiments for pool-and-weir fishway. Using the commercial computer code FLOW-3D for flow calculation, the developed modeling approach provided good results of flow pattern and fish movement. A good agreement between the simulated results and experimental data has been obtained. Further, additional features should be added to the present modeling approach to include the resting zone and the energy consumption in cases

when the fish use combination of both aerobic and anaerobic energy.

Keywords: Fish passage, Individual based model, culvert, pool and weir fishway, tracking Algorithm, Video image processing, Minimum Energy Concept, Turbulent model, Hydraulic model, FLOW-3D.

Zusammenfassung

Ziel dieser Arbeit war die Entwicklung eines numerischen Modells zur Simulation des Aufstiegsverhaltens in Fischpässen. Eine Möglichkeit Untersuchungen zum Schwimmverhalten von Fischen in Fischpässen durchzuführen ist, ihr Schwimmverhalten bei unterschiedlichen hydraulischen Bedingungen aufzuzeichnen und auszuwerten. Aus den Aufzeichnungen lassen sich Aussagen über die Passierbarkeit von Fischpässen gewinnen. Zudem ist es möglich auf die tatsächliche Wanderungsrate von Fischen zu schließen. Darüber hinaus ermöglicht diese Untersuchungsmethode das Verhalten von Fischen bei der Durchquerung einer Geschwindigkeitsbarriere besser nachvollziehen zu können. Für die Auswertung kam eine Video-Bild-Verarbeitungsmethode zum Einsatz, die es ermöglicht die Fischbewegung über die Zeit herauszufiltern und diese in Relation zu den Veränderungen der Geschwindigkeiten, Fließtiefen und anderen hydraulischen Bedingungen zu setzen. Die Bewegungserkennung erfolgte auf Basis der Hintergrundschätzung und –subtraktion. Über dies wird ein Farb-Histogramm basierter Segmentierungsansatz vorgestellt, um dem Schwimmpfad des Fisches über die Zeit folgen zu können und um eine zuverlässige Bewegungserkennung zu gewährleisten. Im Nachgang werden mittels entsprechender Signalaufbereitungstechniken die Bewegungskurven gefiltert und so Ausreißer aussortiert. Drei Testdatensätze wurden mit Hilfe des entwickelten Algorithmus ausgewertet, wovon einer aus der Versuchsanstalt für Wasserbau der Technischen Universität München in Obernach entstammt. Die Ergebnisse sind sehr viel versprechend. Darüber hinaus wurden mögliche Verbesserungs- und Entwicklungsansätze vorgeschlagen.

Im Weiteren wird ein numerisches Modell für den Fischbewegungspfad vorgestellt. Dieses Modell vereint das Niedrigenergiekonzept und Zufallsbewegungen. Des Weiteren werden in diesem Modell Turbulenzeinflüsse und ein Fischgedächtnis berücksichtigt. Die Validierung erfolgte an Hand von Feldmessdaten, die an einem Durchlass im Yellowstone Fluss in Mulherin Creek (USA) aufgenommen wurden. Die Untersuchungen umfassten die hydrologischen und hydraulischen Parameter sowie die gemessenen Fischbewegungspfade. Der Vergleich von Numerik und Feldmessung zeigt, dass die Fischpfade gut übereinstimmen. Die normierte prozentuale Fehlerabweichung lag für die von Turbulenz unbeeinflussten Fälle unter 2,5 % und für die von Turbulenz beeinflussten Fälle zwischen 10 und 20 %. Zudem ist es möglich den Energieaufwand des Fisches innerhalb des Durchlasses an Hand der gemessenen und simulierten Bewegungspfade zu bestimmen. Der mittlere Fehler des simulierten Energieaufwands lag unter 2,5 %. Basierend auf diesem numerischen Modell werden eine neue verbesserte Methode zur Durchlassdimensionierung und Berechnung der tatsächlichen anaeroben Fischenergie vorgestellt.

Das für Durchlässe entwickelte Modell ist für den Fall einer ständigen die Fließrichtungsveränderung (z.B. in einem Beckenfischpass) nicht anwendbar. In diesem Fall orientiert sich der Fisch an der Hauptstromrichtung, wobei er versucht seinen Bewegungsaufwand gering zu halten, indem er gegen möglichst geringe Geschwindigkeiten anschwimmt. Das Bewegungsmodell wurde an Hand zweier experimenteller Beckenfischpassuntersuchungen validiert. Die Ergebnisse zeigen eine gute Übereinstimmung mit der im Experiment gemessenen und numerisch modellierten Strömungsstrukturen und Fischbewegungen. Zur Verbesserung des Modells könnten ein Ruhezonenmodell und ein erweitertes Energiemodell, welches sowohl aerobe wie auch anaerobe Energiezustände berücksichtigt, mit eingearbeitet werden.

Schlüsselbegriffe: Fischpass, individuenbasiert, Fischmodell, Durchlass, Beckenfischpass, Bewegungserkennung, Videoverarbeitung, Niedrigenergiekonzept, Turbulenzmodell, Hydraulisches Modell, Flow3D.

Acknowledgements

With immense pleasure, I would like to express my heartfelt gratitude to my advisor Prof. Dr. Peter Rutschmann for his guidance during the course of this work in institute of Hydraulic and Water Resources Engineering, Technical University of Munich. I render my appreciation to him for giving me a simulating research environment, valuable comments (that I will never forget). Prof. Rutschmann, thanks a lot for your trust and enthusiasm. I would like also to express my deepest gratitude to Dr. Minh Duc Bui for the informative and helpful discussion as well as showing me the importance of using Numerical Simulations in Hydraulic Engineering world through provision of support and valuable advices. He learned me how I can write a good scientific paper, thanks a lot Dr Bui. I graciously thank all my colleges in institute of Hydraulic and Water Resources Engineering who were always ready to help me and give me the feeling that I am at home and between my family.

I would like to express my deepest gratitude to Prof. Joel Cahoon and Dr. Matthew Blank in Montana State University and Dr. Theodore Castro-Santos in USGS Anadromous Fish Research Center in USA for the kind suggestions and help. I would like also to thank Dr. Keiko Muraoka, Kazufumi Hayashida from Watershed Environmental Engineering Research Team, Civil Engineering Research Institute of Cold Region in Japan and Dr. Namihira Atsushi from Institute for Rural Engineering in Japan.

Last and not least I wish to dedicate my entire thesis to my family, my wife, lovely children, mother, brothers and the soul of my father for their encouragement and support.

Table of Contents

Abstract II
Zusammenfassung IV
Acknowledgements VI
Table of Contents VII
List of Figures IX
List of Tables XIII
1. Introduction 1
1.1 Background 1
1.2 Objectives 2
1.3 Outline of thesis 3
2. Hydrodynamics and fish movement behavior 4
2.1 Fish migration 4
2.2 Upstream fish passage 6
2.3 Types of fish passage 6
2.3.1 Culvert fishway 6
2.3.2 Pool-and-weir fishway 7
2.3.3 Vertical slot fishway 8
2.4 Hydraulic factors affecting fish passage 9
2.5 Fish biology 10
2.5.1 Fish muscles 11
2.5.2 Types of fish movement 11
2.5.3 Gills and oxygen respiration 13
2.5.4 Fish vision 14
2.5.5 The lateral line system 14
2.6 Techniques used for fish passage evaluation 15
2.7 Prior research and potential 16
2.8 Summary 19
3. Image processing algorithms for fish path tracking 20
3.1 Datasets 20
3.2 Methodology 23
3.2.1 Motion detection using the motion vector technique 24
3.2.2 Motion detection through frame difference calculation 26
3.2.3 Background subtracted motion detection 29
3.2.4 Using color filtering for robust tracking and multiple fish tracking 30
3.3 Method validation 32
3.4 Suggestions for improvements 39
3.5 Summary 41
4. Numerical model for decoding movement patterns of fish 42
4.1 Numerical modeling 42
4.1.1 Hydraulic model 42
4.1.2 Model for fish movement though a roughened channel with almost uniform main flow directions 45
4.1.3 Model for fish movement in the flow conditions with variable directions 58
4.1.4 Model conversion to 3D 65

4.1.5 Model uncertainty 65
4.2 Summary 65
5. Case study 66
5.1 Case 1: Numerical simulation of energy expenditure of Yellowstone cutthroat trout migrating upstream through a culvert 67
5.1.1 Problem description 67
5.1.2 Data summary 68
5.1.3 Model setup 69
5.1.4 Model calibration 69
5.1.5 Leaping energy 78
5.1.6 Calculation of the actual fish energy 81
5.1.7 Summary 84
5.2 Case 2: Numerical simulation of flow and upstream fish movement through a single pool fishway 86
5.2.1 Experimental data 86
5.2.2 Model calibration 88
5.2.3 Model application 91
5.2.4 Summary 100
5.3 Case 3: Numerical simulation of flow and upstream fish movement through a multiple pool fishway 101
5.3.1 Experimental data 101
5.3.2 Model calibration 102
5.3.3 Model application 105
5.3.4 Summary 111
6. Conclusions and suggestions for further research 113
6.1 Main conclusions 113
6.2 Suggestions for further research 115
7. References 116
Appendix 1: Data collected in a Culvert in Mulherin Creek 125

List of Figures

Figure 2.1: Fish migration cycle between spawning, feeding and refuge (adopted from Lucas and Baras, 2001). 5
Figure 2.2: Culvert fishway (Forest Service Stream-Simulation Working Group, 2008). 7
Figure 2.3: pool-and-weir fishway (California department of transportation, 2007). ... 8
Figure 2.4: Vertical slot fishway (California department of transportation, 2007). 9
Figure 2.5: Distance maximizing strategy for fish traversing velocity barriers in body lengths for still water (A) and in the presence of flow (B) where contours indicate flow velocity (after Castro-Santos, 2005). 12
Figure 2.6: The gill structure of fish (after Bagur, 2009). 14
Figure 2.7: Fish Vision (after Bagur, 2009.)..... 14
Figure 2.8: Organization of CNs and SNs on the goldfish (after Goulet et al., 2008).. 15
Figure 3.1: Positions of the two cameras. 21
Figure 3.2: Side and top view taken of dataset 1. 22
Figure 3.3: An Image from the video of dataset 2. 23
Figure 3.4: An Image from the video of dataset 3. 23
Figure 3.5: Using motion vectors to estimate object movement. 25
Figure 3.6: Fish location at time $t=t_n$ and $t=t_n+1$. Only colored areas will have values different than 0 in the difference image since the background is static. 27
Figure 3.7: Processing steps for moving object detection. 28
Figure 3.8: Median filtering for background estimation. 29
Figure 3.9: Frame #10 from test video (above) and estimated background using pixel-wise median filtering (below). 30
Figure 3.10: Detected moving regions (with centroids and bounding boxes). 30
Figure 3.11: fish color histograms. 31
Figure 3.12: Tracking the fish in dataset 1. 32
Figure 3.13: The estimated fish movement for dataset 1..... 33
Figure 3.14: The estimated vertical fish velocity for dataset 1..... 34
Figure 3.15: Relative error Histogram. 35
Figure 3.16: Snapshots from tracking the blue fish using the color histogram aided fish tracking..... 35
Figure 3.17: The resultant vertical fish movement and velocity for dataset 2. 36
Figure 3.18: Subtraction of the downstream part from the video (dataset 3). 37
Figure 3.19: Relation between the fish position in the pool and its velocity for dataset 3. 38
Figure 3.20: The relation between time and fish velocity for dataset 3. 39

Figure 3.21: SURF features matched between the two frames shown in figure 3.16 (frames are overlaid on one another). 40
Figure 4.1: The structure of the proposed low energy and turbulent model. 46
Figure 4.2: Diagram of decision process following Blank (2008) for estimating Minimum energy expenditure. 47
Figure 4.3: Minimum energy concept with Random movement. 48
Figure 4.4: Effect of turbulence on fish movement. 50
Figure 4.5: The ability of fish to enter the culvert from the downstream (swim or jump). 54
Figure 4.6: A diagram for culvert barrier method. 58
Figure 4.7: Flow pattern in a culvert and in a pool-and-weir fishway. 59
Figure 4.8: The structure of the proposed two dimensions fish model. 60
Figure 4.9: Near opening check. 61
Figure 4.10: Maximum velocity direction. 62
Figure 4.11: Flow direction domain. 62
Figure 4.12: Coordinate conversion From the current coordinate to the local coordinate suitable to the low energy model described in 4.1.2. 63
Figure 5.1: Fish upstream passage through the culvert (photos taken from Blank et al., 2006 and Blank, 2008). 68
Figure 5.2: Overview of study culvert dimension. 69
Figure 5.3: Simulated paths without turbulence effect superimposed on 1st July 2004 (Q = 1.47 m^3/s; observed data from Blank, 2008). 70
Figure 5.4: Simulated paths with turbulence effect superimposed on 1st July 2004 (Q = 1.47 m^3/s; observed data from Blank, 2008)..... 71
Figure 5.5: Comparison between Smoothed and 100 fish average path for fish paths superimposed on 24th June 2004 (Q = 1.55 m^3/s; observed data from Blank, 2008). .. 72
Figure 5.6: Fish paths superimposed on 24th June 2004 (Q = 1.55 m^3/s; observed data from Blank, 2008). 73
Figure 5.7: Fish paths superimposed on 13th July 2004 (Q = 1.44 m^3/s; observed data from Blank, 2008). 73
Figure 5.8: Cumulative distance travelled by the fish. 74
Figure 5.9: Time taken by the fish to travel the culvert. 76
Figure 5.10: Cumulative energy consumed by fish to pass the culvert at different time. 77
Figure 5.11: Summary of fish leaping attempts from June 16th to July 8th, 2004 (after Blank, 2008). 80
Figure 5.12: Outlet region of culvert 1, looking upstream (after Blank, 2008)..... 81
Figure 5.13: Leaping observation at culvert in the 1st of July 2004 (after Blank, 2008). 82

Figure 5.14: Sample of the fish movement results in the model for region 1 and 3. .. 83
Figure 5.15: Sample of the fish movement results in the model. 84
Figure 5.16: Flow stream inside pool-and-weir fishway (Clay, 1961). 86
Figure 5.17: A plan view and longitudinal cross-section view of the pool and weir (Hayashida, et al., 2001). 87
Figure 5.18: A photo for case 2 (L=100 cm, H= 30/20 cm) taken from Hayashida's experimental work..... 87
Figure 5.19: Model setup. 88
Figure 5.20: Mean flow pattern inside the pool tank. 90
Figure 5.21: Maximum velocity paths inside the pool tank 91
Figure 5.22: Maximum velocity near the bed. 91
Figure 5.23: Climbing frequency of each case (after Hayashida et al., 2001). 92
Figure 5.24: simulated flow pattern and fish movement inside the pool tank for case 3 Level 1..... 93
Figure 5.25: Simulated flow pattern and fish movement inside the pool tank for case 2 –Level 2..... 95
Figure 5.27: Simulated 100 fish movements inside the pool tank for case 8 –Level 2. 96
Figure 5.28: Simulated flow pattern and fish movement inside the pool tank for case 4 –Level 3..... 97
Figure 5.29: Simulated flow pattern and fish movement inside the pool tank for case 5 –Level 3..... 98
Figure 5.30: Simulated flow pattern and fish movement inside the pool tank for case 7 –Level 3..... 99
Figure 5.31: typical shape of the hydraulic model. 101
Figure 5.32: Model set up. 102
Figure 5.33: Mean flow pattern inside the pool tank. 104
Figure 5.34: Comparison between measured and simulated maximum velocity near the bed and the walls. 105
Figure 5.35: simulated and observed fish movement inside the pool tank for Type-A Experiment 1 (ΔH = 0.05 m, q=0.021 m^3/s/m.)..... 106
Figure 5.36: Simulated flow pattern and fish movement inside the pool tank for Type-A Experiment 2(ΔH = 0.10 m, q= 0.064 m^3/s/m). 107
Figure 5.37: Simulated flow pattern and fish movement inside the pool tank for Type-A Experiment 4 (ΔH = 0.20 m, q= 0.20 m3/s/m'). 108
Figure 5.38: Simulated flow pattern and fish movement inside the pool tank for Type-B Experiment 1 (ΔH = 0.05 m, q= 0.021 m^3/s/m'). 109
Figure 5.39: Simulated flow pattern and fish movement inside the pool tank for Type-B Experiment 4 (ΔH = 0.20 m, q= 0.2 m^3/s/m). 110

Figure 5.40: Simulated flow pattern and fish movement inside the pool tank for Type-C Experiment 1 (ΔH = 0.05 m, q= 0.021 m^3/s/m.) 111
Figure A1: Location of the culvert (after Blank et al., 2006). 125
Figure A2: Fences that direct fish to the opening of trap #1 (after Blank, 2008)..... 126
Figure A3: Typical measurement of the upstream and Downstream Velocity (after Blank, 2008). 127
Figure A4: Typical inlet and outlet velocity sampling (after Blank, 2008). 127
Figure A5: Location of velocity observations collected on a plane 0.06 m above the culvert bed (after Blank, 2008). 128
Figure A6: Velocity contour line inside the culvert on 1st July 2004 (observed data from Blank, 2008). 128

List of Tables

Table 2.1: Problems of barriers to fish passage and possible effects (Federal Highway, 2007) 10
Table 4.1: Model conversion roles From the current coordinate to the local coordinate suitable to the low energy model described in 4.1.2 64
Table 5.1: Model parameters and calibrated values 71
Table 5.2: Comparison between the measured and average of 100 fish simulated results 78
Table 5.3: Leaping attempts in 1st of July 2004 82
Table 5.4: Leaping attempts in 24th of June 2004 84
Table 5.5: The specifications of the hydraulic model (after Atsushi, 2009). 102
Table 5.6: Discharge conditions (after Atsushi, 2009) 102

1. Introduction

1.1 Background

Habitat fragmentation by road crossing and dam construction has serious effects on river ecosystems. One of these most serious effects is the fish barrierity which can disturb the fish migration through the system and isolate the subpopulation (Morita and Yamamoto, 2002). This reduces the breeding opportunities and interrupts the fish life stages. This type of fragmentation results in a loss of species richness (Castro-Santos and Haro, 2008).

Although the proper design of culvert and other passage can enhance the continuity of the river habitat, most of the current in place culverts were designed to move the water across the roads with no attention or little consideration of fish passage and other ecosystem processes (Jackson, 2006). Makrakis et al. (2012) evaluated 40 culverts in south Brazil and found that most of the studied culverts were considered as potential barrier to fish passage including 45 % classified as impassable, 45 % as high risk and the remaining 10 % as medium risk. Langill and Zamora (2002) found almost the same results in their study of 50 culverts in Nova Scotia, Canada. Culvert can be classified as impassable if one of the following five common conditions happens: excess drop at the culvert outlet, high velocity within the culvert barrel, inadequate depth within the culvert barrel, turbulence within the culvert, and debris and sediment accumulation at the culvert (Washington Department of Fish and Wildlife, 2003).

Although several methods are available in the literature for design of culvert for fish passage, most of these methods are not trivial and two methods can give different values for fish passage (Blank, 2008). Several researches showed the contrast between the methods used to assess barriers to fish passage (Coffman, 2005; Rajput, 2003). Solcz (2007) studied the fish passage in two culverts in Mulherin Creek from 2005 through 2006 using a passive integrated transponder (PIT) tag and found that while the results of the first culvert matched with FishXing Model results, FishXing identified the second culvert as a barrier to fish passage at all flow in contrast to the field observations.

In general, there are two approaches to model the fish passage through a fishway. The first is the traditional approach which depends on fish population characteristics in the fishway site as well as downstream and upstream of it (Burford, 2005). This approach sets a number of equations which can be used for a culvert design. On the other hand, the second approach is the individual based models (IBM) which describe individual fish as a unique entity. In this model, individuals are characterized by a set of variables such as age, sex, weight, etc. The reasons to

represent individuals in ecological models are (Grimm, 2008):

- The behaviors of Individuals usually are different even if they are of the same age.
- While most of the current traditional population models assume global interactions between individuals, the real interactions are local and depend on the local density around the fish.
- Individuals adapt their behavior to the current state of themselves and their biotic and abiotic environment.

The use of individual-based models (IBMs) in ecology started from 1970s and increased greatly during the last decade. IBMs depends on more realistic assumptions than the traditional population models. It can be a bottom up approach starting from individual to reach to population model (Grimm, 1999). In his study of upstream passage through culvert, Pearson et al. (2006) noticed that fish acts as individual rather than school during passage. Hence, it is important for a good passage model to track the individual fish behavior against the change in hydraulic conditions. This approach helps to understand the rules which govern the fish upstream movements inside the culvert and other fishway. Additionally, a random component could be added to mimic the variation between individuals.

In this thesis, an IBM will be developed and applied to fish passage through culvert and other fish passages. The model extracts some rules based on tracking of individual fish during passage. Finally, the model uses some statistical data to get the fish passage percentage.

1.2 Objectives

The main mission of this study is to achieve deeper understanding of fish requirements in culvert and fishway passage, to explore the relation between fish upstream movement and hydraulic condition and to develop a numerical model for fish passage.

The specific objectives of this study are to:

1. Develop an algorithm to extract the fish movement and velocity from a video.
2. Decode a model for flows with almost uniform main directions in culverts as well as in the same passages and develop a numerical model for fish movement through these structures. The fish swims in one go with its burst speed and without rest.
3. Decode a model for flows with variable directions in pool-type channels where

high speeds occur only through the openings of the boulder bars and validate the numerical model for fish movement in these flow conditions

The present study analyzes fish swimming behavior in these artificial environments and explores its implications in the development of new fishway designs. Although further research is needed, the results obtained can contribute to develop robust guidelines for future fishway designs. These results are expected to contribute not only in constructing new one but also evaluating the performance of existing one and rehabilitating it.

1.2.1 Outline of thesis

The thesis contains six chapters covering the listed objective.

Chapter one: includes an introduction and plan of the research work, the objectives and the scope, and the content of the present study are also included.

Chapter two: deals with the literature review of hydrodynamics and fish movement behavior. This section also provides background information on fish passage.

Chapter three: introduces the principal of image processing and develop an algorithm for fish path tracking.

Chapter four: describes the hydrodynamic and fish models used for decoding movement patterns of fish inside the fishway.

Chapter five: presents the application of the model to three different case studies. One of them represents the fish movement through a culvert while the other two cases represent the fish movement through a pool-and-weir fishway.

Chapter six: summarizes conclusions and recommendations for the future studies.

2. Hydrodynamics and fish movement behavior

2.1 Fish migration

Fish populations depend mainly on the characteristics of the river habitat which support its biological functions. This habitat differs according to the main phases of the fish life cycle. The fish has to move from one environment to another in order to survive (Larinier, 2001). Fish can be classified according to migration type to Potamodromous (Northcote, 1997) and Diadromous (Therrien and Bourgeois, 2000). In the first type, fish migrates within fresh water only while in the second one fish migrates in large scale between the ocean and freshwater. Gresswell (1988) categorized the migration of Potamodromous for riverine reproductive migration according to its position in the mainstream, tributaries and lakes into four categories: fluvial, fluvial-adfluvial, lacustrine-adfluvial and allacustrine. Diadromous can be categorized into two following types (Therrien and Bourgeois, 2000):

- Anadromous: where the adults migrate upstream from the saltwater in the seas and oceans to the fresh water in the river for spawning while the juveniles migrate downstream toward ocean for feeding.
- Catadromous: where the adults migrate downstream toward the sea and oceans for spawning while the juveniles migrate upstream to the fresh water in the river for feeding.

In general, there are three reasons for fish migration: spawning, feeding and refuge (Heape, 1931; Northcote, 1997; Lucas and Baras 2001). Figure 2.1 shows the fish movements between these three functional habitats. First, larvae and fry migrate to their first feeding habitat. After that, juveniles migrate to a refuge habitat. Later, subadults move between feeding habitat and refuge habitat. While, maturing adults undertake their first reproductive migration to a spawning habitat and non-maturing adults undertake another refuge migration (Northcote, 1997; Lucas and Baras, 2001).

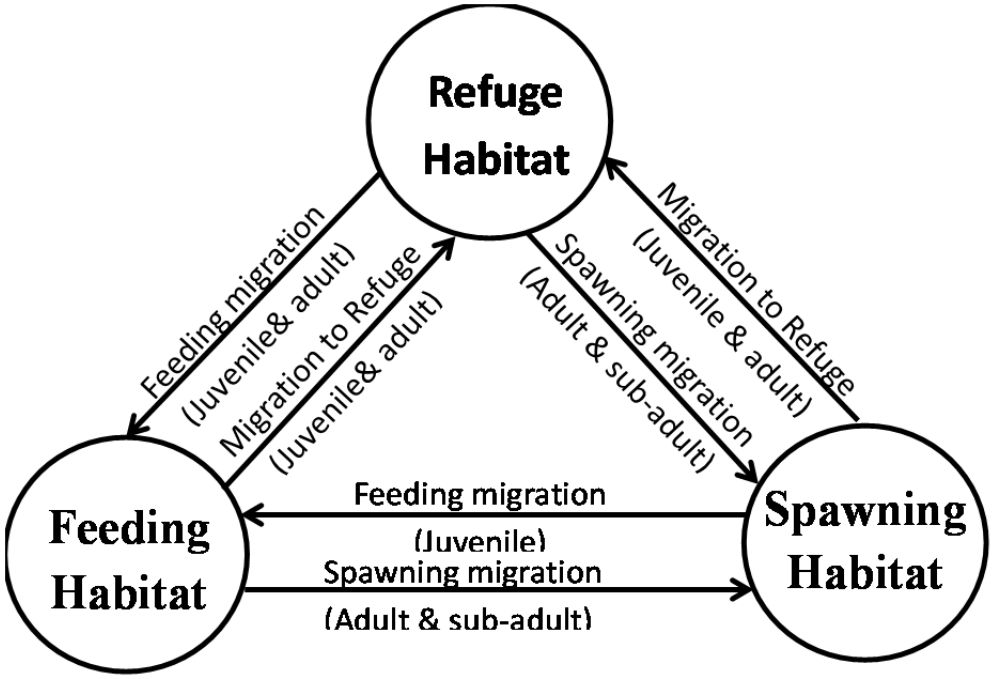

Figure 2.1: Fish migration cycle between spawning, feeding and refuge (adopted from Lucas and Baras, 2001).

Fish migration has great effects on both population and ecosystem. First, it helps fish to attain better growth rates and greater reproductive success by moving between areas to find suitable habitat. This increases the breeding opportunities and prevents inbreeding depression (Morita and Yamamoto, 2002). On the other hand, the fish migration can transport nitrogen, phosphorus, and other nutrients from the sea to the river. Millions of Salmon migrate upstream for spawning and die. Their bodies become an important source for nutrients not only for riverine ecosystems but for the surrounding flora and fauna as well (Castro-Santos and Haro, 2008). Haag and Warren (1998) pointed out in a study of freshwater mussels that, glochidia, a mussel larval stage, can stick to the gill of the passing fish and settle after some time when certain habitats are met. These mussels play an important role in cleaning the water from phytoplankton and zooplankton and saving aquatic ecosystem health.

Due to the great number of dams, roads and other man-made barriers during last century, free fish migration has become partially or totally banned. These migration barriers can earnestly impede the survival of most of the fish species and create barriers to upstream and downstream movement of organisms and nutrients, which hinders biotic exchange (Poff and Hart, 2002). Additionally, these migration barriers subject the fish to migration delays, excessive predation, and high energy expenditure. Therefore, the need for fish passage facilities is widely accepted specially for anadromous fish.

2.2 Upstream fish passage

A fish pass or fishway is any artificial structures built around any man-made flow barrier like dam, locks or culvert that facilitate fish migration. It can be a simple culvert under a country road or a complex bypass system at hydropower facility (U.S. Department of Energy, 1991). Fish passage is needed where a dam prevents a target species from its habitat. Fish are generally incapable of crossing upstream of a dam unless some fish passage facility is presented. There are many factors affecting the success of a fish passage system. It must be designed to be fish friendly by taking into consideration biology and behavior of the target species, in addition to hydrologic conditions both up- and downstream of the project (U.S. Government Printing Office, 1995). There are three challenging points that help to achieve successful passage: guidance to the fishway entrance; entry rate, or attraction into the fishway; and passage rate through the fishway once entered (Castro-Santos and Haro, 2008).

To guide the fish to the place of the fishway, Andrew and Geen (1960) suggested putting the entrance at the farthest upstream point which the fish can reach. The ability of the fish to recognize the entrance of the fish passage downstream of the dam is challenging. The water velocity at the entrance should be high enough to attract the fish to enter the fishway. A velocity of 1.2 m/s is considered minimal for the entrance of the fishway by Andrew and Geen (1960). In case that this velocity is not needed by the fishway, further auxiliary water is added to maintain a flow.

2.3 Types of fish passage

Fish passage can be classified in categories based on hydraulic design and function: culvert, pool-and-weir fishway, Denil fishway, ramp fishway, vertical slut fishway, fish locks, and lifts. Some of these types will be introduced in the following sections.

2.3.1 Culvert fishway

Culverts are structures used to transport water from one side of a roadway embankment to the other. They are constructed with circular, elliptic, pipe-arch, rectangular or square cross-sections (figure 2.2). To design the culvert for fish passage, some considerations features are required to ensure that the fish can enter, pass through and exit the culvert (Minnesota department of transportation, 2000; Katopodis, 1992).

Figure 2.2: Culvert fishway (Forest Service Stream-Simulation Working Group, 2008).

2.3.2 Pool-and-weir fishway

Pool-and-weir fishway consists of a series of pools arranged in a stepped pattern separated by weirs, each of which is slightly higher than the one immediately downstream. Sometimes, this type frequently includes a notch at the weir to ensure minimum overflow depths under low flow conditions, and an orifice placed at the bottom of the weir to provide a passage route for non-leaping swimmers as indicated by figure 2.3 (California department of transportation, 2007).

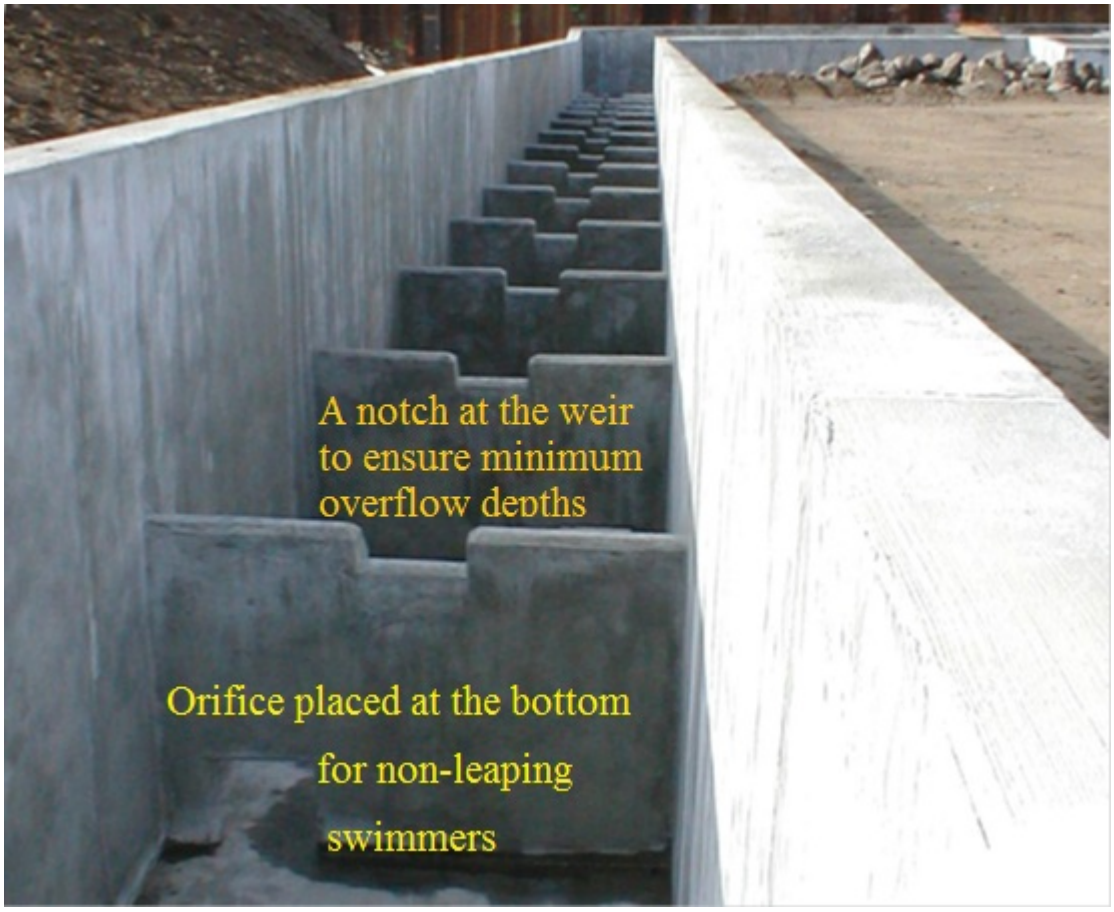

Figure 2.3: pool-and-weir fishway (California department of transportation, 2007).

2.3.3 Vertical slot fishway

In this type, the water flows from one pool to the next through a vertical slot in a baffle forming water jet. This jet causes central turbulence and energy dissipation while each pool is characterized by wide area with low velocity (Figure 2.4). The fish passes through the jet with its burst velocity and the present of the low velocity area allow the fish to take rest (Rodriguez et al., 2006)

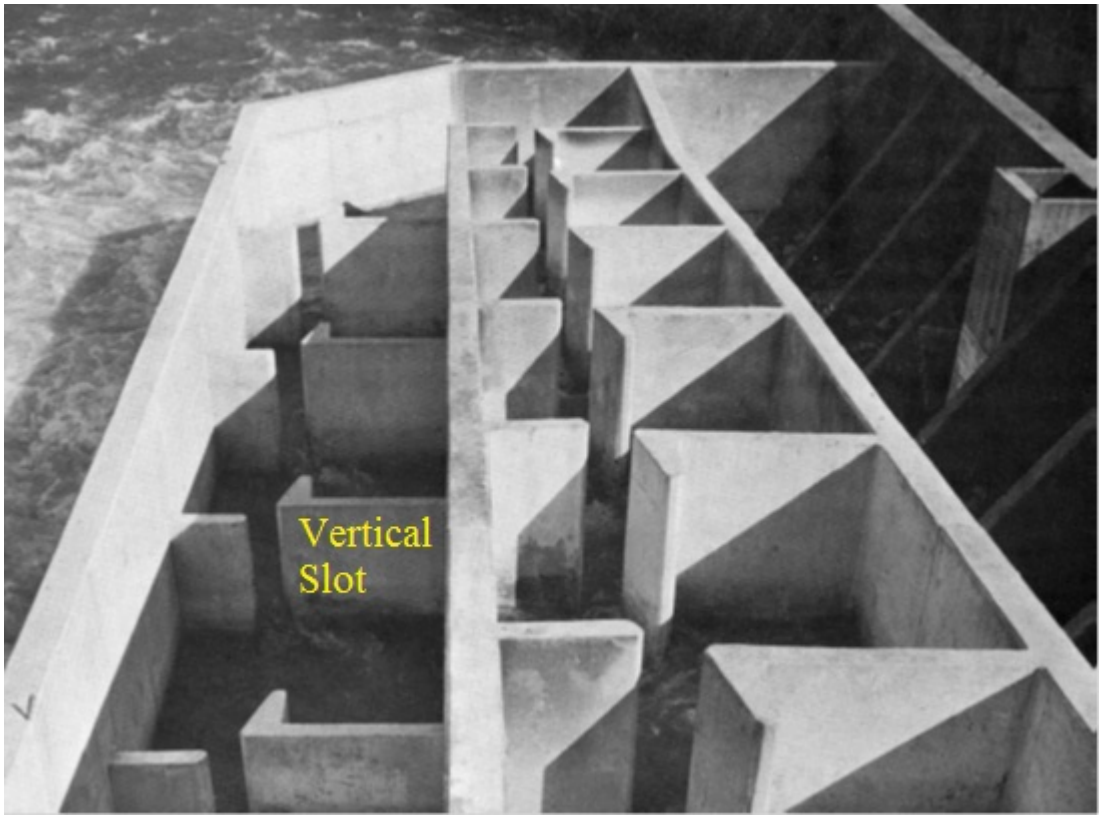

Figure 2.4: Vertical slot fishway (California department of transportation, 2007).

2.4 Hydraulic factors affecting fish passage

A culvert or any other fishway becomes a barrier to fish passage when it demonstrates conditions exceeding fishes' biological ability. The most common obstructions to fish passage are: excessive water velocities, drops at culvert inlets or outlets, physical barriers such as weirs, baffles, or debris caught in the culvert barrel, excessive turbulence caused by inlet contraction, and low flows that provide too small depth for fish to swim. Culverts act as barriers to fish passage by presenting any number or combination of impassable obstacles. Treatments designed to treat one barrier must ensure that another is not created in the process (Federal Highway, 2007). Table 2.1 summarizes the impact of each of these barriers on fish passage.

Table 2.1: Problems of barriers to fish passage and possible effects (Federal Highway, 2007)

Barrier Type	Problem	Impact
Drop	Drop at outlet exceeds fish jumping ability, or jump pool is insufficient to generate sufficient thrust.	Fish cannot enter structure, can be injured, or will expend too much energy entering the structure to traverse other Obstacles
Velocity	High velocity exceeds fish swimming ability.	Fish tire before passing the crossing
Turbulence	Turbulence within culvert prevents fish from entering, or confuses sense of direction	Fish do not enter culvert, or are unable to successfully navigate the waterway.
Length		Fish may not enter structure due to darkness. Fish may fatigue before traversing the structure.
Depth	Low flow depth causes fish not to be fully submerged.	Fish will be unable to swim efficiently or unable to pass the structure.
Debris	Caught within a culvert, debris can block flow, or portions of flow.	Fish will not be able to pass by debris, or constricted flow may create a velocity or turbulence barrier within the culvert.
Cumulative	Series of culverts, each of which stresses fish during passage.	Group of culverts, each marginally passable, may be a combined barrier.

Among these passage barriers, velocity is found to be the only significant parameter in a study of Yellowstone cutthroat trout to indicate the probability of passage through a series of five culverts in Montana (Cahoon et al., 2007). Some of these factors will be discussed in chapter 4.

2.5 Fish biology

Understanding of fish biology will help for better design of the fish passage and other fish way. The effect of some biological aspects on fish passage design will be

explained in this chapter.

2.5.1 Fish muscles

The fish lateral muscle structures are responsible for its swimming and fighting power. When the muscles situated in one side contract, this side will be shortened and the fish tail will be pulled toward this side. By contracting the muscles in the other side, the tail will be swished from side to side (Bagur, 2009). These muscles contribute more than 70 % in Salmonids.

Fish use two types of muscles (red and white muscles) in swimming according to the swimming mode. The function of each of them is quite different according to the type of swimming. The red muscles are responsible for the aerobic energy which is fueled by oxygen while the white muscle is responsible for the anaerobic energy (without Oxygen). As long as a fish swims within the sustained swimming speed only the red muscles are used, while in prolonged swimming at high swim speeds, the white muscles are used, and that leads to fatigue (Bagur, 2009).

2.5.2 Types of fish movement

Fish have three different types of swimming velocities: sustained, prolonged, and burst. While fish can swim with sustained swimming velocities for long time, they can maintain the prolonged velocity for 30 minutes and burst velocity for very short time less than 20 seconds (Katopodis, 1992). The fish can change the swimming type based on the hydraulic conditions they face (Katopodis, 2005). Many studies reported the fish behavior against hydraulic conditions including water velocity, depth and turbulent in term of swimming capability in both laboratory and field conditions (Bagur, 2009).

A good indicator for swimming capability is the fish fatigue time. This is the time taken by the fish under a given set of flow conditions to reach to the exhaustion (fish are unable to swim against the flow) (Nikora et al., 2003). When the fish encounters zones of high velocity flow, it will be forced to swim at speeds greater than their maximum sustained speed (Castro-Santos, 2005). Behlke et al. (1991) mentioned that, fish use their burst speed to pass when they are swimming through velocity challenges. The fish passage should be designed to decrease the fish fatigue time (the time where the fish uses its burst speed) otherwise they would become too exhausted. Several researchers suggest this fatigue time to be in the range between 10-20 seconds (Blaxter, 1969; Dumont, 2012). Based on data of sprint swimming ability of six migratory fish species, Castro-Santos (2005) proposed a new model of distance maximizing strategy for fish traversing velocity barriers (figure 2.5). He took into

account the effect of flow velocity, body length and temperature. No evidence that this model is valid for other species and Castro-Santos is currently in his way to develop a new model for brook trout and brown trout where he found that they behave in different way (Castro-Santos, 2012).

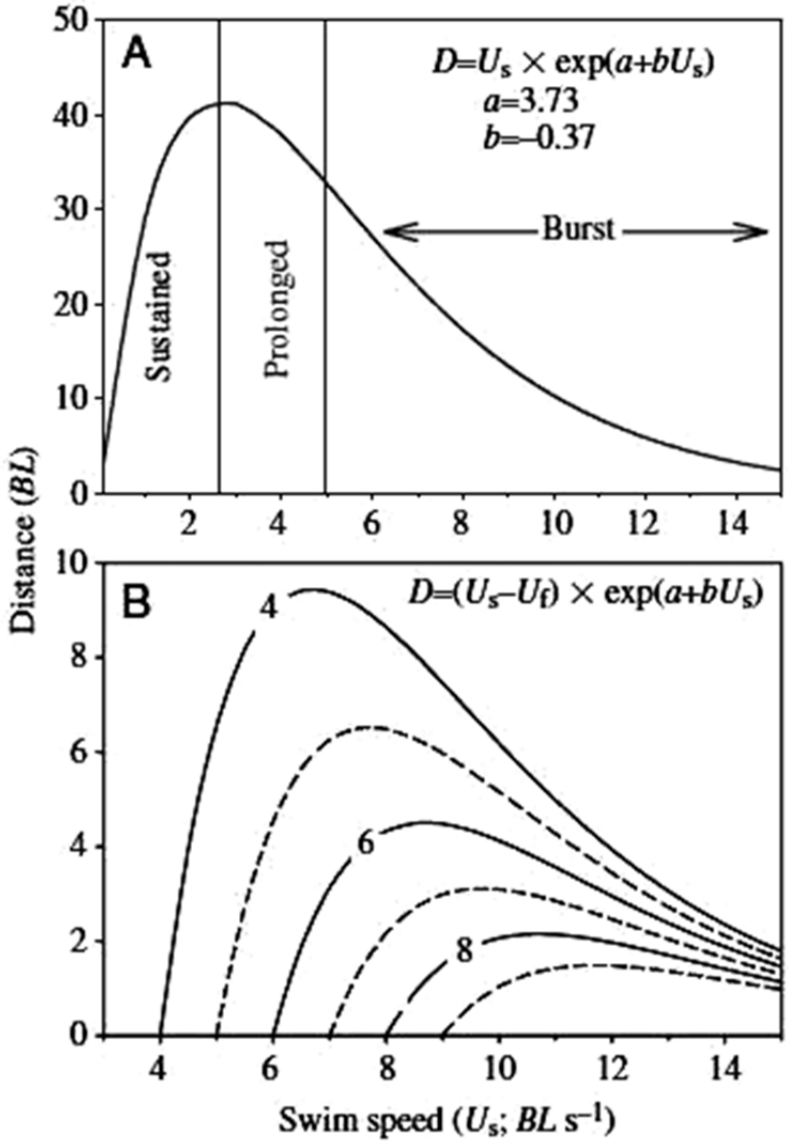

Figure 2.5: Distance maximizing strategy for fish traversing velocity barriers in body lengths for still water (A) and in the presence of flow (B) where contours indicate flow velocity (after Castro-Santos, 2005).

Another indicator for swimming capability is the metabolic cost of swimming performance (Bagur, 2009). It can be measured depending on the oxygen requirement of the fish. Enders and Herrmann (2003) studied the effect of oxygen consumption of the fish in relation to water velocity and turbulence. They found that the breathing rate increases by increasing the water velocity and the fish upstream swimming effort increases in presence of turbulence. The effect of turbulence on swimming capability

is challenging and there is a conflicting finding in published researches (Liao, 2007). More details of the turbulence effect on fish movement are discussed in chapter 4 section 4.4.3.

Mechanism of the swimming speed is another interested topic for both biologist and engineers (Reid, 2011). Several studies concentrated on the relation between the fish swimming speed and some fish kinematic variables such as tail beat frequency (Videler, 1993), tail beat amplitude (Webb, 1971; Liao, 2002), the length and speed of the body wave (Wardle et al., 1995; Tytell and Lauder, 2004) and body undulates (Müller et al., 2001; Blake, 2004). The results of most of these studies are debated and the only accepted result is that the fish swimming increases with tail beat frequency (Reid, 2011). Reid (2011) uses data of 26 species combined from previous studies to test these kinematic variables found that the propulsive body wave is the main reason of the swimming speed. Other variables such as tail beat frequency and amplitude, length and depth of the body, and propulsive body wave length significantly affect the swimming speed.

2.5.3 Gills and oxygen respiration

Two difficulties face fish and other water species in order to extract the oxygen from water. First, the amount of oxygen included in the water is around one - thirteenth of the amount of oxygen in air. Second, water is much denser than air. Fish overcome these challenges by pumping larger amounts of water over their respiratory organs and increasing the surface area of them (Bagur, 2009). The role of the fish's gills is to maximize the gases exchange of gasses between fish's blood and water. The fish has four gills in each side and each of them is covered of two rows of gill filaments (Kisia, and Onyango, 2007). To increase the surface area, filaments are further folded into V-shape and Filaments divided into thin lamellae which further aids gas exchange (figure 2.6).

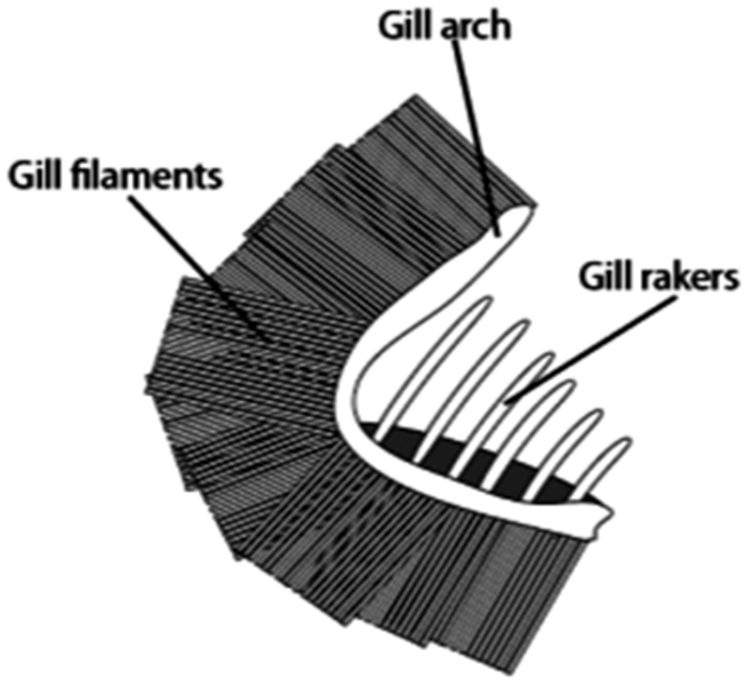

Figure 2.6: The gill structure of fish (after Bagur, 2009).

2.5.4 Fish vision

The fish eyes have a wide area to view including two types of vision in addition to a small blind area behind the fish as indicated in figure 2.7 (Bagur, 2009):

- The front vision where there is overlap between its two eyes to provide an area of binocular vision. This allows the fish to accurately determine the distance of prey items.
- The side monocular vision is to monitor the horizon in each side

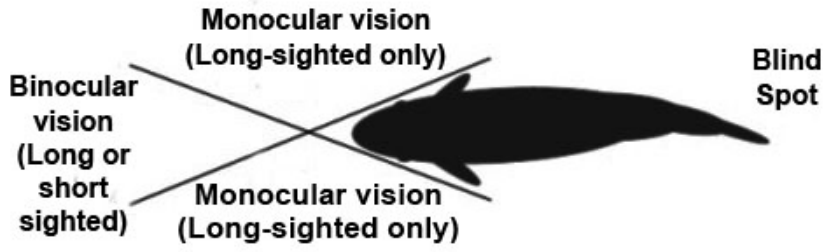

Figure 2.7: Fish Vision (after Bagur, 2009.)

2.5.5 The lateral line system

The lateral line system (LLS) is an organ consists of series of neuromasts (pores) spread over the fish body arranged. Each neuromast has a series of sensory hair cells which have the ability to detect the sound and other sensory functions (Bagur,

2009). There are two types of neuromasts, superficial neuromasts (SNs) that are situated on the surface of the skin, and canal neuromasts (CNs) that are situated within a system of subdermal canals. The canal fluid is in contact with the outside water through a series of pores. Neuromasts are sensitive either to water velocity (SNs) or pressure differences (CNs). Using CNs, the fish can recognize small local pressure gradients over the body due to hydrodynamic motion (see Webb et al., 2008) (figure 2.8). Several researches showed the ability of the blind fish to detect and recognize stationary objects in its surroundings with the aid of its LLS (Campenhausen et al., 1981; Weissert and Campenhausen, 1981; Hassan, 1989). Chagnaud et al. (2007) studied the responses of anterior lateral line nerve fibers of goldfish to unidirectional water flow and to running water vortex. They found that the vortex shedding frequency can be retrieved from the responses of anterior lateral line nerve fibers.

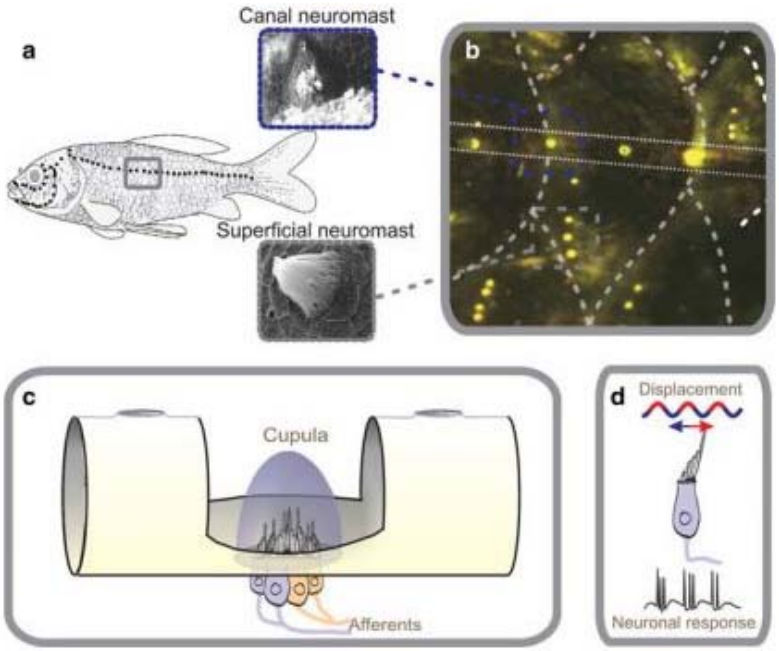

Figure 2.8: Organization of CNs and SNs on the goldfish (after Goulet et al., 2008). a) distribution of the neuromasts on fish body; b) close up of CNs and SNs; c) the shape of CN; d) the impact of sinusoidal stimulas on a single hair cell.

2.6 Techniques used for fish passage evaluation

Unfortunately, there are no widely accepted standards to evaluate the constructed fish passage. One evaluation method is the presence of evidence of reproduction by species which could not spawn previously in the upstream habitat. Brown (2006) studied spawning of green sturgeon, acipenser medirostris, in the upper Sacramento River, California. He concluded that green sturgeon spawn in the upper Sacramento River, both above and below Red Bluff Diversion Dam.

Another evaluation method is to count the individual species that pass the structure manually (Wibe et al., 2001) or automatically (Beach, 1978; Burwen et al., 1995; Suzanne and Gove, 2004). Manual counting is often difficult to do, especially in situations with low visibility or high turbulence (Tiffan and Rondorf, 2004). Automatic counting using remotely-operated electronic monitoring device is another option. Several types of electronic monitoring devices are available in literature including infrared counters (Beach, 1978), multi-beam sonar (Suzanne and Gove, 2004) or split-beam acoustics (Burwen et al., 1995). However, most of these techniques have a limited application in a specific situation (Baumgartner et al., 2010). Baumgartner et al. (2010) performed a field and laboratory study on the effectiveness of an infrared fish counter. The laboratory results show that the unit was often under estimate the number of fish especially when multiple fish passed through the counter at the same time. On the other hand, the unit showed much better results in counting the fish in field study than the laboratory results. Fish behaved differently around the unit and some of them actively avoid the unit.

Tracking the fish movement is the third evaluation method. It can be used for both upstream and downstream migration. Several techniques are available including Radio telemetry (Gowans et al. 1999), Passive integrated transponder tag (Zydlewski et al., 2001), ultrasonic (Egli and Babcock, 2004) and video-based techniques (Kane et al., 2004). Most of the used methods required human interaction with fish like Passive integrated transponder tag (PIT-tag). In PIT-tag method, an electronic microchip is inserted into the fish body with a unique code. This code can be registered when the fish passes an antenna. While using a network of antennas, the spatial and temporal fish movements can be provided. This technique was used in several studies of individual fish movements and migration ((Prentice et al., 1990; Hockersmith et al., 2003; Cookingham and Ruetz Iii, 2008). Although this method and probably other similar methods are the only practical way to follow the fish path in some cases, the change in fish behavior because of human interaction is unknown and it is difficult to quantify (Hubert, 1985).

A video based technique is another way to track the fish movement in the field and in the laboratory (Spampinato et al., 2008; Pinkiewicz, 2012). Spampinato et al. (2008) developed an automated Video Processing system for detecting, tracking and counting underwater fish. They used 20 underwater videos to test the developed algorithm and achieved an overall accuracy as high as 85 %. The basic of this technique is introduced in chapter 3.

2.7 Prior research and potential

Combining the observed fish behavior and hydraulic measurement give more

understanding of the fish pathway into, through and out of the fish passage. Hydraulic conditions like velocity, water depth and turbulent are varied in space and time. Thus, it is better to relate the fish passage success to fine scale structure and dynamic of the hydraulics rather than the average. Although the field studies of the individual fish movements in fine scale help to understand the factors affecting the ability of fish to pass barriers, the work in this direction is very limited and most of these studies have been either laboratory experiments (Atsushi, 2009 and Hayashida et al., 2001) or studies of fish movements on the large scale (Maselko et al., 2003) in addition to very few field studies with reasonable scale (Blank, 2008 and Fitch, 1995). Following individual fish movement in the field is very difficult. For example, Fitch (1995) could not recapture any of his tagged trout in a study of nonanadromous trout passage in culverts in Virginia. In the remaining part of this section, samples of some of these studies are presented.

Several studies are concentrated on the detail structure of the hydraulic conditions inside the culvert as well as other fish passage (Katopodis, 1993; McArthur, 2011; Wu et al., 1999). Wu et al. (1999) studied the structure of mean flow in a vertical slot fishway and found that the flow at the slot could be considered roughly as plane jet while the slot velocities were not uniform and the stream lines were not perpendicular to the slot opening. He could differentiate two pattern of flow according to the bed slope. For slope of 5.0 %, the flow inside the pool can be considered as 2D with two recirculation zones around the main jet. One the other hand, for slopes of 10 % and 20 %, the main flow should be considered as 3D as part of the flow rises to the surface before travelling through the outlet. Tarrade et al. (2008) used Particle Image Velocimetry (PIV) to calculate the mean velocity in a vertical slot fishway in addition to various kinematics parameters characterizing the flow like kinetic turbulent energy, the vorticity and the flow instationarity.

Numerical simulation is another way to study the flow characteristics inside the fishway with more details and less efforts. It can avoid major problems during the design stage of fish passage structures and, it can improve the structure's hydraulic performance. Khan (2006) employed modeling tools for 3D flow simulation of a seven-pool vertical slot fishways. He found that the flow inside the fishway is a strong 3D velocity field characterized by eddies, flow separations, vortices, upwellings and downwellings.

Haselbauer (2008) carried out a series of biological, hydraulic and numerical experiments on a new type of fishway. He used a system of sequential sluices and baffles in between to avoid the entrainment of air into the water. This reduces the disturbances in the fish pass due to air bubbles and decreases the noise level in the water and in the air along the fish pass. Further, he applied an existing numerical code

FLOW-3D to simulate his laboratory experiment. The turbulence models applied were Reynolds averaged Navier-Stokes (RANS) and large eddy simulation.

Several researches showed that fish movement inside the fish passage is individual rather than school (Pearson et al., 2006). Therefore, studying the rules governing the fish upstream movements inside the culvert and other fishway poses a great challenge in this research field. Unfortunately, the available studies concern the individual fish movements inside passage are very limited and more detailed studies are required.

Guiny (2001) constructed two typical physical models to study the behavior of juvenile salmon and hydraulic conditions for a range of small structures including vertical slots, orifices, weirs and combinations of all three. He found that higher percentage of fish moved through orifices or vertical slots than through weirs for a given flow rate and velocity. He noticed also that in order to pass through the weir or the orifice, salmon parrs prefer to follow the path near the bottom and along the sides of the arena where velocities is low.

Pearson et al. (2006) conducted fish-passage tests to evaluate passage success in a 40 ft corrugated culvert with slope 1.14 %. The culvert has three weir baffles and tested under five different flow conditions (1.5, 3.0, 6.0, 8.0, and 12.0 cfs). The successful passage was varied from 40.0 % at 1.5 cfs to 70.0 % at 3.0 cfs, and 10.0 % at 12.0 cfs. They noticed that the fish follow the low velocity pathways for upstream passage. These pathways differ according to flow conditions and differ between baffled and unbaffled conditions.

One of the most important and effective tool to study fish passage is a numerical model. Several models were presented in the literature (Haefner and Bowen, 2002; FishXing, 2006; Goodwin et al, 2006). A model presented by Haefner and Bowen (2002) described the fish movements through the louver type fish collection facility. In this model, the fish swimming behavior was studied using a set of simple decision rules that govern fish swimming intensity and direction according to its current position. Khan (2006) studied the flow and the energy expenditure in a vertical slot fishway and developed a model for the energy expenditure and drag forces along different flow paths. Goodwin et al. (2006) developed an Eulerian–Lagrangian–Agent Method (ELAM) for mechanistically decoding and forecasting 3-D movement patterns of individual fish. In this model, the physical and hydrodynamic (Eulerian) are coupled with the movement of individual fish (Lagrangian) in addition to the behavior decisions of individuals (agent). Goodwin et al., (2006) applied ELAM to the fish passage systems in the Pacific Northwest, USA.

Based on the literature review, I believe that the best way to design structures in which the fish move as individual rather than population, is to combine the individual

based model with some statistical data which describe the variation between individuals.

2.8 Summary

In this chapter, the most important fish passage characteristics that affect the ability of the fish to pass the fishway were discussed. This serves as a step for the introduction of the next two chapters where I investigate the conceptual applicability of image processing techniques for tracking fish path in a real dataset captured by off-the-shelf video cameras in chapter three and developed a numerical model of fish passage through culvert and other fish barrier in chapter four.

The important of this chapter for fish passage that it gives an overview on the important of fish passage, its types, hydraulic and biological factors that affect it, the techniques used for its evaluation, and the previous works that studied it both experimentally and numerically.

3. Image processing algorithms for fish path tracking

The study of fish behavior has always been a topic of interest amongst hydraulic engineers as well as biologists. Recent studies have emphasized the in-depth assessment of fish behavior for efficient design of the hydraulic structures that concern them. In order to make studies on fish path movement and how it is affected by water flow, we have to first acquire datasets that capture fish movement in moving water streams. As a first part of my study, I shall present an image processing-based approach to which I developed for this particular purpose.

Traditionally, several methods are used to capture a moving fish track. These included the mark and recapture technique (Blank, 2008; Warren and Pardew 1998), casting nets for collecting and examining fish, human underwater observation and photography (Rouse, 2007; Schlieper 1972), combined net casting and acoustic tracking (sonar) (Brehmera et. al, 2006) and, more recently, human hand-held video filming (Spampinato et. al, 2008). Videler and Weihs (1982) used a high-speed camera (up to 200 frames/s) fixed over the middle of a tank to measure the fish Burst speed. From these frames, the displacement of the head and the tip of the tail in a horizontal plane is traced by digitizing the position every 0.01s. Xingqiao et al. (2008) proposed a particular and real-time image processing application to detect pathological changes to fish. They acquired Images from a video source periodically using specialized control software and convert it to gray Image. Then they removed its noise interference to enhance the quality. Finally they statistically recognized pathological changes of the fish. On the other hand, Wu and Zeng (2007) introduced a video system for tracking a free-swimming fish two-dimensionally. They used two CCD (charge coupled device) cameras to obtain three-dimensional kinematic parameters of the tail and pectoral fin of the fish in forward, backward and turning swimming modes.

In this study, I investigate the conceptual applicability of image processing techniques for tracking fish path in a real dataset captured by off-the-shelf video cameras, emphasizing low acquisition cost. The aim of this part is to extract the fish path and velocity from a video camera.

3.1 Datasets

Three sets of data are used in this study. The first was captured in the Laboratory of Hydraulics in Obernach of the Technische Universität München (TUM) while the second one was downloaded previously from internet from following location http://www.youtube.com/watch?v=0jbrSgTmb0&feature= related. The last one was taken from a previous work of Hayashida et al. (2001) in the Watershed

Environmental Engineering Research Team, Civil Engineering Research Institute of Cold Region (Japan), who studied the fish movement in a single pool-and-weir fishway.

In the first dataset, a primary investigation of the fish movement inside a Plexiglas channel that is 50cm wide, 80cm deep and 12m long with gravel bed material was done with two video cameras as shown in figure 3.1. One of them was set up horizontally while the other was in the vertical direction. The fish was allowed to move only in 1.5m distance by two grids. The fish length was around 29.4 cm. Figure 3.2 depicts the camera locations with which the dataset was captured.

Figure 3.1: Positions of the two cameras.

a. Vertical plane camera

b. Horizontal plane camera

Figure 3.2: Side and top view taken of dataset 1.

The second dataset shows the movement of 7 fish with different colors in a fish tank. This dataset was primarily used to validate the proposed methods and develop them, since it posses a higher quality and clarity than that of dataset 1. Figure 3.3 shows an image from the video of the second dataset.

Figure 3.3: An Image from the video of dataset 2.

The third dataset shows the movement of the fish inside a pool-and-weir fishway taken from Hayashida et al. (2001). The experiment was done in a two-dimensional water channel 60cm wide consisting of two 20cm thick weirs 20cm and one pool. The model will be applied to case 1 where the pool length was 50 cm, and the pool water depth 30 cm. Figure 3.4 shows an image from the video of the third dataset.

Figure 3.4: An Image from the video of dataset 3.

3.2 Methodology

In this section I will explain the applied and tested methods. The concepts will be explained and some details of implementation will also be provided, since in image

processing algorithms have to be adapted to the specific application.

3.2.1 Motion detection using the motion vector technique

Block segmentation of video frames combined with motion vectors make up the most fundamental components of almost all video compression standards (Jenq-Neng, 2009). Videos are made up of a series of images (called frames) taken at short time intervals such that the human eye cannot perceive the discrete transitions from frame to frame (typically 25 fps or 30 fps). Hence consecutive frames are temporally correlated over localized spatial domains. This temporal correlation is exploited in video compression: The idea is to segment each frame into a series of blocks (typically of size 8x8 or 16x16 pixels) as shown in figure 3.5.a. It is highly probable that a visually similar block can be found in the immediate (spatial) vicinity in the previous frame. Hence a similar image patch is looked for in a search field. Once such a similar block is found, the video codec simply stores the spatial offset values from the center of the block (the so-called motion vector) and no longer needs to store all pixel values. Such a motion vector shown in figure 3.5.b can effectively capture small-scale motion and encode them efficiently.

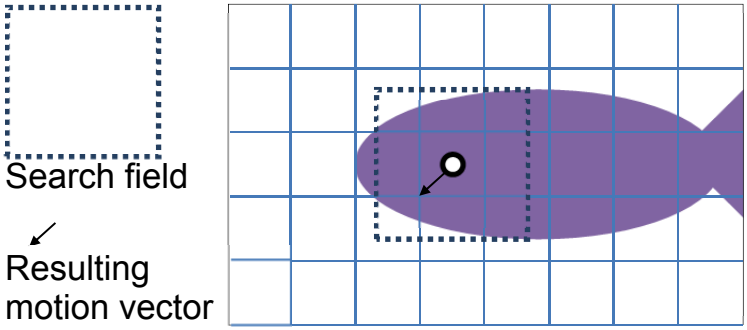

a. Block segmented frame ($t=t_n$) with motion vector shown for one of the blocks. The motion vector encodes the relative displacement of the most similar image patch found in the frame $t=t_{n-1}$.

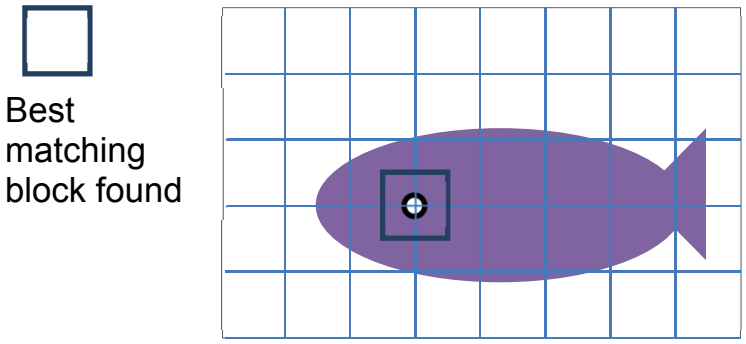

b. Most similar image patch found in the search area shown in figure (a) to the block encompassing the fish eye.

Figure 3.5: Using motion vectors to estimate object movement.

We used motion vectors to capture fish movement. The idea I exploited is again the high temporal correlation between consecutive frames. In essence, since a fish movement is constrained and changes within certain limits, I expected that a block search with motion vectors can sufficiently capture the fish movement if the background is static and the only moving objects are the fish.

The motion vectors are typically calculated for each color channel separately (Jenq-Neng, 2009), since each color layer is typically compressed independently For our application, however, it suffices to perform motion estimation on the gray-level intensity image. For that, the gray-level intensity at any location (u, v) at time (t) can be simply calculated from the three color intensity values I_R (for red), I_G (for green) and I_B (for blue) using equation 3.1 (Solomon & Breckon, 2011):

$$I(u,v,t) = 0.3I_R(u,v,t) + 0.59I_G(u,v,t) + 0.11I_B(u,v,t) \quad (3.1)$$

The different factors account for the color-dependent sensitivity of the eye (the eye is much more sensitive to the green color than the blue color). To calculate the motion vectors (and hence the amount of movement) for a particular block, the most similar patch of the same size in the previous frame has to be determined. The most similar patch in the previous frame is determined as being the one within the search field that has the smallest sum of squared differences (SSD). The SSD between any two patches of image intensity of size NxN is defined as:

$$SSD = \sum_{i=1}^{N}\sum_{j=1}^{N}(I_{curr}(i,j) - I_{cand}(i,j))^2 \quad (3.2)$$

In this specific case I_{curr} denotes the block in the current frame for which a similar patch in the previous frame is being looked for and I_{cand} being the currently considered patch in the previous frame. In other words, the most similar patch is the one that minimizes the difference energy.

The motion vector technique has a fundamental limitation: it does not always perform true motion estimation since the focus is on finding the most similar patch only. Hence, sometimes the motion vectors do not really represent the true motions of the objects over time. Moreover, the search range is typically limited to a small rectangular area around the center point of the block whose match is to be found. This is necessary since the SSD is computationally expensive if performed using the exhaustive search (ES) technique (O (N^2)). More efficient search algorithms exist (Manikandan et al., 2006). Nevertheless, the search field would have to be adapted according to the speed of the fish and the video sampling rate adding complexity to the algorithm.

3.2.2 Motion detection through frame difference calculation

Due to the issues presented in the motion vector technique, I decided to use another method of motion detection based on calculating differences between consecutive frames. This is justified if the background is static which can be insured using a proper capturing arrangement (static cameras, appropriate lighting, etc.). In this case, as can be seen in figure 3.6, only the area covered by the fish in two consecutive frames will have values different from 0 after the subtraction operation since the pixels outside that area will remain the same. Hence by identifying the locations where this is

the case and looking for the center of mass of this area, the approximate location of the fish can be identified.

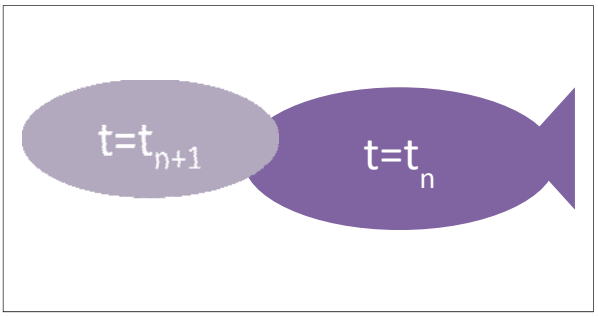

Figure 3.6: Fish location at time $t=t_n$ and $t=t_n+1$. Only colored areas will have values different than 0 in the difference image since the background is static.

The difference is calculated using the gray-level image representation as in the motion vector technique case. The calculation of the gray-scale image is followed by three processing steps:

1. Calculating the absolute difference image between frame n and frame n+1 as shown in figure 3.7.a.
2. Converting the gray-scale image to a binary image by applying thresholding (Figure 3.7.b). The threshold is calculated using the method described in (Otsu, 1979).
3. Filtering the binary image using an opening operation (figure 3.7.c). This type of morphological filtering is effective in filtering out small particles stemming from noise and smaller insignificant objects (Russ, 1995).

a. Absolute difference image

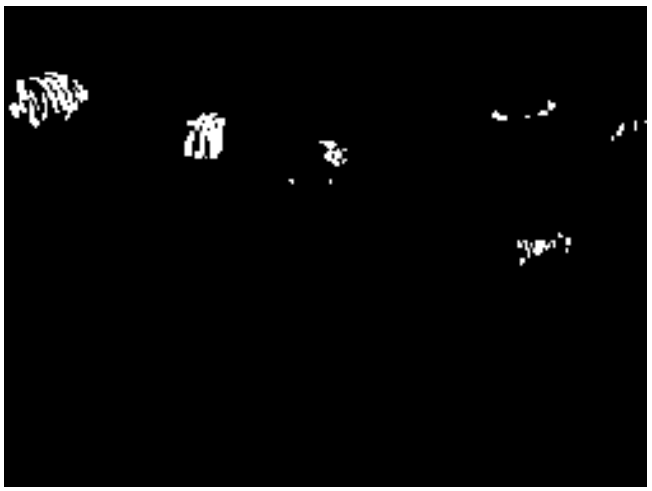

b. Threshold difference image

c. Filtering using image opening

Figure 3.7: Processing steps for moving object detection.

The problem with this technique is that the retrieved location always deviates from the true one as it lies somewhere between the old and new fish locations (The centroid of the area where the absolute difference is bigger than zero). Furthermore,

after implementing this technique, I noticed an oscillatory behavior of the tracking point. Hence, I applied the refinements described in Section 3.3 and Section 3.4.

3.2.3 Background subtracted motion detection

We have seen that the location is always biased behind the fish when it is moving forward, and that a static or slow-moving fish cannot be tracked. To solve these two problems I decided to estimate the background first and use this as a reference frame out of which each video frame is subtracted. Insuring that the fish is the only moving object, this helps in identifying the true fish location. This method also works when the fish is suddenly static or moves slowly.

To estimate the background I again use morphological filtering. More specifically I filter each pixel along the t dimension with a structuring element of width 41 pixels (the same pixel in the previous 20 frames and the next 20 frames). The median value is taken as background value at that particular frame. This is exemplary shown in figure 3.8. The fish body is temporarily seen on the location (u, v) and changes the intensity of the pixel over a short period of time. If the structuring element length is chosen appropriately, this temporary change in the intensity will be filtered out and the prevailing intensity value (that of the actual background) will be chosen as the background intensity value.

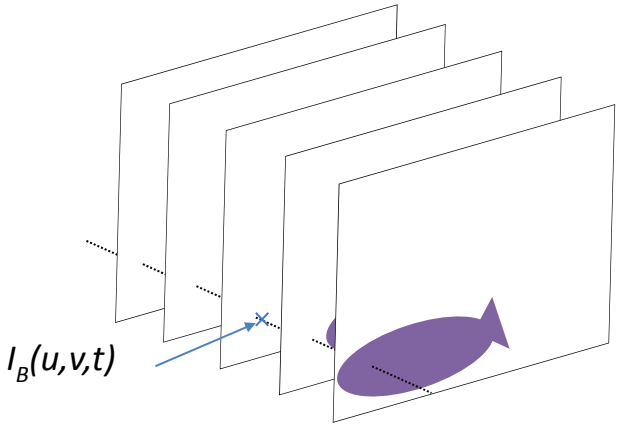

Figure 3.8: Median filtering for background estimation.

In figure 3.9, the estimated background at time t=10 frames is shown for the actual test sequence captured in our lab.

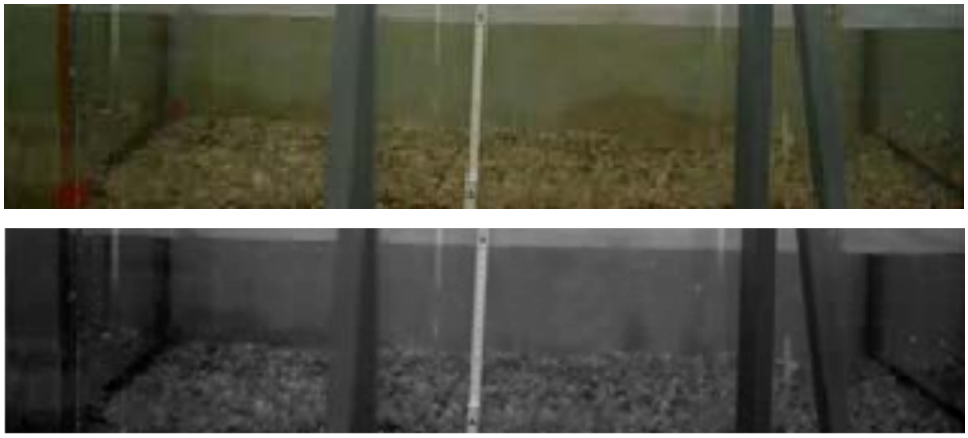

Figure 3.9: Frame #10 from test video (above) and estimated background using pixel-wise median filtering (below).

3.2.4 Using color filtering for robust tracking and multiple fish tracking

The background subtraction motion detection technique delivered the required improvement. Nevertheless, I needed a method to filter outliers (sudden jumps in tracking point). Also I needed a method to associate tracking points to multiple fish tracked over time. The problem can perhaps be seen in figure 3.10 more clearly: - While individual fish can be detected and tracked (red dots representing centroids of detected moving regions), these dots cannot be assigned to the different fish over time.

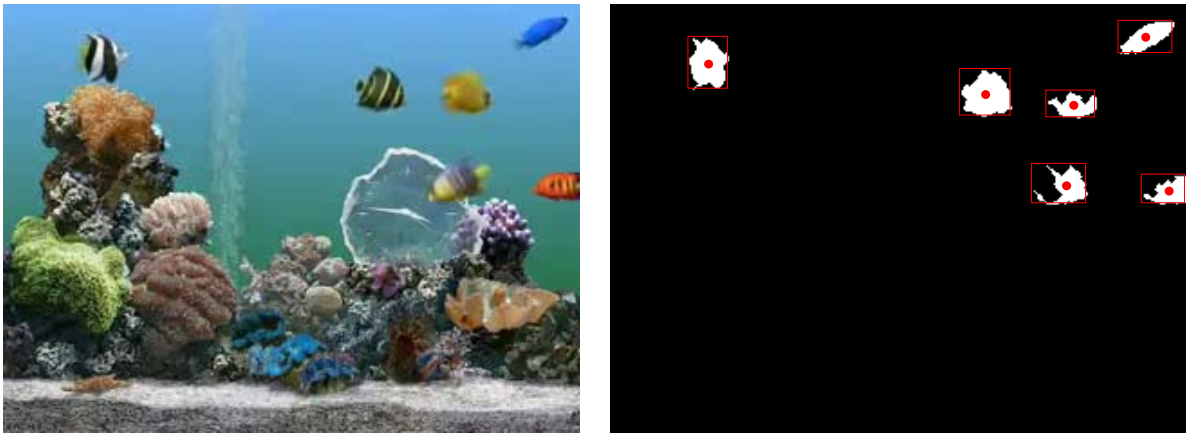

Figure 3.10: Detected moving regions (with centroids and bounding boxes).

Simply assigning the found locations to the fish based on the area size does not work well. Figure 3.10, however, shows that color might be a good information source upon which to identify which location belongs to which fish. Matching colors can be achieved using matching of color histograms. Such histograms are shown for two of the fish in figure 3.11. It can be seen that the histogram of the blue channel for the blue fish has most energy concentrated in the higher values range. A similar thing can be observed for the orange fish where the histogram of the red channel has a big part of

its energy in the high values range.

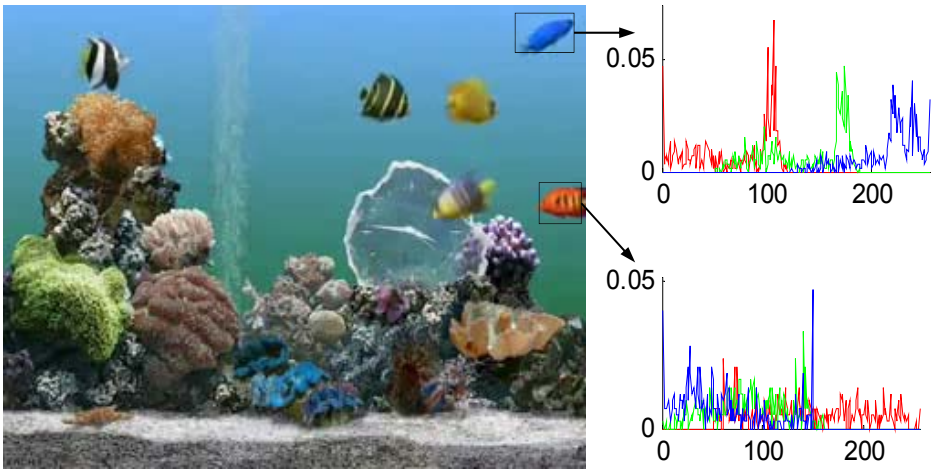

Figure 3.11: fish color histograms.

The idea is to extract the color histogram of each fish to match them to color histograms extracted from the bounding box regions out of each frame. This way, each detected region can be uniquely assigned to one fish; namely that with the most similar color histogram.

The only thing that remains to be explained is how color histograms can be compared. There exists a number of metrics to compare color histograms. Two notable metrics are the *Kullback-Leibler divergence* and the *Bhattacharyya distance*. I have chosen to use the Bhattacharyya distance where the similarity between two discreet histograms expressed as vectors of length M can be calculated using:

$$D_B(\boldsymbol{h_1}, \boldsymbol{h_2}) = -\ln\left(\sum_{i=1}^{M} \sqrt{\boldsymbol{h_1}(i)\boldsymbol{h_2}(i)}\right) \tag{3.3}$$

$\mathbf{h_1}$ and $\mathbf{h_2}$ being color histograms expressed as vectors having M bins (in our case I use M=256 bins since intensity values for each channel range from 0 to 255 since our videos have 8 bit color depth). Since there are three channels per image patch and consequently three histograms, there needed to be a way to combine them together. The most simple is to perform distance calculation between patches using each channel histogram separately and then calculate one distance score by linearly combining the individual distances using a weighting equal to that found in equation 3.1.

3.3 Method validation

Dataset 1 is used to verify the algorithm without the color filtering technique, since only one fish is moving. The two videos included in this datasets show that the fish rested in its place for some time before starting to move quickly with high speed. The recorded video has a frame rate of 25fps and spans a period of 10.5s. Figure 3.12 shows three frames of the resulting tracking. The successful fish tracking outcome can better be seen in the video I provide at (http://www.wb.bv.tum.de) under Research Video Section (Dataset_1.avi).

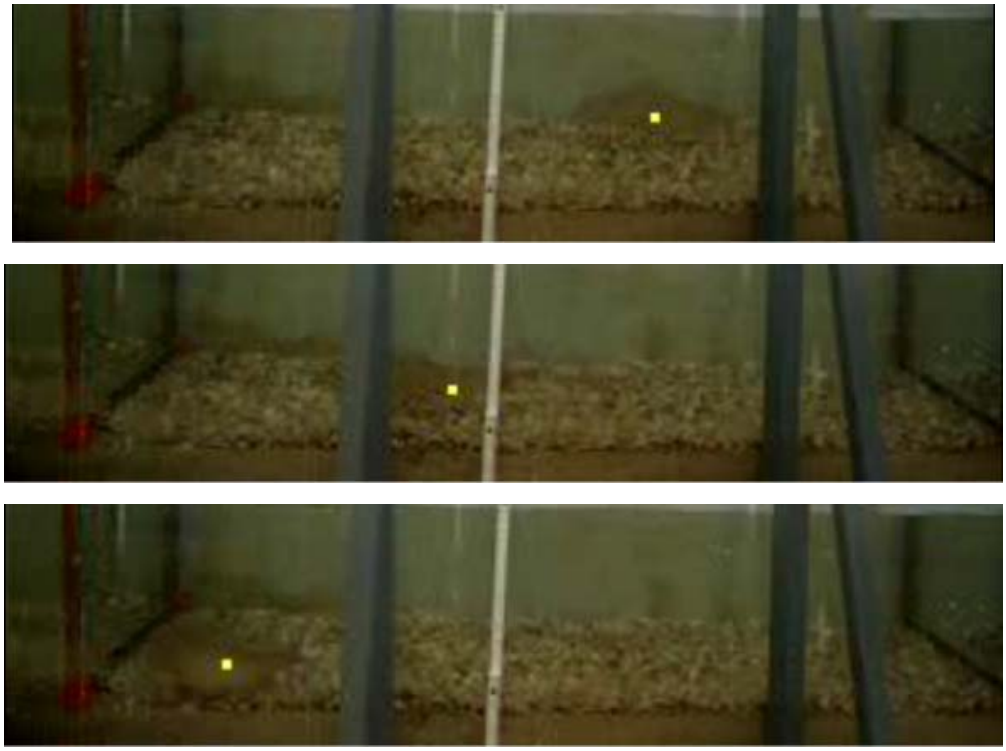

Figure 3.12: Tracking the fish in dataset 1.

Figures 3.13 and 3.14 show the smoothed fish path and velocity as captured in the vertically and horizontally aligned cameras. While the vertical velocity was captured by the developed algorithm, the tracking method could not work with the other camera (the one looking at the fish from above) due to the randomly changing lighting reflections (water surface specularities) resulting from the water surface turbulence and the lighting of the test setup. Hence, I suggest capturing a new dataset where the camera capturing the horizontal plane is placed below the fish tank to avoid this problem. I are confident however, that the method would work just as well if a proper dataset is captured for the horizontal plane and thus providing us with the 3D location of swimming fish over time. The results of the horizontally aligned camera were extracted manually by programming a Matlab tool that displays the frames and captures the location which the user clicks on. With this tool I manually recorded the

true fish location at every 5th frame (corresponding to 0.2s time space). The same method was used to verify that the results I got are accurate; the true fish vertical location was manually determined and recorded by human observation using the mentioned tool. I calculated the difference between the estimates using our proposed fish tracking method and the ground truth locations. The determined accuracy is best seen in an error histogram showing the distribution of absolute location error in the estimated location compared to the ground truth location.

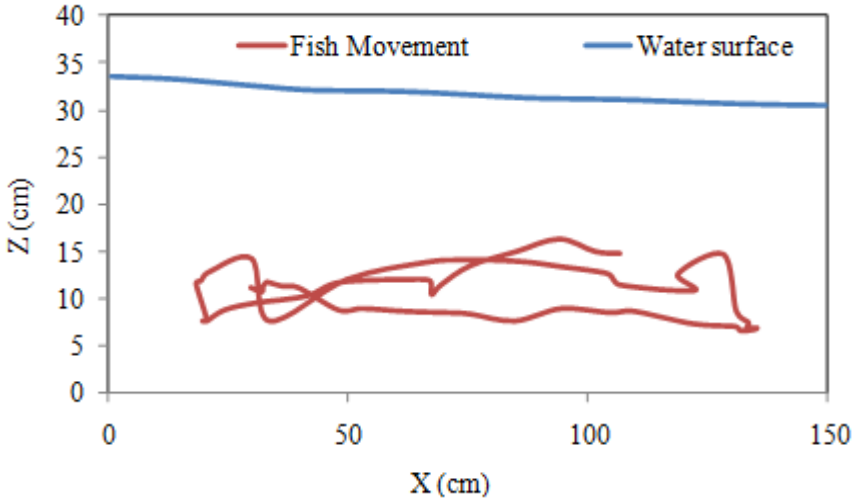

a. Vertical fish movement

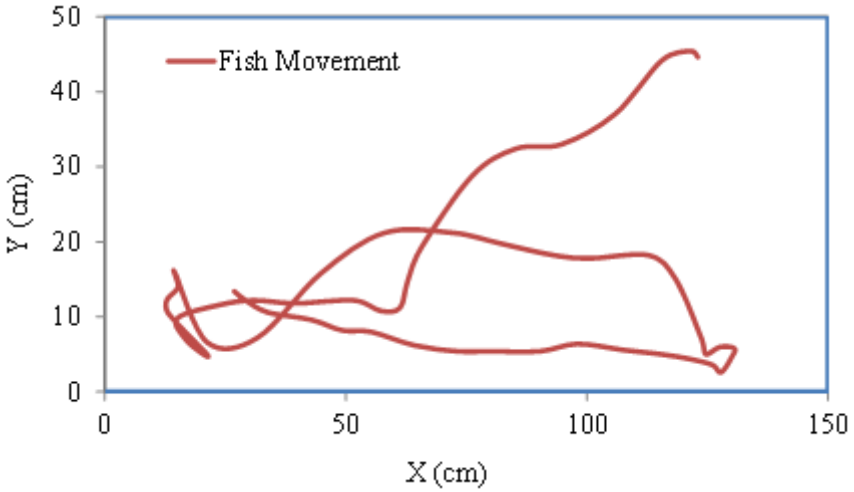

b. Horizontal fish movement

Figure 3.13: The estimated fish movement for dataset 1.

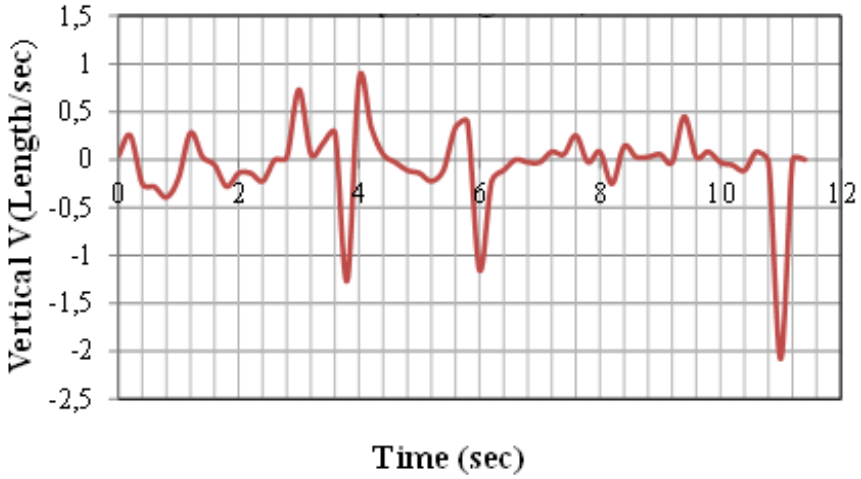

a. Vertical fish velocity

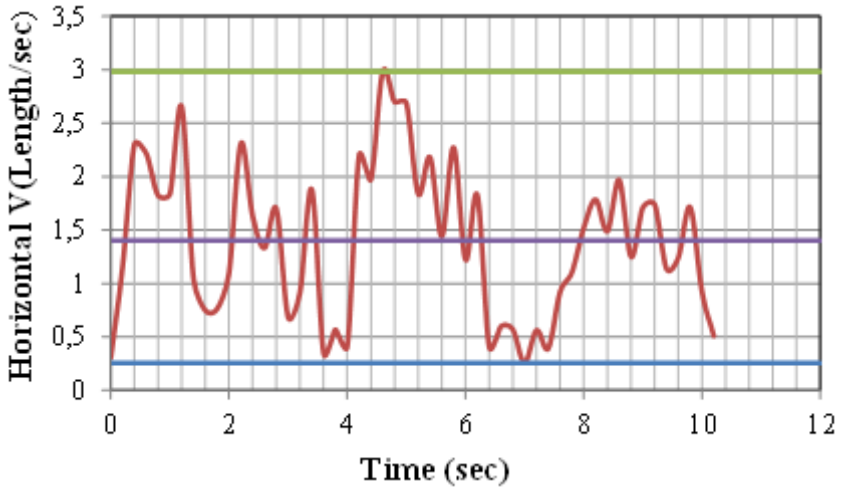

b. Horizontal fish velocity

Figure 3.14: The estimated vertical fish velocity for dataset 1.

The relative error histogram was calculated relative to the fish length as shown in figure 3.15. The mean error in X and Y directions are 0.1490L ± standard deviation 0.1471L and 0.0635L ± 0.0537L respectively (where the tolerance values indicated by the ± sign represent the standard deviation). The main reason for this small difference is the presence of some supporting beams (see figure 2(a)) which partially occlude the scene.

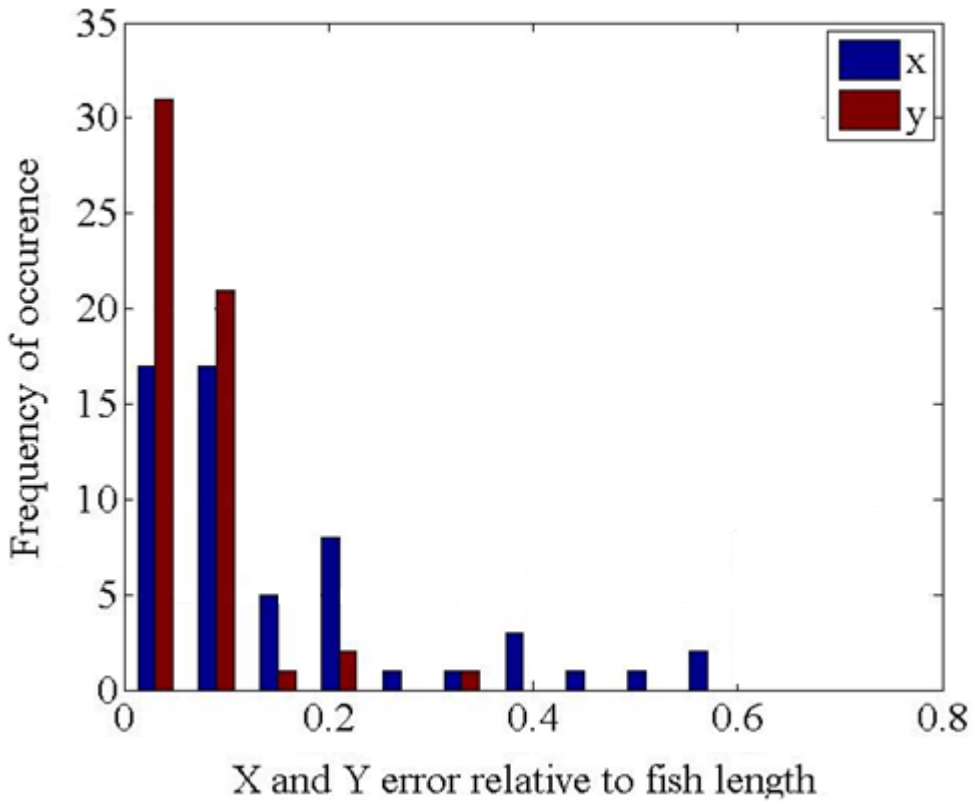

Figure 3.15: Relative error Histogram.

To also verify that the suggested improvement of using color filtering (histogram matching) does bring the expected gains, I ran the the refined method on dataset 2. More specifically, I provide the color histogram of the blue fish in the fish tank as template and with that successfully track and distinguish the blue fish. Figure 3.16 shows two frames of the resulting tracking. The resulting tracking can better be seen in the video on (http://www.wb.bv.tum.de) under Research Video Section (Dataset_2.avi). Figure 3.17 shows the blue fish movement and velocity.

Figure 3.16: Snapshots from tracking the blue fish using the color histogram aided

fish tracking.

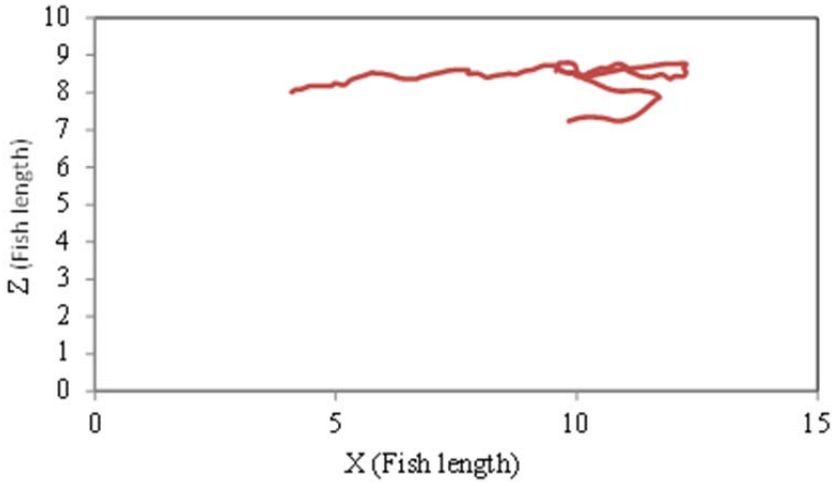

a. Vertical fish Movement

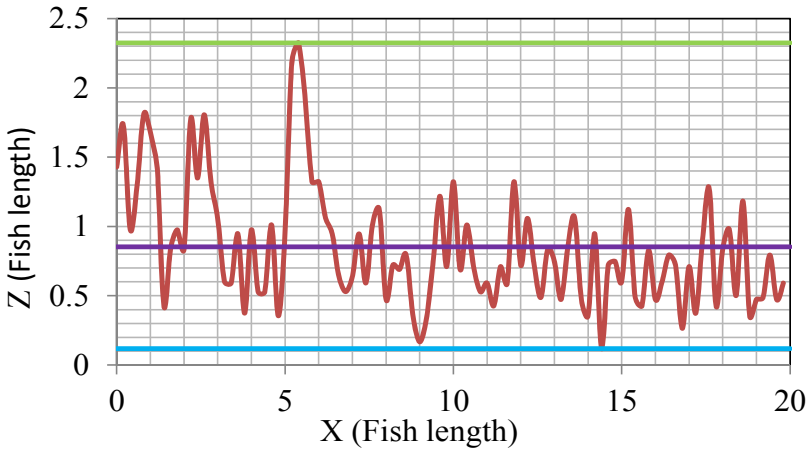

b. Vertical fish velocity

Figure 3.17: The resultant vertical fish movement and velocity for dataset 2.

The method was applied to extract the fish movement inside the pool-and-weir fishway (dataset 3). In this case, the fish enter the pool from the downstream part and swim to the bottom of it and finally the fish start moving individually upstream against the flow direction. Although all the fish have almost the same size and color, only one fish is moving and the others are stationary. To simplify this video, the part where the fish are appear together in a swarm is cut out from the video and the algorithm is applied to the remaining part as shown in figure 3.18. The movement of the fish and its velocity were extracted with the same algorithm while some corrections were done manually using the prescribed Matlab tool. Figure 3.19.a shows the fish movement path where the fish moves from the downstream to the upstream direction. The figure shows that the fish moves against the high flow direction and away from the turbulent area in the middle of the pool. Figure 3.19.b shows the change of velocity while the

fish moves upstream. Figure 3.20, on the other hand, shows the change of velocity with time. The fish velocity is varied from zero to 12.0 fish length per second. The velocity drops down when the fish changes its direction from the horizontal to the vertical direction and reaches its maximum value as it swims up through the upstream weir.

a. Before extraction b. After extraction

Figure 3.18: Subtraction of the downstream part from the video (dataset 3).

The distribution of the fish velocity indicates that the fish velocity inside the fishway is varied from point to point starting from very small velocity at the resting zone to more than 10.0 fish length per second over the weir. This indicates that the fish uses a combination of aerobic and anaerobic energy when passing through the fishway.

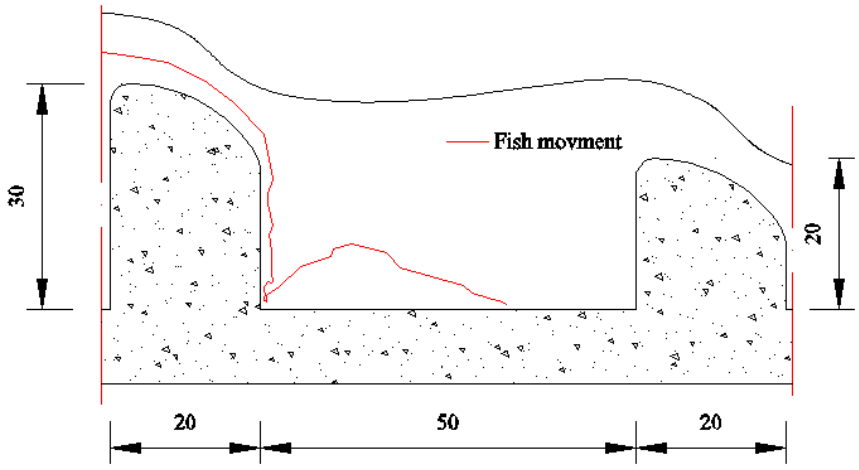

a. Fish movement

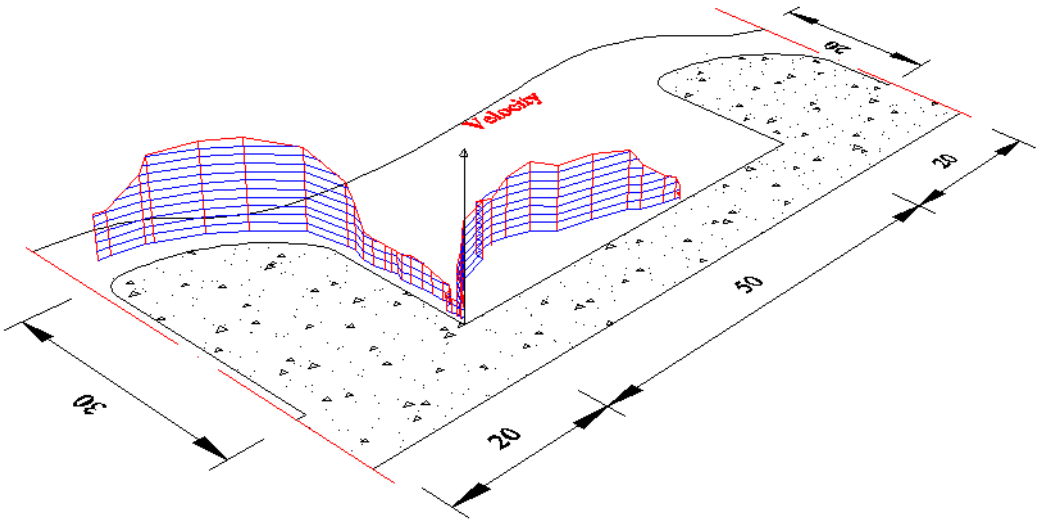

b. Fish movement and related velocity

Figure 3.19: Relation between the fish position in the pool and its velocity for dataset 3.

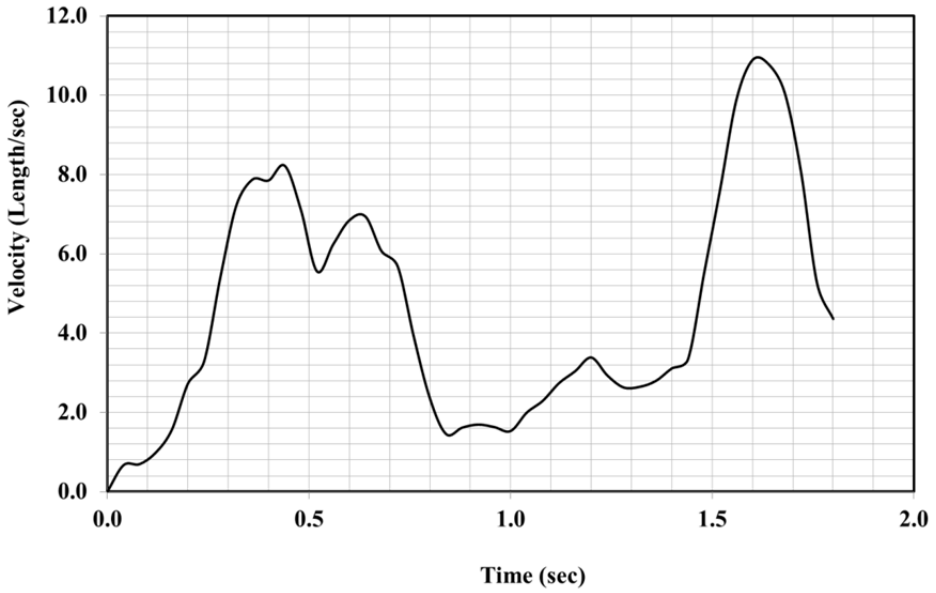

Figure 3.20: The relation between time and fish velocity for dataset 3.

3.4 Suggestions for improvements

We have seen that it is important not to only detect fish, but also track them across frames. In the presented approach, I used the concept of color histogram matching for that purpose. It is interesting to look at a complimentary approach, namely that of object matching using local invariant texture features. In contrast to color histograms, such features compare texture, i.e. appearance in the grey-scale image.

Comparing two images or identifying the same object in two different images is not a straight-forward task. Typically, “features” are employed for this purpose. Features are numerical entities (typically high dimensional) that provide an alternative representation to the standard pixels of images or image patches. These representations are mathematical functions of the image intensity values (the pixel values). The mathematical functions are designed so that the resulting feature vectors (also called feature descriptors) possess certain desirable properties.

For the particular application of fish tracking one particular class of features is interesting: local-invariant features. These features describe small image patches. They are required to have following properties: “lighting-invariance”, “rotational-invariance” and “scaling-invariance”. A lighting invariant feature means that two similar image patches with different lighting (i.e. contrast and brightness difference) would result in the same feature descriptor. Invariance against scaling and rotation accordingly means that the same patch would result in the same feature descriptor even if it is captured in a rotated manner and from a different distance resulting in a

different size inside the image. The perhaps most widely used features are the Scale Invariant Feature Transform (SIFT) (Lowe, 2004), the Speeded-Up Robust Features (SURF) (Bay et al., 2004), and table External Regions (MSER) (Matas et al., 2002). SIFT features typically detect edge-like patches, while SURF features mainly fire on "blobs". MSER is sensitive to homogenous connected surfaces.

Local features can be matched across images representing different perspectives of the same scene. Figure 3.21 shows SURF features extracted and matched on the two images shown in figure 3.16.

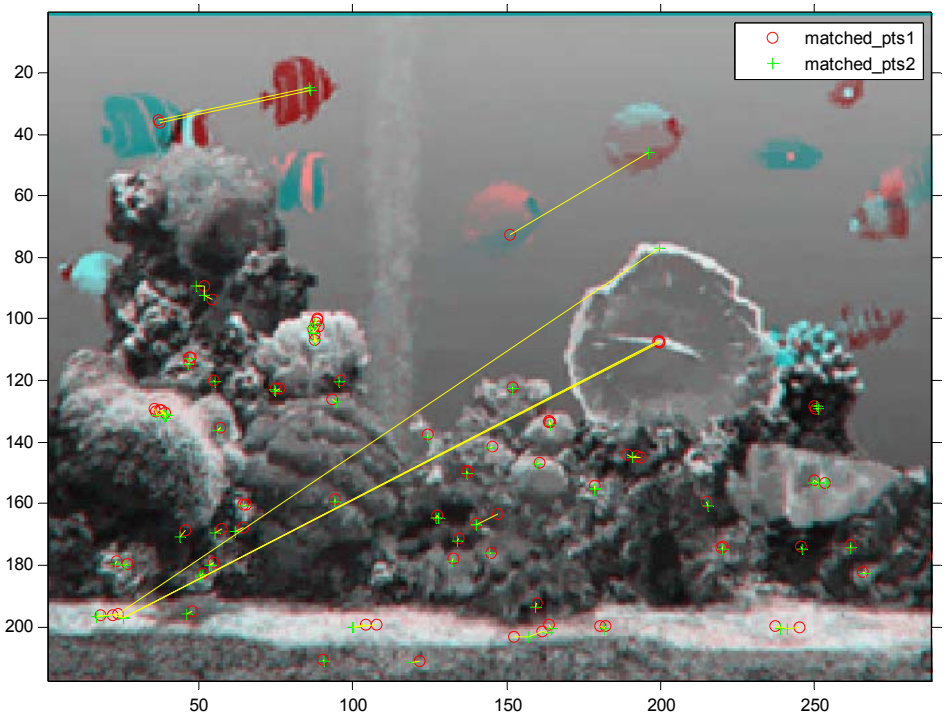

Figure 3.21: SURF features matched between the two frames shown in figure 3.16 (frames are overlaid on one another).

Figure 3.21 shows how promising this idea is. Two of the fish have been matched perfectly without the need for background estimation subtraction and color histogram matching. It also reveals some of the short comings. The blue fish on the right edge of the image was not matched across the images because the (textural) appearance changes substantially as the fish is turning. The two other fish on the right edge are not matched as well. This is perhaps due to the background which affects the calculated descriptors. Two of the fish on the left edge are not matched as well. However this is because one of them actually disappears behind stones and the other comes out of it (i.e. due to "occlusion"). This is however, not a short coming of the approach. In fact if the frame rate is higher, then the inter-frame change is low and features of similar objects are very similar and can be matched robustly.

In short, this approach is very promising. There is a large body of research concerned with features and there are large possibilities to reap off the benefits of using features for the purpose of fish tracking. It remains to be said that features are much better used to complement the already implemented system than be used in a feature-only system. One example is the blue fish. While features failed to track it as it turned, the color-histogram matching approach tracked it successfully since the color did not change in that case.

3.5 Summary

In this chapter, I presented a method that I have developed to capture fish movement. The method is based on techniques from the area of image processing. Particularly, the methods of motion vector-based motion estimation and frame difference-based motion estimation are investigated towards their usability to track swimming fish for the purpose of automatic path capturing. The motion vector technique is found to be of limited performance. The frame difference technique is improved by performing background estimation and subtraction using morphological filtering, resulting in accurate fish tracking in a realistic dataset captured at our lab. I furthermore add color filtering for fish identification in a multiple fish tracking scenario and demonstrate the principal capability to track and identify different fish.

Although I achieve good results in tracking fish in realistic scenarios, I consider this chapter as a foundation for more elaborate methods that could result in more accurate and robust tracking by incorporating suitable post-processing techniques (outlier removal and adaptive smoothing). This is mainly motivated by the fact, that I have been able to acquire higher quality data later from Blank (2008), Hayashida, et al., (2001), Atsushi *et al.*, (2008) and Atsushi (2009). Nevertheless, researchers who want to study the field of fish behavior even further are encouraged to consider and improve the proposed method so as to be able to capture more datasets in quick time.

4. Numerical model for decoding movement patterns of fish

Studying the fish upstream movements through culvert and other fish passages is very important from the ecological and culvert construction point of view. This can provide information of the proportions of the migrating populations that actually move upstream and help to better understand the mentality of the fish for traversing a velocity barrier.

In this study, a numerical model of fish passage through culvert and other fish barrier is developed and incorporated in a computational fluid dynamics (CFD) code FLOW-3D for flow simulation. The model distinguishes between two different fish passage types. The first is the roughened channels where the fish have to swim through them in one go with their burst speeds. The second is pool-type channels where high speeds occur only through the openings of the boulder bars. Accordingly, two different models will be presented in the following sections.

4.1 Numerical modeling

The numerical modeling employs a discrete and particle-based representation of individual fish migrating through or swimming inside a structure. It relies on detailed water velocity fields and turbulent flow characteristics, which can be obtained from the observed data or applying a computational fluid dynamics (CFD) code. The model releases a number of simulated fish and tracks their movements using a concept of minimum energy expenditure, with a discrete random-walk method and other special fish behaviors. The simulated particles do not have time-varying attributes (other than location) which affect their simulated behavioral responses. However, it is individual-based in the sense that the detailed movements and exposure histories of individual fish are simulated.

4.1.1 Hydraulic model

In the commercial computer program FLOW-3D, the hydrodynamic module is based on the solution of the three-dimensional Navier-Stokes equations and the continuity equation for incompressible flows. The governing equations can be written in a tensor form for a control volume as follows (Flow Science Inc., 2008):

$$\frac{\partial(u_i A_i)}{\partial x_i} = 0 \qquad (4.1)$$

$$\frac{\partial U_i}{\partial t}+\frac{1}{V_f}\left(U_j A_j \frac{\partial U_i}{\partial X_j}\right)=-\frac{1}{\rho}\frac{\partial P}{\partial X_i}+f_i \tag{4.2}$$

where:

$$\rho V_f f_i=\tau_{b,i}-\left[\frac{\partial}{\partial X_j}\left(A_j S_{ij}\right)\right];\quad S_{ij}=-\mu_{tot}\left[\frac{\partial U_i}{\partial X_j}+\frac{\partial U_j}{\partial X_i}\right] \tag{4.3}$$

where U_i (1, 2, 3) = the velocity components; P = pressure; A_i = fractional area open to flow in the i-direction; V_f = fractional volume open to flow; f_i = the gravity force per unit volume; S_{ij} = strain rate tensor; $\tau_{b,i}$ = wall shear stress; ρ = density of water; μ_{tot} = total dynamic viscosity, which includes the effects of turbulence ($\mu_{tot}=\mu+\mu_T$); μ = dynamic viscosity; and μ_T = eddy viscosity.

In FLOW-3D, alternative schemes for turbulence closure, namely one-equation for turbulent energy k, standard k-ε, renormalization-group (RNG) k-ε, and large eddy simulation (LES) models, can be applied. The k-ε closure schemes will be considered in this model, where the turbulent viscosity can be expressed as the product of the turbulent velocity and length scale. Therefore,

$$\mu_T=\frac{\rho C_\mu k^2}{\varepsilon} \tag{4.4}$$

The closure equations for the turbulent kinetic energy k, and the dissipation rate ε, are given in a tensor form by:

$$\begin{aligned}&\frac{\partial k}{\partial t}+\frac{1}{V_f}U_i A_i \frac{\partial k}{\partial X_i}=C_{sp}\frac{\mu}{\rho V_f}\left[2A_i\left(\frac{\partial U_i}{\partial X_i}\right)^2+\left(\frac{\partial U_i}{\partial X_j}+\frac{\partial U_j}{\partial X_i}\right)\left(A_j\frac{\partial U_i}{\partial X_j}+A_i\frac{\partial U_j}{\partial X_i}\right)\right]\\&-\frac{1}{V_f}\frac{\partial}{\partial X_j}\left[\frac{A_i}{\rho}\left(\mu+\frac{\mu_T}{\sigma_k}\right)\frac{\partial k}{\partial X_j}\right]\end{aligned} \tag{4.5}$$

where C_{sp} is an empirical factor called the shear production coefficient with default value=1.0

$$\frac{\partial \varepsilon}{\partial t}+\frac{1}{V_f}U_i A_{xi}\frac{\partial \varepsilon}{\partial x_i}=C_{\varepsilon 1}\frac{\varepsilon}{k}\left(C_{sp}\frac{\mu}{\rho V_f}\left(2A_{xi}\left(\frac{\partial U_i}{\partial X_i}\right)^2+\left(\frac{\partial U_i}{\partial X_j}+\frac{\partial U_j}{\partial X_i}\right)\left(A_{xj}\frac{\partial U_i}{\partial X_j}+A_{xi}\frac{\partial U_j}{\partial X_i}\right)\right)\right)$$
$$-\frac{1}{V_f}\frac{\partial}{\partial X_j}\left[\frac{A_{xi}}{\rho}\left(\mu+\frac{\mu_T}{\sigma_k}\right)\frac{\partial k}{\partial X_j}\right]-C_{\varepsilon 2}\frac{\varepsilon^2}{k} \tag{4.6}$$

The closure coefficients and auxiliary relations in case of the standard k-ε model are: ($C_{\varepsilon 1}$= 1.44, $C_{\varepsilon 2}$ = 1.92, C_μ = 0.09, σ_k = 1.0, σ_ε = 1.3). The RNG approach is a mathematical technique that can be used to derive a turbulence model similar to the k- ε, results in a modified form of the ε equation which attempts to account for the different scales of motion through changes to the production term. The RNG model uses the same equations like k-ε model with different coefficients values ($C_{\varepsilon 1}$= 1.42, $C_{\varepsilon 2}$ is computed based on the values of *k*, *ε* and the shear rate, C_μ = 0.085, σ_k = 0.72, σ_ε = 0.72).

The wall boundary conditions are evaluated differently based on the chosen turbulence closure scheme. Transport turbulence closure scheme uses a law of the wall formulation. In FLOW-3D, the combined smooth and rough logarithmic law of the modified wall equation is iterated in order to solve for the shear velocity u_* (Flow Science Inc., 2008):

$$u_o=u_*\left[\frac{1}{\kappa}\ln\left(\frac{\rho u_* y_o}{\mu+\rho a u_* k_s}\right)+5.0\right] \tag{4.7}$$

where κ = von Karman constant; a is a constant, which is equal to 0.247 for standard and RNG k-ε models; k_s = wall roughness; and y_0 = distance from the solid wall to the location of tangential velocity, u_0. The denominator of Eq. (8) represents an effective viscosity due to the effect of the rough boundary (μ_{eff} =μ+ρau_*ks). If the cell is within the laminar sublayer (where ρ$u_*$$y_0$ /μ≤5.0), the solution for the shear velocity is defined with:

$$u_*=\sqrt{\frac{\mu.u_o}{\rho y_o}} \tag{4.8}$$

The solution for the shear velocity is used as the wall boundary conditions for the turbulent transport equations. At wall boundaries k and ε are defined with:

$$k = \frac{u_*^2}{\sqrt{C_\mu}}; \varepsilon = \frac{u_*^3}{\kappa y_o} \tag{4.9}$$

FLOW-3D handles free surfaces using the Volume of Fluid (VOF) technique pioneered by Hirt and Nichols (1981). This technique consists of three components: A method for finding the free surface, an algorithm for tracking the free surface as a sharp interface moving through the computational mesh and a process for applying boundary conditions to the surface. The method makes use of the simple principle of assigning a single variable F (fluid fraction) to each cell that has a value of 1.0 if the cell is occupied by fluid and a value of 0.0 if the cell is completely empty. Therefore, if the cell has a value of F between 0.0 and 1.0 then the cell contains a free surface. In addition, the normal to the surface can be calculated from the direction in which F changes most rapidly applying boundary conditions to the surface.

$$\frac{\partial F}{\partial t} + \frac{1}{V_f} A_i U_i \frac{\partial F}{\partial X_i} = 0 \tag{4.10}$$

FLOW-3D permits the modeling of complicated geometries by allowing the partial blockage of each cell in a regular mesh. The partial blockage of mesh cells is represented by associating a single open volume fraction (V_f) and three open area fractions (A_i) with each computational mesh cell. The volume fraction is the fraction of the cell volume which may be occupied by fluid. It is, therefore, one minus the fraction of the cell volume which is occupied by solid material. The area fractions are defined as the fraction of the area of each mesh cell face through which fluid may flow. Those associated with a particular cell are the faces between it and the next higher cell in i-directions. The other three faces of a particular cell have area fractions that are associated with the next lower cell in each direction (Sicilian, 1990).

4.1.2 Model for fish movement though a roughened channel with almost uniform main flow directions

Based on the water velocity and the observed fish paths extracted from the work of Blank (2008), a model for fish movement though a roughened channel with almost uniform main flow directions is developed. Figure 4.1 shows the flowchart that summarizes the structure of the proposed model. According to this flowchart, the main steps of the model can be summarized as follow:

1. To start the model, the data related to the culvert geometry, the measured or

simulated velocity and the coordinates of the fish at the entrance of the culvert are required.

2. Based on these flow data, the model checks whether there is high turbulence or not.
3. In case of high turbulence the turbulence avoidance model will be applied.
4. Otherwise, the model checks the velocity at the next three points in the upstream direction searching for the lowest velocity. In this case the minimum energy expenditure model with random probability will be applied.
5. In case that the three points have the same velocity, the fish will search in its memory if there was a turbulence in one side within the specific number of previous movements, then the turbulence avoid technique will be applied.
6. Otherwise, the fish will give equal probabilities to the three directions.
7. The steps are repeated until the fish reaches to the most upstream part of the culvert.
8. Finally the calculated path is smoothed using the moving average filter method.
9. The energy expenditures are calculated from the smoothed simulated path.

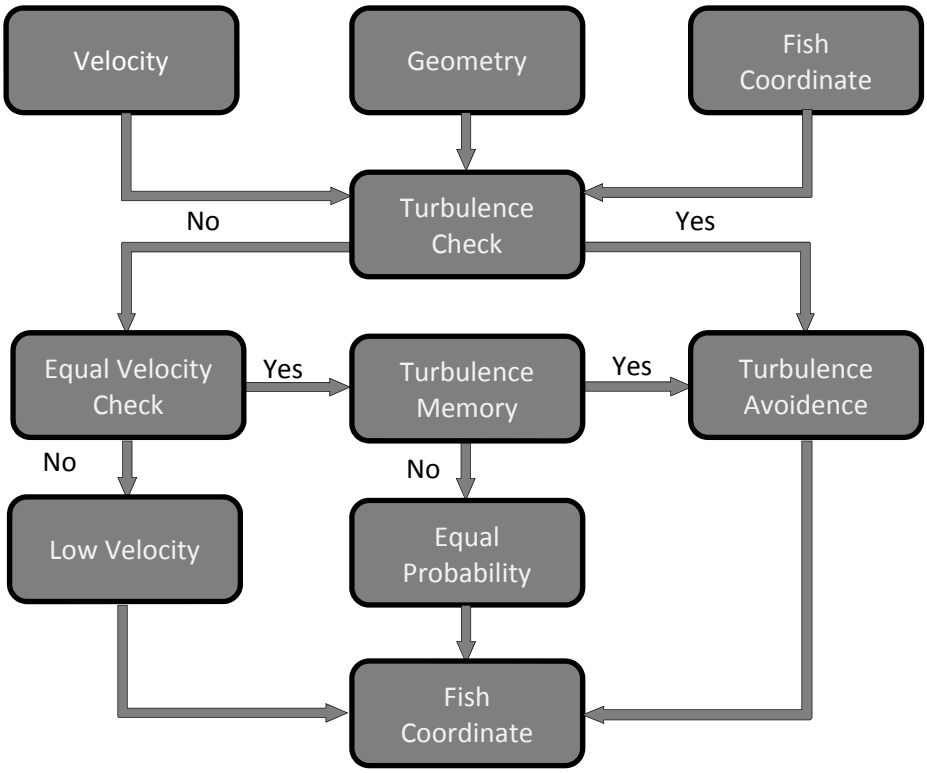

Figure 4.1: The structure of the proposed low energy and turbulent model.

A detailed description of the fish movement model is introduced in the remaining part of this section.

4.1.2.1 Minimum Energy Concept

According to many investigators the fish seeks to minimize their energy expenditure by travelling against the lower velocities (see for example Kane et al., 2000; Pearson et al., 2005). Blank (2008) studied the fish energy expenditures inside the culvert and found that the total energy expenditures by the fish is very close to the minimum possible energy expenditures. This indicates that the fish will follow the low velocity path when migrating upstream through the culvert.

Following Blank (2008) work, a model was developed at the Institute of Hydraulic and Water Resources Engineering, Technische Universität München (TUM). In this model, when starting from the downstream, the fish will select the path by searching and comparing the velocities in the grid upstream, upstream left and upstream right. The path with the lowest velocity is the minimum energy path. The fish moves to the grid point with the lowest water velocity and the procedures are repeated until the fish has ascended the entire structure. If the velocity at each of the three points is more than the fish burst speed, the model will stop and the fish will be assumed to go back with flow direction (see figure 4.2).

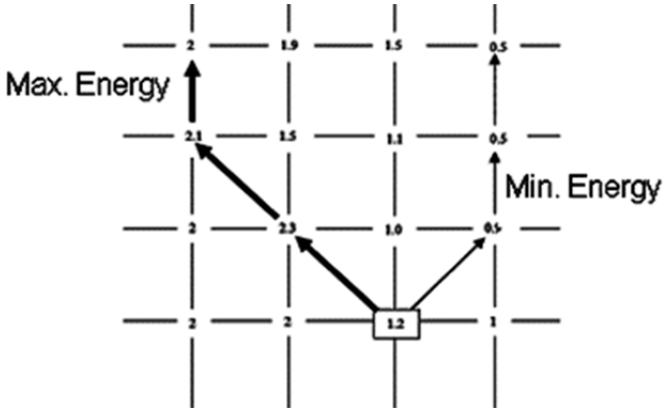

Figure 4.2: Diagram of decision process following Blank (2008) for estimating Minimum energy expenditure.

4.1.2.2 Minimum energy concept with random movement

Random movement was widely used in the fish orientation models (Warburton and Lazarus, 1991; Huth and Wissel, 1994; Stöcker, 1999). The model of Clark and Rose (1997) assumes that a fish randomly picks a movement direction (upstream or downstream) and then examines locations that are accessible considering barriers (due to high velocity or cascades), a minimum depth requirement, a maximum slope limit, and a maximum movement distance.

In our model, once the fish enters the culvert, it tries to get out the culvert by

going randomly in the forward direction. The fish simultaneously tries to minimize energy expenditure by seeking the low velocities. A series of trials were made and tested to optimally combine the random movement with the minimum energy expenditure of the fish. Finally, the following concept was chosen to fit best the observations:

1. The velocities in the nearby grid cells, namely upstream U_p, upstream left U_l, and upstream right U_r were compared with each other. The path with the lowest velocity takes higher probability P_1, while the middle velocity has the probability P_2 and the highest velocity takes probability P_3.
2. The values P_1, P_2 and P_3 are model parameters. They are selected in a way that the sum of them equals to 1.0; P_1 is greater than P_2 and P_2 is greater than P_3. These values are problem-dependent and must in general be adjusted to the flow domain and the fish the observed path during the model calibration.
3. A pseudo random value between 0 and 1.0 was calculated using Wichmann-Hill's random number generator (Wichmann and Hill, 1982).
4. If the random value falls between 0 .0 and P_1, the fish will go to the lowest point.
5. If the random value falls between P_1 and P_1+P_2, the middle velocity will be selected. Otherwise, the highest velocity will be selected (figure 4.3).

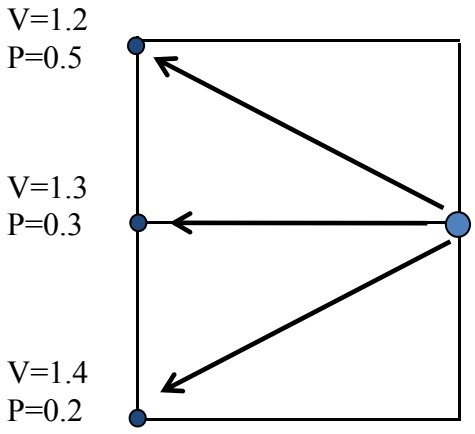

Figure 4.3: Minimum energy concept with Random movement.

4.1.2.3 Turbulence avoidance

While turbulence has been known to be characteristic of aquatic environments, only in the last 25 years, the ecological effects of turbulence on animal behavior have been recognized (Smith et al. 2005). Turbulence is an interdependent natural hydraulic phenomenon that is important to fish, and consequently it is important to develop an

understanding of how fish sense, react to, and perhaps utilize turbulence criteria in river flows. It is well known that fish sense and respond to shear stress and turbulence in natural water. Dijkgraaf (1963) mentioned that fish can sense variations in pressure and water velocity on the body surface, especially by means of their lateral line and inner ear. Olla and Davis (1990) found turbulence avoidance behavior in laboratory experiments with larvae of the Walleye Pollock. Further, Pavlov et al. (1994) found that increasing the turbulence intensity decreased the fish's critical velocity, i.e., the maximum velocity at which a fish can sustain itself in a stream. They concluded that energy expenditures will be greater for fish attempting to maintain position in streams with turbulent flows because such streams possess more kinetic energy. Mackenzie et al. (1994) showed that high levels of turbulence decreased the capture success as the prey moved out of the capture region quickly. On contrary, Nikora et al. (2003) found that turbulence effect on *Glaxias Maculatus* appeared to be not noticeable and he concluded that the interaction between fish movement and turbulence differs according to the turbulence energy and scales. Goulet et al. (2008) proposed a mechanism of both superficial (SNs) and canal (CNs) that sense perturbations in water surrounding them.

The shear stress in turbulent flow, known as Reynold's stress, can be written as:

$$\tau_{ij} = (\mu + \eta)\frac{\partial u_i}{\partial x_j} \tag{4.11}$$

where μ is the dynamic viscosity; η is the eddy viscosity, which accounts for the extra resistance conferred by eddy currents and u_i is the i-component of the average velocity. According to the available data of measured mean velocities, the velocity gradient $\partial u_j/\partial x_i$ was selected as a good indication to define the turbulence. The higher is the velocity gradient, the higher is the turbulence. The critical velocity gradient is the maximum velocity gradient where the fish can pass the flow without taking the effect of turbulence avoidance into account. This value can be adjusted during the model calibration.

The decision-making information related to high turbulence is represented as a sensory ovoid. The sensory ovoid was used before in the work of Railsback et al. (1999), Goodwin et al. (2006) and Nestler et al. (2002). Sensory Query Distances SQD_s characterize the range of the sensory ovoid from the fish centroid parallel SQD_x and perpendicular SQD_y to the flow direction. The detection range of the lateral line mechanosensory system and, therefore SQD_s is a function of fish length. Longer fish are able to detect hydrodynamic stimuli from greater distances (Denton and Gray, 1988; Kalmijn, 1989; Coombs, 1999; Goodwin et al., 2006). In the current study, SQD_x and SQD_y were calibrated within a range from 0.5 to 5.0 times the fish length.

Since the water depth is very small and there are no data available for the vertical distribution of the water velocity, the Sensory Query Distances in z direction will be set to zero (see figure 4.4).

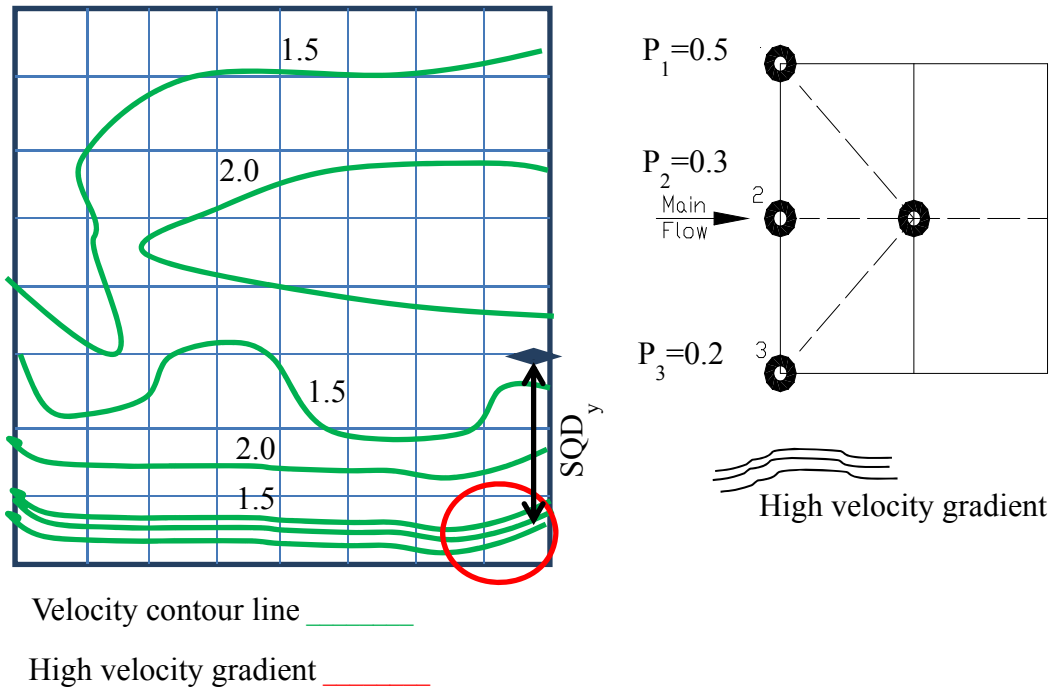

Figure 4.4: Effect of turbulence on fish movement.

When the velocity contour lines are perpendicular to the stream direction, the mean flow velocities in the surrounding cells of the fish location are equal (U_p=U_l=U_r). In this case, the presence of turbulence effect has a certain role in the selection of the fish path. In this model, it can be estimated as follows:

1. If no turbulence effect is included, the probabilities of the fish to swim upstream, upstream right or upstream left are equal (P_1=P_2=P_3=0.333).
2. When the fish passes a turbulence area, it will try to avoid high turbulence (sensory ovoid). In this case, the fish will select the path according to the lowest velocity gradient.
3. After some movements, the distance between the fish position and the detected turbulence place will be greater than SQDs. Although there is no turbulence flow any more in the domain surrounding the new location, the fish will still prefer to move in the same direction away from the turbulence zone.
4. After a certain time period, the fish will forget totally the turbulence effect and the swim probabilities will be defined as described in the case (1). This forget-time-period will be adjusted with a constant number of movements and can be defined during the model calibration.

Due to the random effect, an abrupt change in the fish movements can be seen in the simulation results. This change does not match the measured data. This increases the length of the fish path and accordingly, increases the amount of energy consumed. One of the most common filter methods is the moving average filter. As its name suggests, the moving average filter operates by averaging a number of points from the input to generate each point in the output signal. This procedure is repeated so that a moving window of M points is used to calculate the average of the data set. The algorithm takes the mathematical expression:

$$Y(i) = \frac{\sum_{K=i-(M-1)/2}^{K=i+(M-1)/2} Y(K)}{M} \tag{4.12}$$

Where: M is an odd number, changes according to the mesh resolution. It will be taken here as 5.0.

4.1.2.4 Energy expenditure through passage structure

The energy fish deliver, if they are to pass through passage structures, is a combination between the energy expenditure inside the structure and the energy expenditure at the entrance and the exit of the structure.

4.1.2.5 Energy expenditure through fish movement

A swimming fish experiences several different forces as it moves through flowing water, including the virtual mass force due to fish acceleration F_{VM}, the drag force F_D, the buoyancy force B, the gravity force G and the thrust force F_T. Assuming that the streamlines are straight, parallel, and horizontal, and the fish is swimming at a constant speed, then the forces acting on the swimming Cutthroat in this study, as suggested by Behlke (1991) and Blank (2008), will be the drag force F_D and the thrust force F_T

The drag force F_D refers to forces which act on a solid object in the direction of the relative fluid flow velocity. Unlike other resistive forces such as dry friction, which is nearly independent of velocity, drag forces depend on velocity. The fluid drag on a given object is characterized by presentation of a plot of drag coefficient (C_D) versus a representative Reynolds number (Re). In this case, a support holds the body in a rigid state is used in measuring the drag force. The profile drag on fish cannot be measured by the same methods as those outlined above for bodies which rely on an outside source for support in the moving fluid (Behlke, 1991). Biologists attempted to define

the profile drag for on fish analytically (Webb, 1971; Webb, 1975; Blake, 1983). They adopted the following drag force equation as their standard

$$F_D = 0.5\rho C_d V_f^2 S \tag{4.13}$$

where C_d is a profile drag coefficient in the usual engineering sense, ρ is the mass density of water, S is the surface area of the fish, and V_f is its swimming velocity with respect to the surrounding water. The drag coefficient is composed of a frictional component C_f and a pressure component C_p and can be represented as a function of the Reynolds number as follows:

$$C_d = C_p + C_f = 1.2C_f = 1.2\left(0.074\,\mathrm{Re}^{-0.2}\right) = 0.0888\left(\frac{\nu}{V_f L_f}\right)^{0.2} \tag{4.14}$$

where ν is the kinematic viscosity of water, L_f is the length of the fish. The surface area of a fish can be expressed as $S = \alpha_f (L_f)^{\beta f}$, where α_f is equal to 0.465; β_f is equal to 2.11 for this study (Khan, 2006). Combining equations 3 and 4 the thrust force can be calculated as:

$$F_T = F_D = 0.020646\rho\nu^{0.2} V_f^{1.8} L_f^{1.91} \tag{4.15}$$

The power P_f that a fish will expend to overcome the drag force is a product of the drag force and the velocity of the fish V_f.

$$P_f = F_D V_f \tag{4.16}$$

Finally, the energy expended by a cutthroat to pass through the culvert can be expressed as follows:

$$E_f = \sum_{i=1}^{n} P_f t_i \tag{4.17}$$

The time it takes for a fish to swim an increment (i) of the path length is estimated using the following equation:

$$t_i = \Delta t = \frac{\Delta x}{V_f + V_w} \tag{4.18}$$

where Δx is the increment of the path length; V_w is the velocity of water parallel to the fish swimming direction.

4.1.2.6 Energy expenditure culvert downstream entrance

The ability of fish to enter the culvert from the downstream depends mainly on the outfall drop, the fish swimming performance, the hydraulic conditions in the downstream pool depth and the characteristics of the plunge plume (Pearson et al., 2005). If the difference in height is more than a specific value, the fish is forced to jump out of the water to pass the obstacle. Several researchers observed that fish will swim up rather than leap at very low falls (Orsborn and Aaserude 1985, Mayama 1987, Stuart 1962). FishXing (2006) assumes that the fish is able to swim rather than jump if any of the following conditions are satisfied (figure 4.5):

- Tail water Elevation > Outlet Bottom Elevation,
- ½ Fish Length > Outlet Drop, or
- Fish Length > Hypotenuse formed by the plunge height and distance.

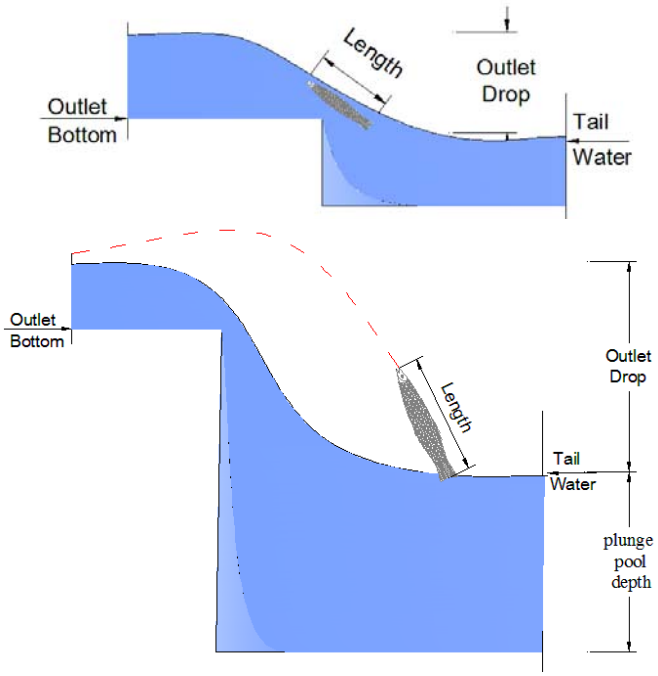

Figure 4.5: The ability of fish to enter the culvert from the downstream (swim or jump).

Stuart (1962) was the first to study the fish leaping ability. Based on a series of laboratory flume tests and field observations, he investigated the leaping behavior of juvenile salmon and trout and found that most of the fish were observed leaping from the water surface. He added that, the plunge pool depth should be 1.25 the outfall drop in order to establish the hydraulic conditions for leaping. In a study of the behavior of adult sockeye salmon, Lauritzen (2002) observed that most adult salmon initiated their leap from depth, bursting to the surface at high speed. Mayama (1987) noticed the same behavior in his study of Juvenile Salmonids.

Neglecting air resistance, Powers and Orshorn (1985) described the motion of the leaping fish in waterfall as curved two-dimensional motion with constant acceleration

$$X=(V_o \cos\theta)t \tag{4.19}$$

$$Y=(V_o \sin\theta)t-(1/2)gt^2 \tag{4.20}$$

Where X = Vertical leap distance, Y = Horizontal leap distance, V_0 = initial leap velocity, θ = Leaping angle, g = Gravitational acceleration and t = Time. According to Stuart (1962) and Guiny (2001), the leaping angle is typically between 60˚-70˚. This value increased to 75˚ in case of standing wave. The initial leaping velocity will be taken, according to Lauritzen (2002) and Mayama (1987), as the burst speed.

The total energy consumed by the fish during jumping combined of the energy consumed to overcome the weight in air in addition to the takeoff and landing. Unfortunately, no data is available related to the takeoff and landing energy. Guiny (2001) calculated the leaping energy ($E_{leaping}$) based on its weight (W), the height it was to jump (Δh) and the leaping angle as:

$$E_{Leaping} = W \frac{\Delta h}{sin^2\theta} \tag{4.21}$$

In case of the present of standing wave downstream of the waterfall or the weir, Guiny (2001) suggested to decrease the leaping energy to:

$$E_{Leaping} = W \frac{\Delta h}{sin^2\theta} (1 - \sqrt{0.024})^2 \tag{4.22}$$

In a study of Brook Trout, Kondratieff and Myrick (2006) identified the probability of successfully leaping over an obstacle as a function of waterfall height (H_1), pool depth (H_2), total fish length (TL), condition (C), and trial duration (D) as well as the second-order interactions between the variables. Blank (2008) mentioned several reasons for the fish to fail leap into the structure. First of all, the fish may start jumping from a position away from the structure; secondly, they may jump to a direction that did not take them toward the culvert entrance; and thirdly, they may not jump high enough to clear the downstream invert of the structure. The fish may do several trial before successfully leap to the structure. This may increase the fish energy consumption and affect the ability of the fish to pass the fish passage. The number of trials, the fish will do before succeed to jump into the culvert; can be calculated according to a primary study to the site or by the equation given by Kondratieff and Myrick (2006).

4.1.2.7 Actual fish energy

The total anaerobic energy expenditure (AEE) in the white muscle of fish from each exercise treatment group can be expressed according to the following equation (McFarlane and McDonald 1998; Pearson et al. 1990):

$$AEE = 1.5\Delta lactate + \Delta ATP + \Delta PCr \tag{4.23}$$

where Δ represents the difference between control and exercise values, ATP is

adenosine triphosphate, and PCr is phosphocreatine.

Norton et al. (2000) suggested that for both sustained swimming, powered by red muscle and burst swimming, powered by white muscle; it seems likely that the red muscles of small fishes, like white muscles, have faster contraction and relaxation times. Which mean that the red muscle of small fishes may contribute power to support burst swimming, enabling these vulnerable fishes to use more of their total muscle mass (red and white) for high-speed locomotion at a stage in their life history when predation pressure is likely to be high. In this study, no attempt will be done to provide a detailed physiological model. Rather, I assume that a fish is capable of swimming for period of time during which burst mode swimming can be performed. Beyond this time, the concentration of lactic acid in white muscle fibers allows swimming by red fibers only (sustained swimming). Haefner and Bowen (2002) model the fish energy with a random initial energy determined by assuming a uniform random distribution with mean of fatigue time. Following the same technique, I assume that the initial fish energy can be calculated using the energy expenditure method using Burst speed and fatigue time. Hoar and Randall (1978) suggested the burst speed fatigue time range is up to 15 seconds. Due to the lack of data related to Cutthroat fatigue time in burst speed, rainbows can be suggested as a possible surrogate species for cutthroat trout (Blank, 2008). Several researches gave fatigue time for Rainbow to in a range from 1-20 seconds (Bainbridge, 1960; Beamish, 1978). For the current work, the fatigue time will assumed to vary randomly between t_{min} and t_{max} seconds where t_{min} and t_{max} are the minimum and maximum fatigue times. They can be adjusted during the model calibration. Based on the burst speed and fatigue time, the actual fish energy can be simply calculated using equations 4.15, 4.16 and 4.17 to be:

$$E_f = 0.020646\rho v^{0.2} V_f^{2.8} L_f^{1.91}\left[t_{\min} + (t_{\max} - t_{\min})rand\right] \tag{4.24}$$

where rand represent a uniform random value.

4.1.2.8 Depth barrier

During the low flow condition, the culvert shallow water depth may work as a barrier for fish movement if the water could not fully submerge the fish species. The fish submergence prevents the fish oxygen starvation and decrease the risk of injury through contact with the culvert bottom (Forest Practices Advisory Committee on Salmon in Watersheds, 2001). The water depth should be greater than the fish body thickness plus additional depth. The additional depth takes into account the variation in

individual fish size and the change in bed level due to sediment deposit or debris (Powers and Orsborn, 1985; Webb, 1975; Fishxing, 2006). ADF&G and ADOT&PF (2001) recommended the water depth to be 2.5 the depth of a fish's caudal fin while Maine Department of Transportation (2004) suggested the water depth to be either 1.5 x the body thickness or the documented depth during the known fish movement. Everest et al. (1985) documented the minimum depth requirement for a variety of salmonid and trout species from the Pacific Northwest.

4.1.2.9 New method for culvert barrierity

Determining the fish barrierity of a culvert is not trivial and the classification of barrierity from different methods are not congruent (Blank, 2008). This emphasizes the need of a good method to determine culvert barrierity. In this part, a new method for culvert barrierity will be described as follows:

1. The actual fish energy is calculated based on the fish fatigue time and the burst speed. The fish fatigue time is assumed as a random value varies according to the fish exhaustion.
2. The culvert leaping barrierity is determined according to the minimum pool height and the maximum vertical leap distance.
3. The culvert will be considered as fish leap energy barrier if the actual fish energy is less than the required leaping energy.
4. The culvert depth barrierity will be considered if the water depth at any part of the culvert is less than the minimum depth suitable for fish swimming. Additionally, the culvert velocity barrierity is considered when the minimum velocity at any cross-section is more than the burst speed.
5. The remaining fish energy is calculated at each time step and if this energy is less than zero. The culvert will be considered as culvert energy barrier.

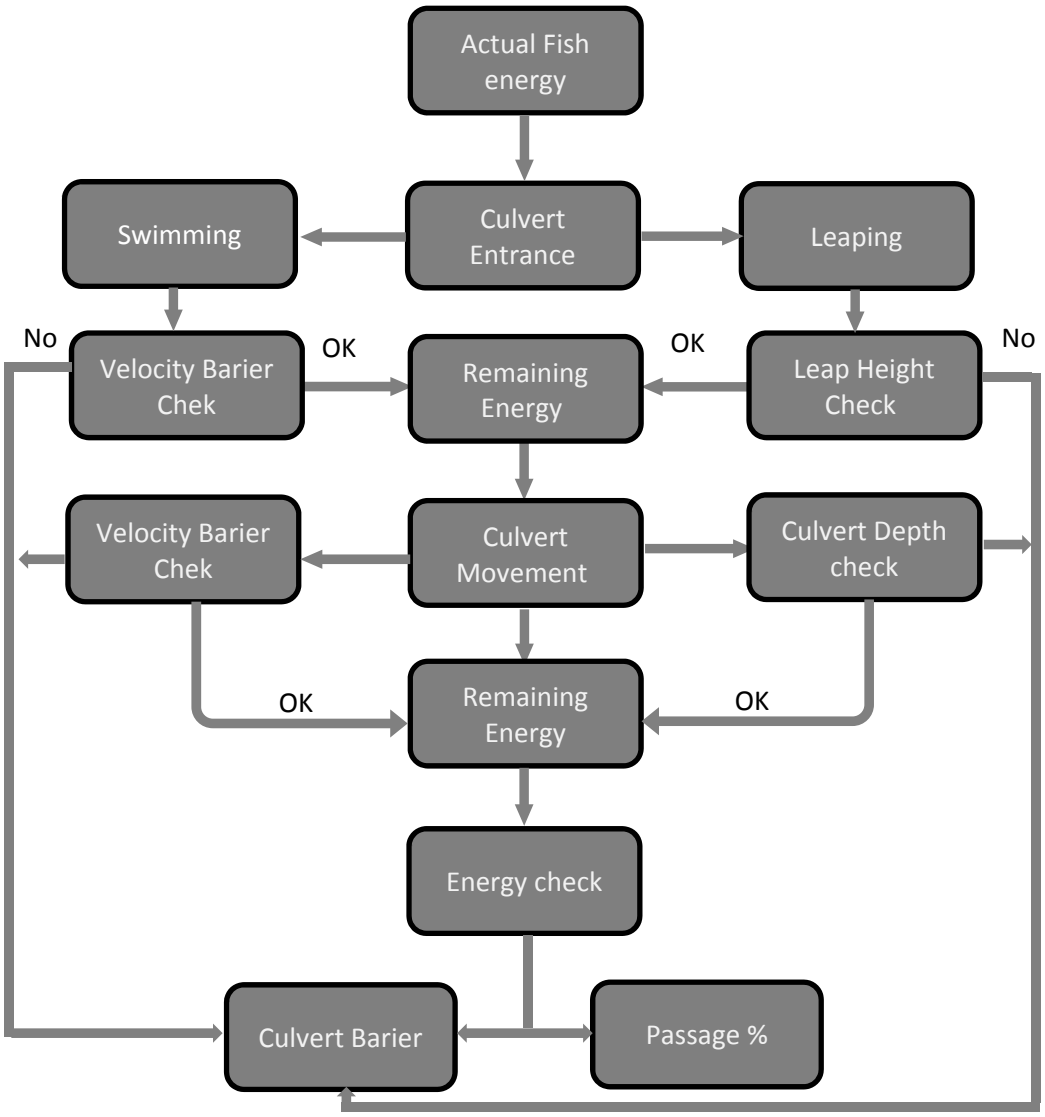

Figure 4.6: A diagram for culvert barrier method.

4.1.3 Model for fish movement in the flow conditions with variable directions

In the previous part I introduced a model based on the concept of energy expenditure with random movements and turbulence effects to simulate the fish upstream movement inside the culvert, where the direction of main flow was almost uniform. This technique is not valid for the case, when the flow direction changes point by point e.g. in a pool-and-weir fishway. In this case, based on high water flow the fish recognizes the direction of the fishway (figure 4.7). At the same time, the fish tries to minimize the energy expenditure by travelling against the lower velocities. Powers et al. (1985) suggested that the fishway entrance should site as close as possible to the source of the competing flow from the turbine. Another strategy suggested by Castro-Santos and Haro (2008) is to supplement the flow at the fishway entrance. This increases the ratio of flow at the fishway entrance to turbine flow without increasing the total flow passed through fishway itself.

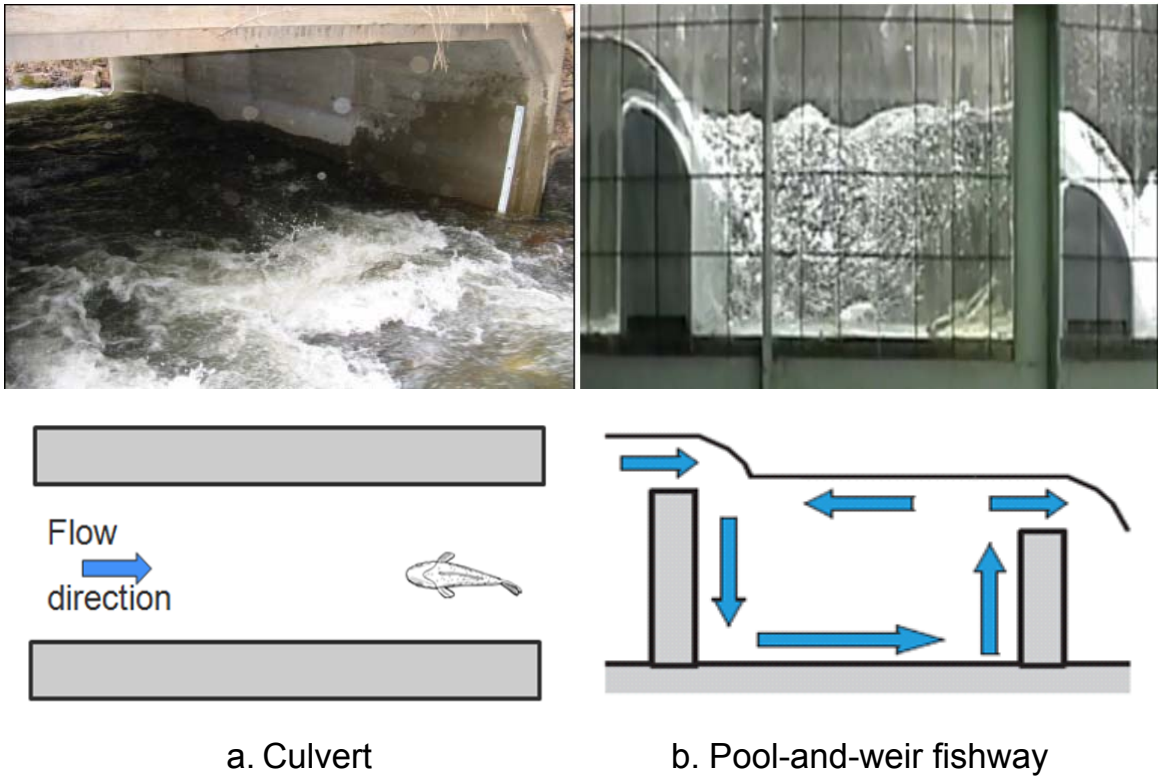

Figure 4.7: Flow pattern in a culvert and in a pool-and-weir fishway.

Combining this idea with the previous model, the following modification to the previous model can be suggested. Figure 4.8 shows the flowchart of the proposed model. According to this flowchart, the main steps of the model can be summarized as follow:

1. To start the model, the data related to the culvert geometry, the measured or simulated velocity and the coordinates of the fish at the entrance of the culvert are required.
2. Based on these data, the model checks whether there is an opening within a distance around the fish in the upstream direction or not.
3. In case of the presence of the opening, the fish will go directly toward the opening.
4. Otherwise, the model checks the maximum velocity within a distance around the fish in the upstream direction.
5. If the maximum velocity around the fish is less than a special value which can be determined during model calibrations (e.g. a half of the fish length/s), the fish could not recognize the flow direction and the random movement will be selected.
6. On the other hand, if the velocity is high enough for the fish to recognize the upstream direction, the fish will go in a direction against the direction of the high flow.
7. In this case, the direction conversion will be done to allow the low energy and

turbulent model to be applied.

8. The steps mentioned above are repeated until the fish reaches to the most upstream part of the culvert.
9. Finally the path is smoothed using the moving average filter method.
10. The energy expenditures are calculated from the smoothed simulated path.

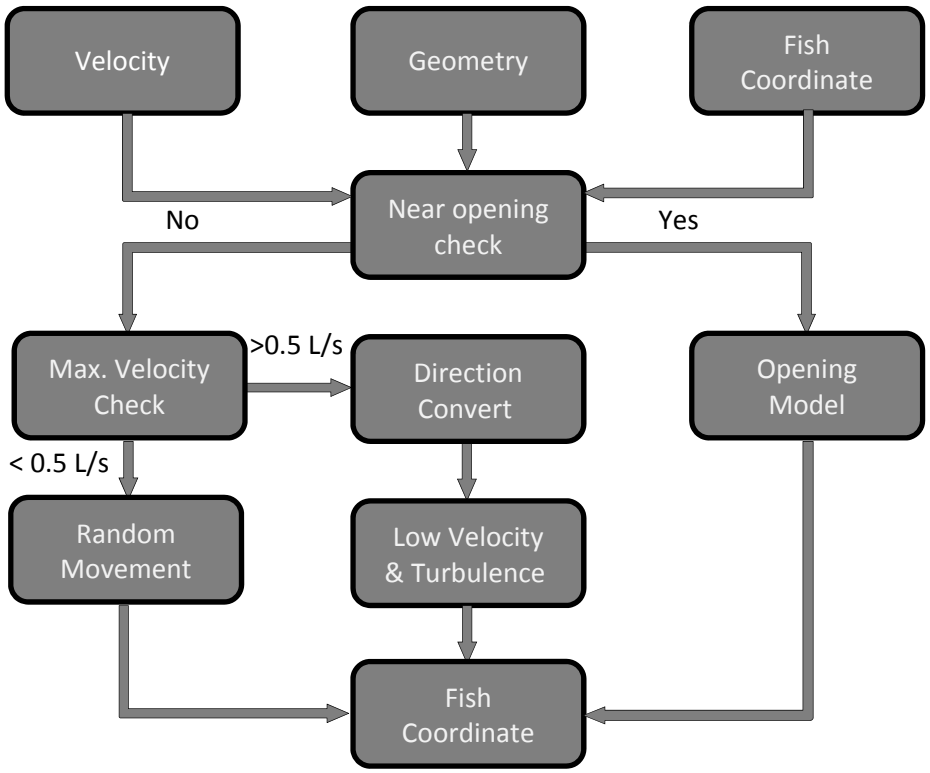

Figure 4.8: The structure of the proposed two dimensions fish model.

4.1.3.1 Near opening check

The decision-making information related to the near opening check is represented also as a sensory ovoid. The fish searches if there is an opening within a specified distance SQDx and SQDy in X and Y directions. In this case, the near opening model will be applied (see figure 4.9). In this model, the fish directs itself toward the opening unless the water velocity is higher than the fish burst speed. Once the fish reach the opening, it tries to swim upstream through the opening.

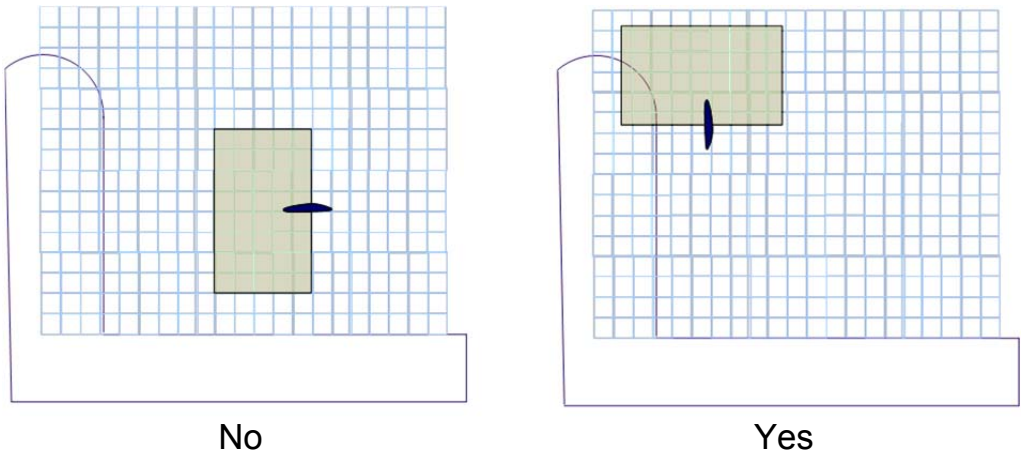

Figure 4.9: Near opening check.

4.1.3.2 Velocity check

As mentioned above, the flow pattern around the fish in a Pool-and-Weir fishway is not uniform and the upstream direction is changeable. The fish examines the velocity within a distance SQDx and SQDy in all direction except the downstream part in order to find its way. If the maximum velocity magnitude around the fish is less than a specific value which can be determine during the model calibration, the model assumes that the fish will not be able to recognize the flow direction. Hence, the random model will be applied and the fish will go randomly in one of its surrounding 8 points. The area will be considered as a rest zone and the fish velocity will convert to sustained velocity (half fish length/ sec). In a study by Pearson et al. (2006), it was found that, fish at a discharge of 1.5 ft^3/s exhibited more exploratory behavior than those at higher flows. The study suggested that for larger juvenile coho, consistent of upstream movement required flow higher than 1.5 ft^3/s.

On the other hand, in case that the maximum velocity is higher than this specific value, the fish will find the upstream direction by following the Maximum velocity direction. At this velocity, the angle of flow can be determined using the horizontal and vertical component of this velocity. Based on the flow direction, the fish will select the direction of the next movement. Four cases can happen as indicated in figure 4.10:

1. If the angle is signed between -45^0 to 45^0, the fish will move horizontally in the direction of –X.
2. If the angle is signed between 45^0 to 135^0, the fish will move vertically in the direction of –Y.
3. If the angle is signed between 135^0 to 225^0, the fish will move horizontally in the

direction of X.

4. If the angle is signed between 225^0 to 315^0, the fish will move vertically in the direction of Y.

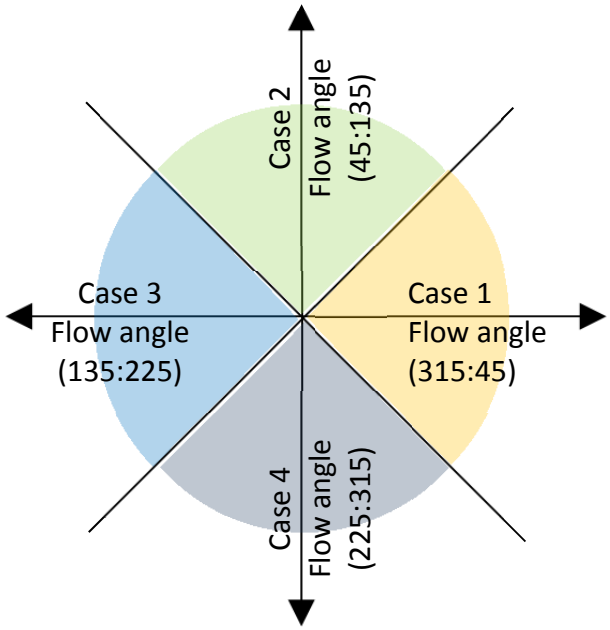

Figure 4.10: Maximum velocity direction.

Based on the direction of the maximum velocity around the fish, the fish determine the domain where they can move against this direction. This Domain can be determined by the area where the difference in angle between the direction of the maximum velocity around the fish and the velocity at each point is less than a specific value which can be determined during model calibration (see figure 4.11).

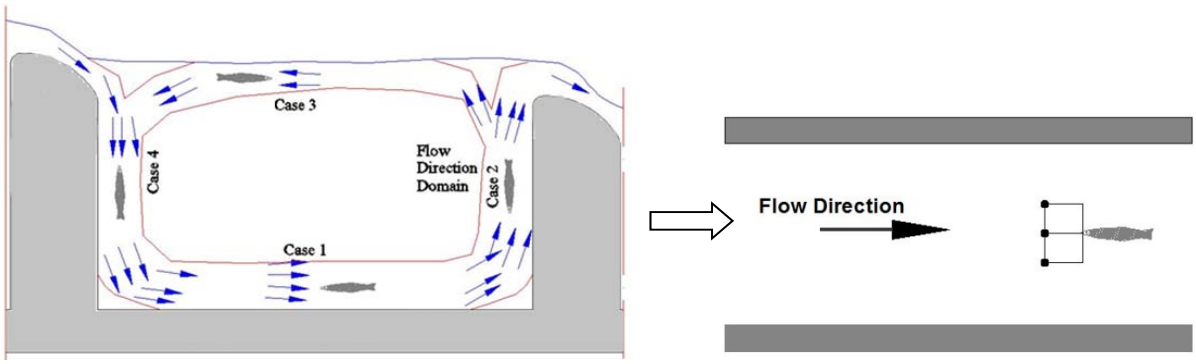

Figure 4.11: Flow direction domain and conversion to the low energy and turbulent model.

Within this domain, the fish tries to minimize its energy by following the low energy concept with random movement and turbulence avoidance model which was described in 4.1.2. Before applying this model, A coordinate conversion should be applied first in order to convert the current model coordinates to local coordinate with

flow direction in +ve X and the fish move against the flow (see figure 4.12). The data related to the fish current position, the velocity component in X and Y directions, and the flow angle should be converted to the local coordinate.

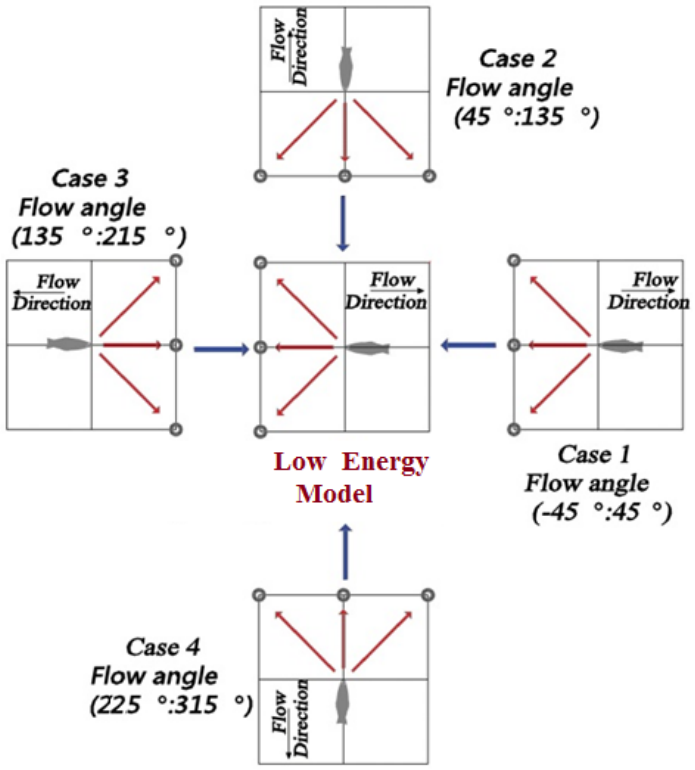

Figure 4.12: Coordinate conversion from the current coordinate to the local coordinate suitable to the low energy model described in 4.1.2.

Table 4.1: Model conversion roles From the current coordinate to the local coordinate suitable to the low energy model described in 4.1.2

Case	Conversion roles
Case1 **Flow angle (315:45)**	$Max\_i_L = Max\_i_G$, $Max\_j_L = Max\_k_G$, $i_L = i_G$, $j_L = k_G$, $X_L(i_L) = X_G(i_G)$, $Y_L(j_L) = Z_G(k_G)$, $V_L(i_L,j_L) = V_G(i_G,k_G)$, $dif\_V\_angel_L(i_L,j_L) = dif\_V\_angel_G(i_G,k_G)$, $xfish_L = xfish_G$, $yfish_L = zfish_G$
Case2 **Flow angle (45:135)**	$Max\_i_L = Max\_k_G$, $Max\_j_L = Max\_i_G$, $i_L = k_G$, $j_L = i_G$, $X_L(i_L) = Z_G(k_G)$, $Y_L(j_L) = X_G(i_G)$, $V_L(i_L,j_L) = V_G(i_G,k_G)$, $dif\_V\_angel_L(i_L,j_L) = dif\_V\_angel_G(i_G,k_G)$, $xfish_L = zfish_G$, $yfish_L = xfish_G$
Case3 **Flow angle (135:225)**	$Max\_i_L = Max\_i_G$, $Max\_j_L = Max\_k_G$, $i_L = Max\_i_G - i_G + 1$, $j_L = k_G$, $X_L(i_L) = x_G(i_G)$, $Y_L(j_L) = Z_G(k_G)$, $V_L(i_L,j_L) = V_G(i_G,k_G)$, $dif\_V\_angel_L(i_L,j_L) = dif\_V\_angel_G(i_G,k_G)$, $xfish_L = xfish_G$, $yfish_L = zfish_G$
Case4 **Flow angle (225:315)**	$Max\_i_L = Max\_k_G$, $Max\_j_L = Max\_i_G$, $i_L = Max\_k_G - k_G + 1$, $j_L = i_G$, $X_L(i_L) = Z_G(k_G)$, $Y_L(j_L) = X_G(i_G)$, $V_L(i_L,j_L) = V_G(i_G,k_G)$, $dif\_V\_angel_L(i_L,j_L) = dif\_V\_angel_G(i_G,k_G)$, $xfish_L = zfish_G$, $yfish_L = xfish_G$
*where:	i, j, k are the point id in X, Y,Z directions; Max_i, Max_j, Max_k is the total number of point in X and y directions; V is the velocity magnitude; dif_V_angel is the difference in angle between the direction of the maximum velocity around the fish and the velocity at each point; xfish, yfish, zfish are the fish position in x, y and z directions; subscribts L and G are the indications for the local and glopal coordinates.

4.1.4 Model conversion to 3D

The model described in 4.1.3 is valid for the situations where the fish moves in 2D and the movement in the transverse direction is neglected. The model can be applied to vertical or horizontal flow and The level which includes the main flow direction in 3D cases is determined by calculating the average velocity gradient in X, Y and Z directions (du/dx, dv/dy and dw/dz). The model starts with the two directions which include the highest two values of the average velocity gradient. if the velocity gradient in the third direction cannot be neglected, then the model will run in two steps. The first step is to calculate the fish movement in the main level and in the next step the fish will follow the direction of the maximum flow in a domain around it in the third direction. On the same time within the domain of the maximum flow direction the fish try to minimize the energy expenditure by going through the lowest velocity within this domain.

4.1.5 Model uncertainty

One of the most difficult problems in IBMs is the too many parameters included in this model. These parameters are uncertain or even completely unknown. Additionally the complexity of IBMs leads to error propagation. Although calibration of these models decreases the uncertainty, the lack of field and experimental data limits the progress of these models and increases the model uncertainty. In the next chapter, the model will be validated and applied to three case studies. The values of all parameters will be calculated during the calibration of the model.

4.2 Summary

In this chapter, a new method for culvert design was suggested. The method compare between the actual fish energy and the energy consumed inside the culvert. In this method, the fish movement depends on a low energy concept and random movements. The effects of turbulence and fish memory were also taken into account.

This technique is not valid for the case, when the flow direction changes point by point e.g. in a pool-and-weir fishway. Hence the model was modified and adopted to solve this situation. In this case, based on high water flow the fish recognizes the direction of the fishway (figure 4.7). At the same time, the fish tries to minimize the energy expenditure by travelling against the lower velocities.

5. Case study

Three case studies are presented which cover two different types of fish passage. They are presented to demonstrate the two proposed models described in chapter 4. The first case study includes field data for hydraulic conditions and fish movement inside a culvert in a Mulherin Creek tributary of the Yellowstone River near Gardiner, Montana, USA presented by Blank (2008). The last two cases present two examples of pool-and-weir fishway experiments in Japan. The second case study is a single pool-and-weir fishway from a previous study by Hayashida, et al. (2001). While the third case study presents an application to multiple pool-and-weir fishway by Atsushi (2009). Since all of the data are obtained for 2D areas, in this study I assume flows are two dimensional.

Each study is presented in the form of a short problem description, the completed data summary, model setup, calibration and applications. A summary of the unit is provided at the end of the case studies.

5.1 Case 1: Numerical simulation of energy expenditure of Yellowstone cutthroat trout migrating upstream through a culvert

5.1.1 Problem description

The ability of cutthroat trout and other salmon fish to pass a culvert is a function of its anaerobic energy. The fish anaerobic energy should be enough to allow the fish to jump inside the culvert, swim against flow in the upstream direction through the culvert and exit the culvert as seen in figure 1. Several factors affect each of these steps. The ability of a fish to jump inside the culvert from the downstream part depends on the pool water depth, the jumping height and the fish size. On the other hand, water depth, water velocity, water temperature, turbulence, the length of the culvert, the availability of resting areas, culvert slope and length in addition to the fish sex and species are the main factors influence the fish movement inside the culvert. Excessive sediment can deposit on the upstream end of the culvert resulting in high water velocities which can prevent fish from moving upstream. The main interest of this part will be the fish movement inside the culvert. This study is a trial to understand the relationship between the fish movement and the hydraulic condition inside the culvert.

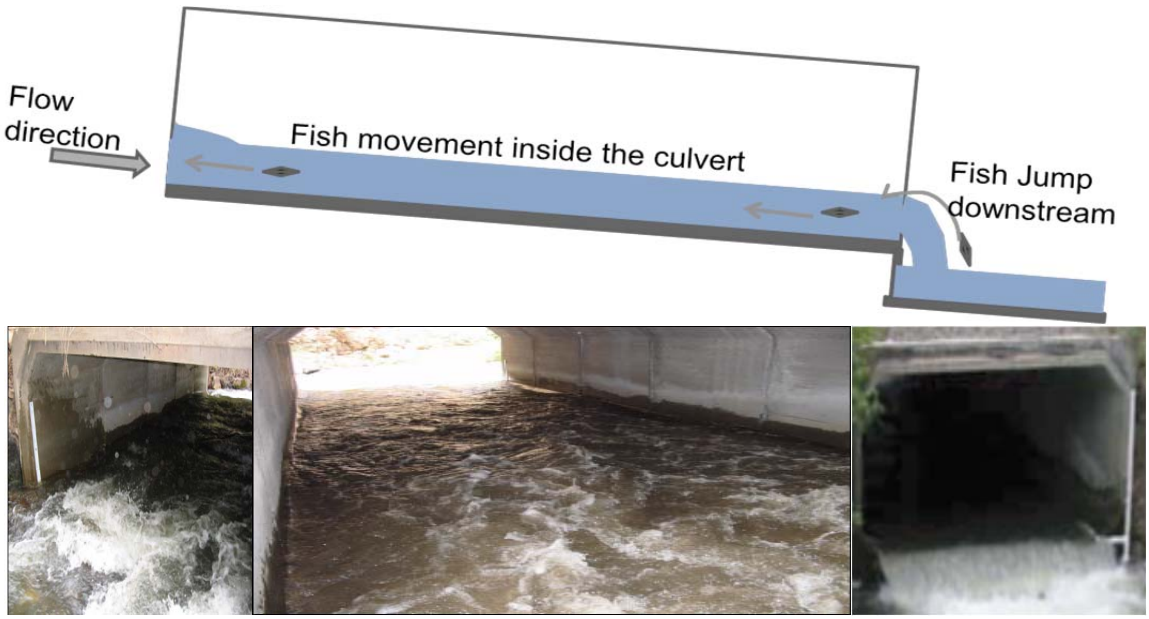

Figure 5.1: Fish upstream passage through the culvert (photos taken from Blank et al., 2006 and Blank, 2008).

5.1.2 Data summary

The field data were collected at Mulherin Creek, a tributary to the Yellowstone River with the confluence near Gardiner, Montana, USA during the summer of 2004. This tributary is characterized by the high gradient stream with an average of 11.6 % from the headwater to the mouth and 2.0 to 5.0 % in the study area. The stream has a variety of flow ranging from base flow around 0.28 m^3/s to a measured flow 3.1 m^3/s recorded on June 6, 2004 (Blank et al., 2006 and Blank, 2008). The studied culvert was a concrete box culvert with chamfered corners. The culvert had a slope of 1.1 %, length of 11.13 m, width of 3.6 m and an outlet drop that is 0.49 m on the average during the course of the study (figure 5.2). The study focused on Yellowstone cutthroat trout as a native species (Cahoon et al., 2007; Blank et al., 2006 and Blank, 2008). A short description of this study can be found in Appendix 1.

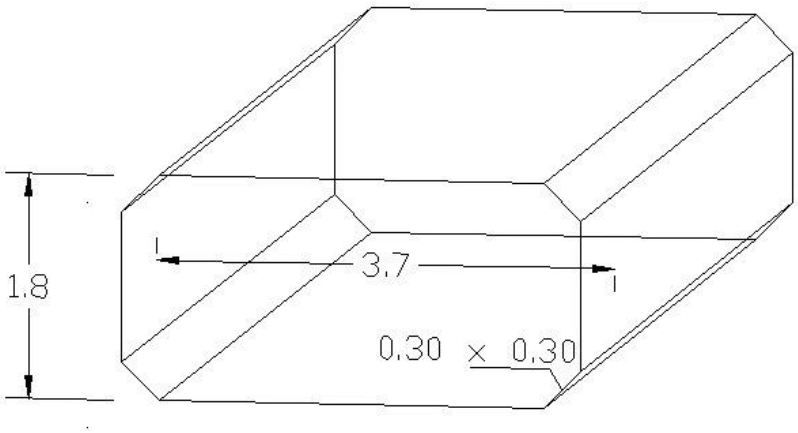

Figure 5.2: Overview of study culvert dimension.

5.1.3 Model setup

From the data of Blank (2008), a 2D grid (5 cm × 5 cm) was constructed and the measured velocity contour lines at 0.06 m height from the bed were used to interpolate the velocity at the grid intersections using The Surface-water Modeling System (SMS version 10.0). The following model parameters need to be adjusted according to the fish type, weight, and length:

- Probability values P1, P2 and P3 for random movement,
- Maximum critical velocity gradient,
- SQDx and SQDy,
- Number of movements before the fish forgets the presence of turbulence.

5.1.4 Model calibration

To calibrate these parameters, the data of culvert velocity contours of July 1, 2004 was selected. After analyzing the calculated results with different value sets of the swimming probability P_1, P_2 and P_3 a value set of (0.5; 0.3; 0.2) gives generally good agreement between calculations and observations. Figure 5.3 shows the simulated fish path without including turbulence effect. In the figure, the contours with numbers give the measured mean velocities in m/s. A good agreement between the model and the measured fish paths can be seen in the case of the combination of random movement effects with the minimum energy concept. A normalized error (NE) of 1.925 % and 2.420 % are calculated for the fish which started from points 6 and 8 as respectively.

In the domain with large mean velocities, there is a high velocity gradient and

therefore higher turbulence, so the simulated fish paths do not match the observed paths (fish starts from point 2, s. Fig. 5.3). It can be seen that the fish does not follow the minimum velocity direction and pass through the high velocity contour in order to escape from the turbulent zone.

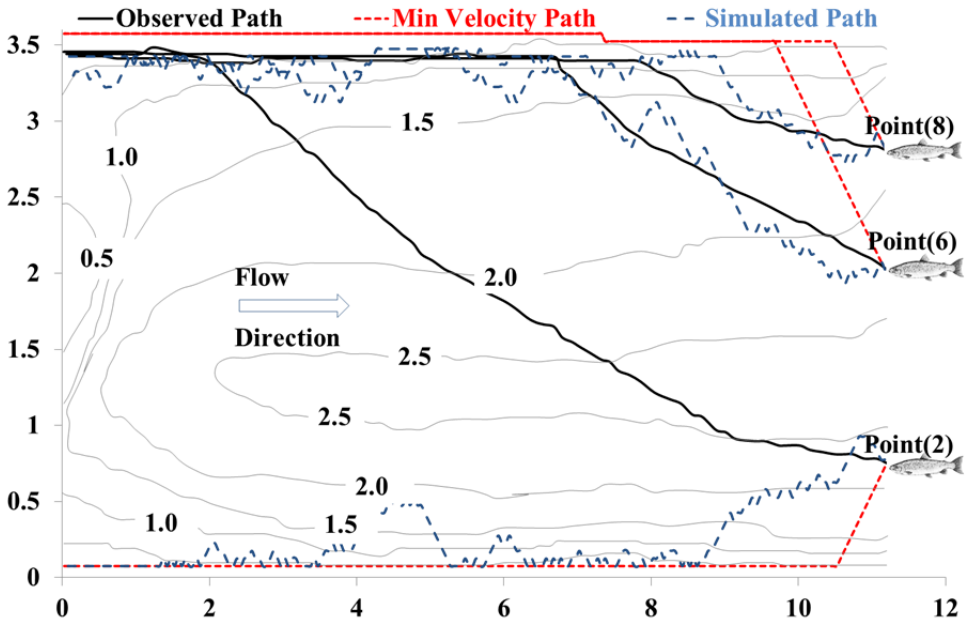

Figure 5.3: Simulated paths without turbulence effect superimposed on 1st July 2004 ($Q = 1.47\ m^3/s$; observed data from Blank, 2008).

Figure 5.4 shows the simulated fish paths including turbulence effects. For all cases, the model shows a better agreement between the modeled and the measured fish paths especially after adding the turbulence memory effects on fish path simulation. Several trials were made to adjust the sensory distance and memory distance. In this case, the normalized error NE for the fish which started from point 2 decreased from more than 50.0 % to 18.0 %

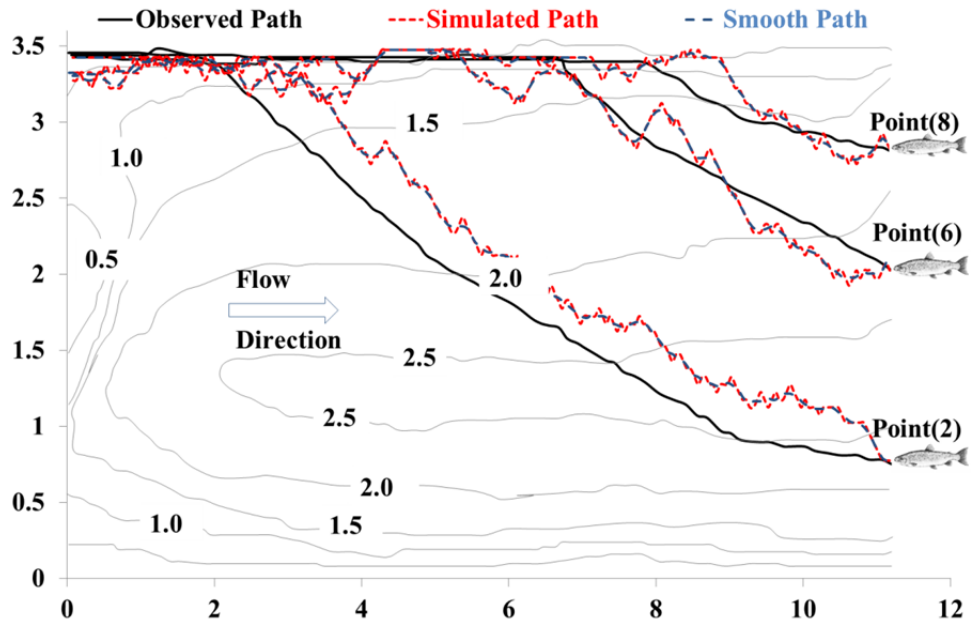

Figure 5.4: Simulated paths with turbulence effect superimposed on 1st July 2004 (Q = 1.47 m^3/s; observed data from Blank, 2008).

Further sensitivity analysis has been done to define the model parameters in this studied case. Table 5.1 summarizes the calibrated values for the model, which will be used for future predictions.

Table 5.1: Model parameters and calibrated values

Probability	**P_1**	**P_2**	**P_3**
No turbulence effect	0.50	0.30	0.20
Turbulence effect	0.50	0.30	0.20
Equal velocity no turbulence	0.33	0.33	0.33
Equal velocity after a turbulent zone	0.50	0.30	0.20
Other parameters:			
Maximum critical velocity gradient (m/s/m)		5.00	
Sensory Query Distances in x direction (m)		0.10 (0.3 L_f)	
Sensory Query Distances in y direction (m)		0.75 (2.26 L_f)	
Number of movements before memory loss		17	

*where: L_f is the fish length.

The simulated fish path could suffer an abrupt change in the fish movements due to random effects. This increases the total distance the fish should travel compared to the measured distance. Smoothness of the simulated fish paths using equation 4.12 may enhance the results and decreases this difference. Another method which could be applied is to run the model for a number of times (here I run it for 100 times) and take

the average path. This method is suitable for the cases when the fish has one direction to go like in culvert. In this case, the fish always move against the flow direction in the direction of –ve X and select one of the three points namely upstream, upstream left, and upstream right. It can be concluded that only the values of y for the same movement in all runs is changed. Taking the average of these values for each movement could remove the abrupt change in the fish movements due to random effect especially when the model uses high number of trials. Figure 5.5 shows the results for the smoothed paths in addition to the average path of the simulation of 100 fish.

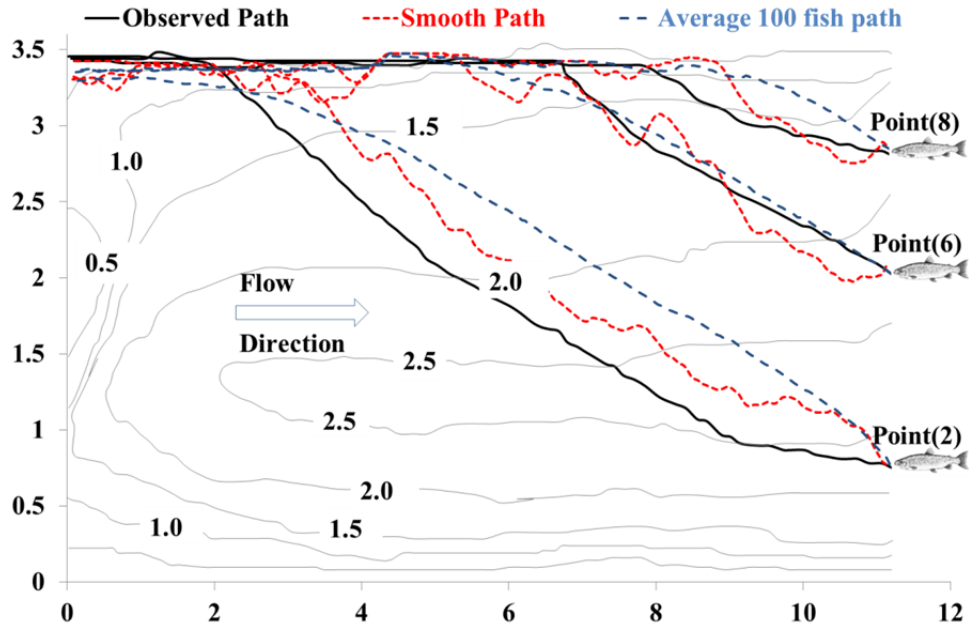

Figure 5.5: Comparison between Smoothed and 100 fish average path for fish paths superimposed on 24th June 2004 (Q = 1.55 m^3/s; observed data from Blank, 2008).

The model was applied to different efflux discharges through the culvert, on 24 June, 2004, with Q = 1.55 m^3/s (figure 5.6) and on 13 July, 2004, with Q = 1.44 m^3/s (figure 5.7). Although the fish start points in figures 5.6 and 5.7 are the same, the presence of the turbulence in figure 5.7 affected the fish path. It can be seen from the two figures that for all the cases with different flow characteristics the predicted results show a good agreement with the observations. The normalized error NE % values are always less than 2.5 % for the cases where the effect of turbulence is not appearing and 10-20 % in the cases with turbulence. Accordingly, the fish consumes more energy. Figure 5.8 shows the difference between the simulated and the measured distance for all the simulated fish.

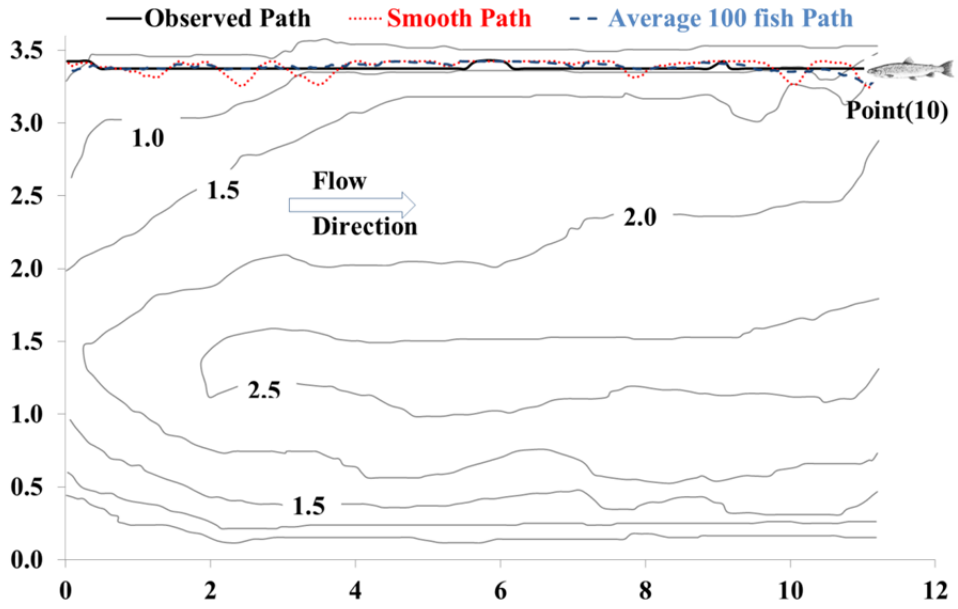

Figure 5.6: Fish paths superimposed on 24th June 2004 (Q = 1.55 m^3/s; observed data from Blank, 2008).

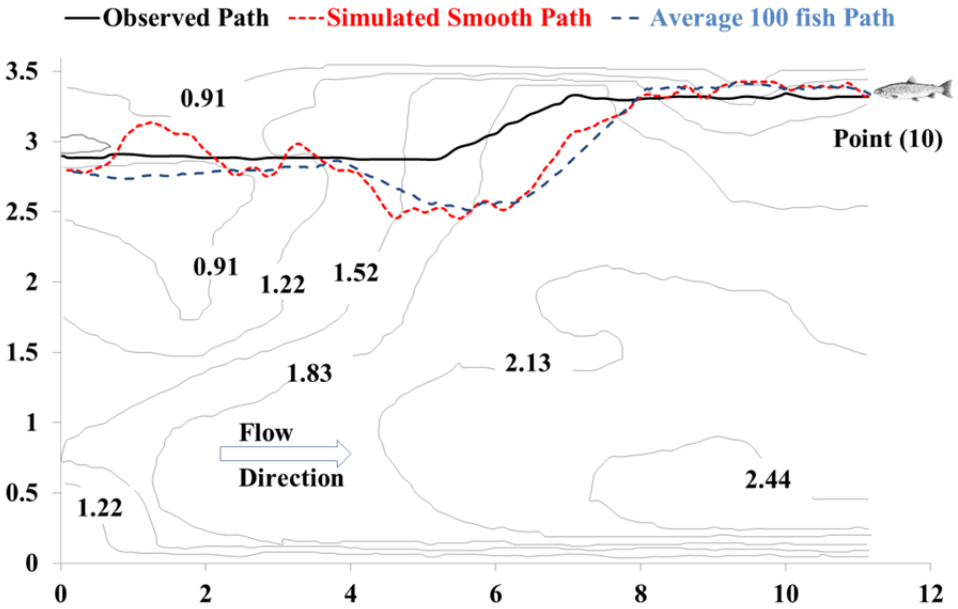

Figure 5.7: Fish paths superimposed on 13th July 2004 (Q = 1.44 m^3/s; observed data from Blank, 2008).

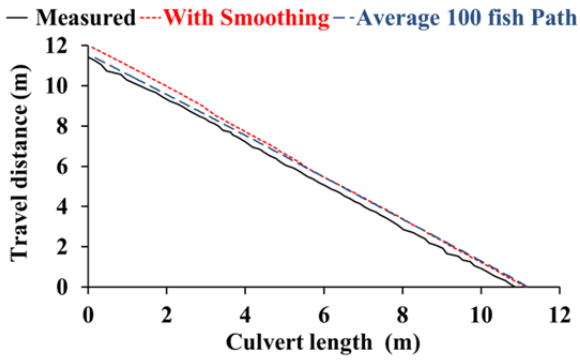

1st of July 2004 from point (2)

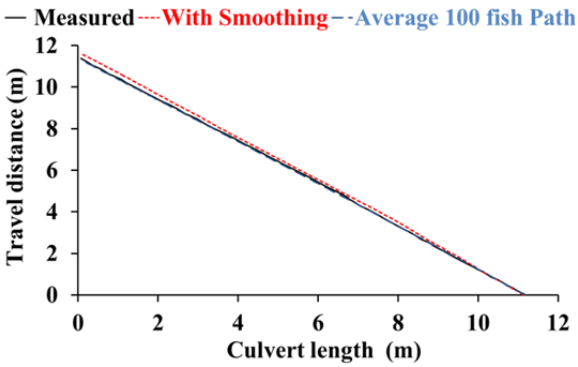

1st of July 2004 from point (6)

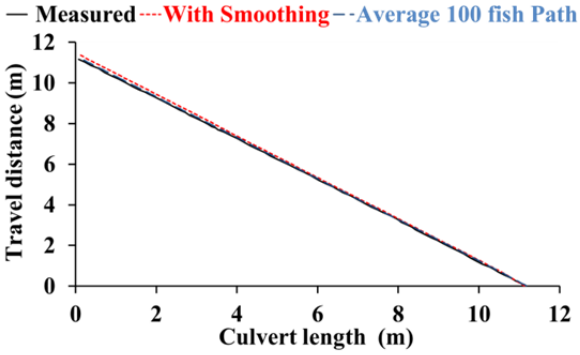

1st of July 2004 from point (8)

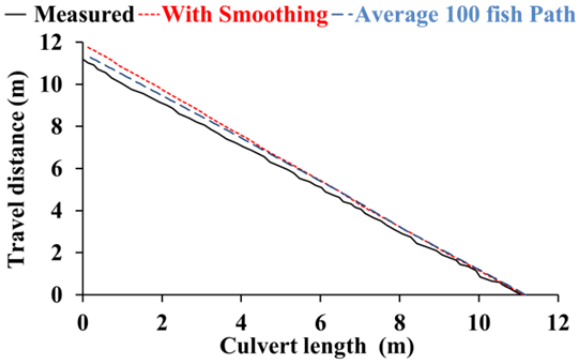

24th of June 2004 from point (10)

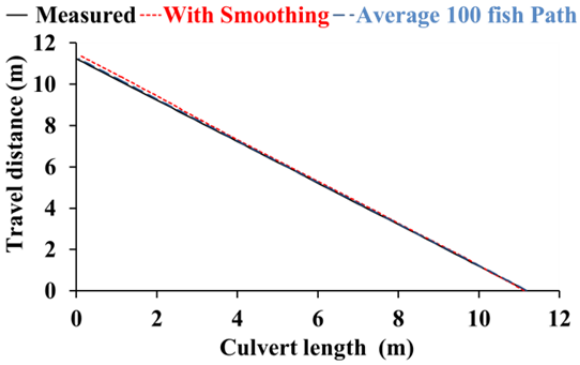

13th of July 2004 from point (10)

Figure 5.8: Cumulative distance travelled by the fish.

To calculate the passage time by the fish to travel the culvert, the burst speed for cutthroat trout is required. Several researchers mentioned burst speed amounts to be 10-12 body-lengths per second. Bell (1991) reported the burst speed of cutthroat trout as 4.1 m/s. Using Burst speed according to Bell (1991), the passage time was calculated using the measured and simulated path. Figure 5.9 compares the time taken by the fish to travel the culvert. The average error in the time taken by using the 100 fish average simulated path compared to the measured path was about 3.37%. The calculated time varies according to the flow velocity distribution and the point where the fish enter the culvert. The maximum time taken by the fish based on the measured path was 5.35 seconds for fish starting at point (2). Fish have an exhaustion point

related to burst swimming up to 15 seconds (Hoar and Randall, 1978). This time includes the attempts made by the fish to jump inside the culvert in addition to the fish movement inside the culvert. In a study by Cahoon et al. (2007) for the fish passage in the same culvert using passive integrated transponders (PIT tags), they found that the fish can successfully pass the culvert after an average number of attempts varied from 2 to 11 trials with mean 5 trials. The study was done in the period from 19 May to 17 September 2005 and repeated in the period from 9 April to 25 May 2006 and from 27 June and 30 September 2006.

Energy expenditure through the culvert was calculated based on the measured and simulated fish path. The average fish length was taken according to Blank (2008) as 331 ± 31 mm of length based on the data from 322 Yellowstone cutthroat trout captured during the study. Figure 5.10 compares the energy expenditure between the simulated and the measured path. The measured energy expenditure ranged from a minimum of 28.44 J to a maximum of 44.44 J. The average error in the 100 fish simulated energy was 2.42 %. Table 5.2 summarizes the results of the distance, the time consumed and the energy expenditure of the fishway for the measured and simulated path.

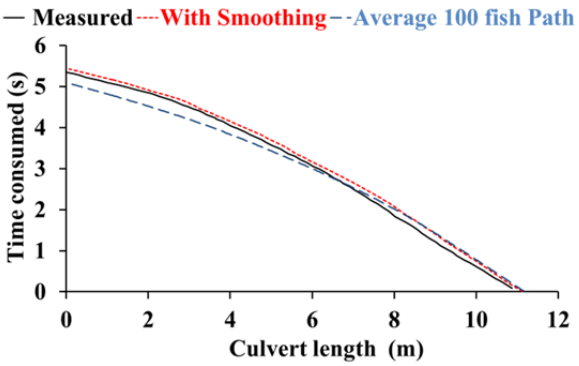

1st of July 2004 from point (2)

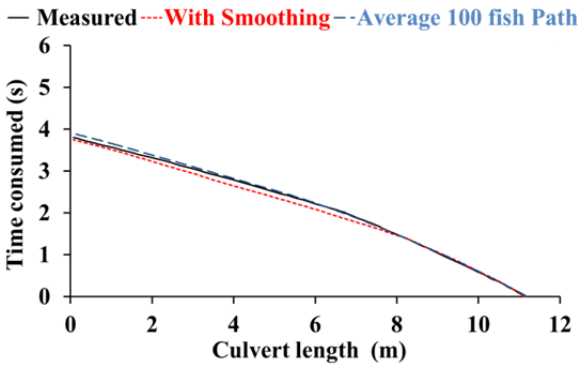

1st of July 2004 from point (6)

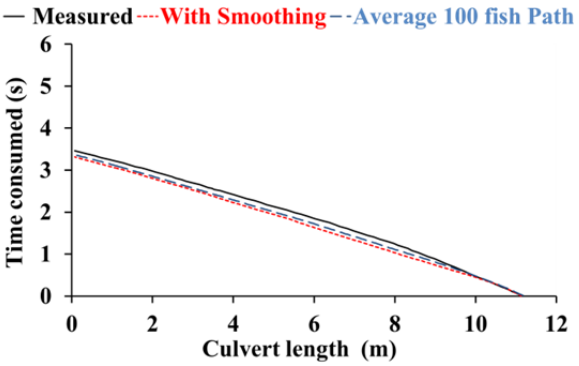

1st of July 2004 from point (8)

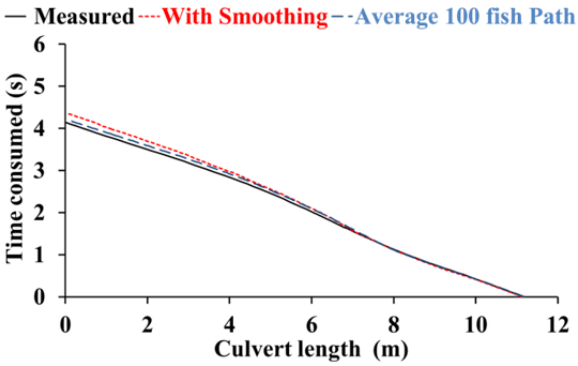

24th of June 2004 from point (10)

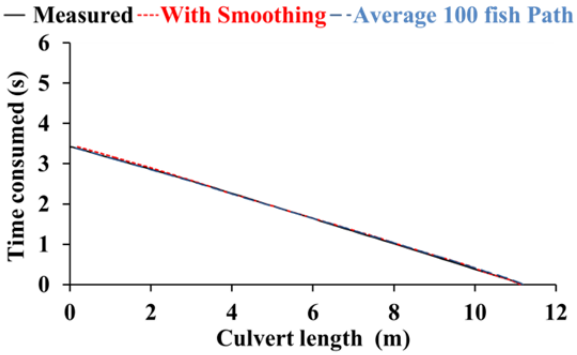

13th of July 2004 from point (10)

Figure 5.9: Time taken by the fish to travel the culvert.

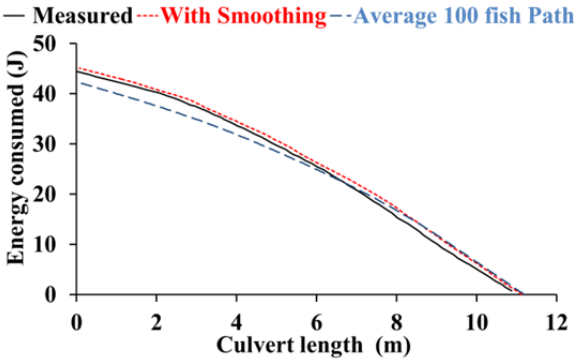

1st of July 2004 from point (2)

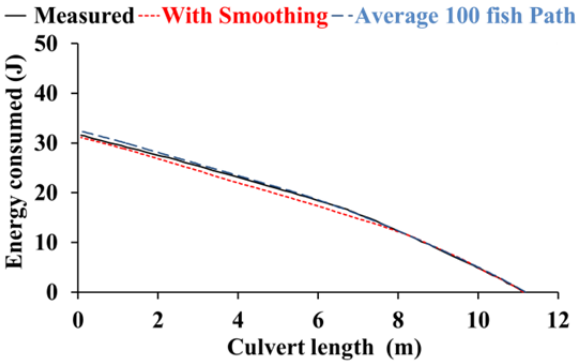

1st of July 2004 from point (6)

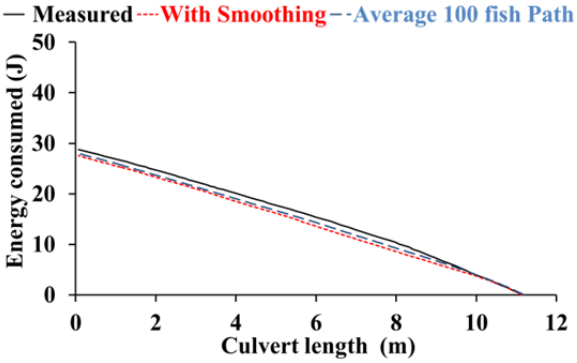

1st of July 2004 from point (8)

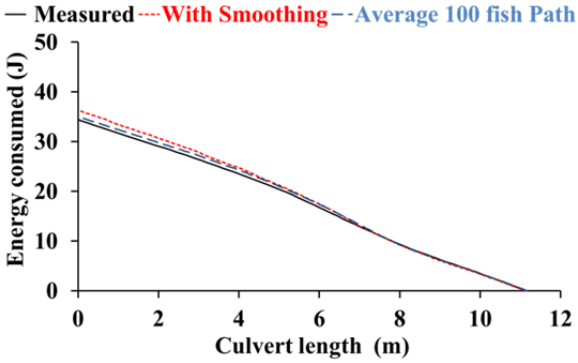

24th of June 2004 from point (10)

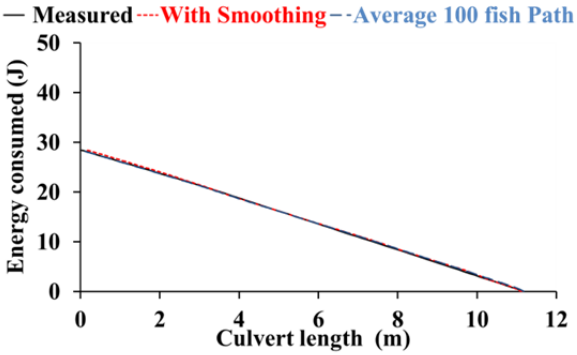

13th of July 2004 from point (10)

Figure 5.10: Cumulative energy consumed by fish to pass the culvert at different time.

Table 5.2: Comparison between the measured and average of 100 fish simulated results

Fish starting point	Distance(m)			Time (sec.)			Energy consumed(j)		
	Measured	Simulated	Error (%)	Measured	Simulated	Error (%)	Measured	Simulated	Error (%)
2 (01st July 2004)	11.53	11.49	0.35	5.35	5.08	5.03	44.40	42.16	5.04
6 (01st July 2004)	11.37	11.31	0.53	3.80	3.90	3.42	31.59	32.36	2.45
8 (01st July 2004)	11.16	11.25	0.81	3.46	3.37	0.29	28.75	27.96	2.74
10 (24th June 2004)	11.17	11.40	2.04	4.14	4.19	0.24	34.37	34.84	1.35
10 (13th July 2004)	11.21	11.23	0.14	3.42	3.41	7.89	28.44	28.30	0.50
Average error (%)	0.77			3.37			2.42		

5.1.5 Leaping energy

Leaping into the culvert is the first obstacle the fish meets during passage. The energy consumed by the fish to pass this obstacle depends on the jumping height and the leaping angle in addition to the fish weight. The leap height measured from water surface in the plunge pool to the water surface in the culvert averaged 0.60 m during the observation period. Unfortunately, there is no data available related to fish weight in this study. Several weight equations have been developed in the literature for many warmwater and coolwater species (see Anderson and Neuman 1996). Murphy et al. (1990) suggested the regression line percentile (RLP) technique when developing the standard weight (W_s) equations. This technique formulates W_s equation based on $\log_{10}$ (weight)-$\log_{10}$ (length) regression equations. Schoby and Curet (2007) described equation (5.1) for the length-weight relationship for westslope cutthroat trout captured and tagged in the Upper Salmon River Basin. The total length (L_f) in this study was in range 330 to 480 mm and the weight was in range of 345 to 1200g.

$$\log_{10} W_s = -4.46 + 2.79 \log_{10} L_f \quad (5.1)$$

Based on a samples of 117 cutthroat trout population (48 lentic and 69 lotic), Kruse and Hubert (1997) developed standard weight (W_s) - length equation for inland cutthroat trout. They developed separate W_s equations for lentic (relatively still water like lakes) and lotic (flowing water like rivers) populations in addition to the overall equation:

Lentic (N=48) $log_{10} W_s = -5.192 + 3.086\, log_{10}\, L_f$

Lotic (N=69) $log_{10} W_s = -5.189 + 3.099\, log_{10}\, L_f$ (5.2)

Overall (N=117) $log_{10} W_s = -5.139 + 3.072\, log_{10}\, L_f$

where N is the number of populations, W_s is weight in grams and L_f is the fish length in millimeters.

Using equation (5.1) and the lotic population in equation (5.2), the standard weight for a fish with 331 mm length is 371.81 and 416.82 g respectively. The leaping angle is typically between 60˚-70˚. Based on this data, the energy consumed by the fish during jumping can be calculated according to equation (4-21) as 2.27 J for 70˚ leaping angle and 3.27 J for 60˚ leaping angle. This value does not include the energy consumed during takeoff and landing which assumed here equal to the energy consumed during jumping.

The presence of enough energy inside the fish does not mean that the fish will successfully leap into the culvert. Figure 5.11 shows the summary of the fish attempts to leap into the culvert during the period from June 16th to July 8th, 2004. Among 89 leaping attempts observed, Blank (2008) noticed that there was only 34 successful leaps into the culvert (38.2 %). There are several reasons for these unsuccessful attempts:

- The fish did not jump high enough to clear the downstream invert of the culvert.
- The direction of the fish leaping was not in the direction of the culvert entrance.
- Some fish started leaping from a point away from the culvert entrance

Figure 5.11 shows that part of the fish, which successfully leapt into the culvert, could not pass the culvert. Among 34 successful leaps attempts, only 18 fish have successfully passed the culvert. The reason for that could be the direction of the trout landing angle. Additionally, some trout landed at an angle not parallel to the flow direction.

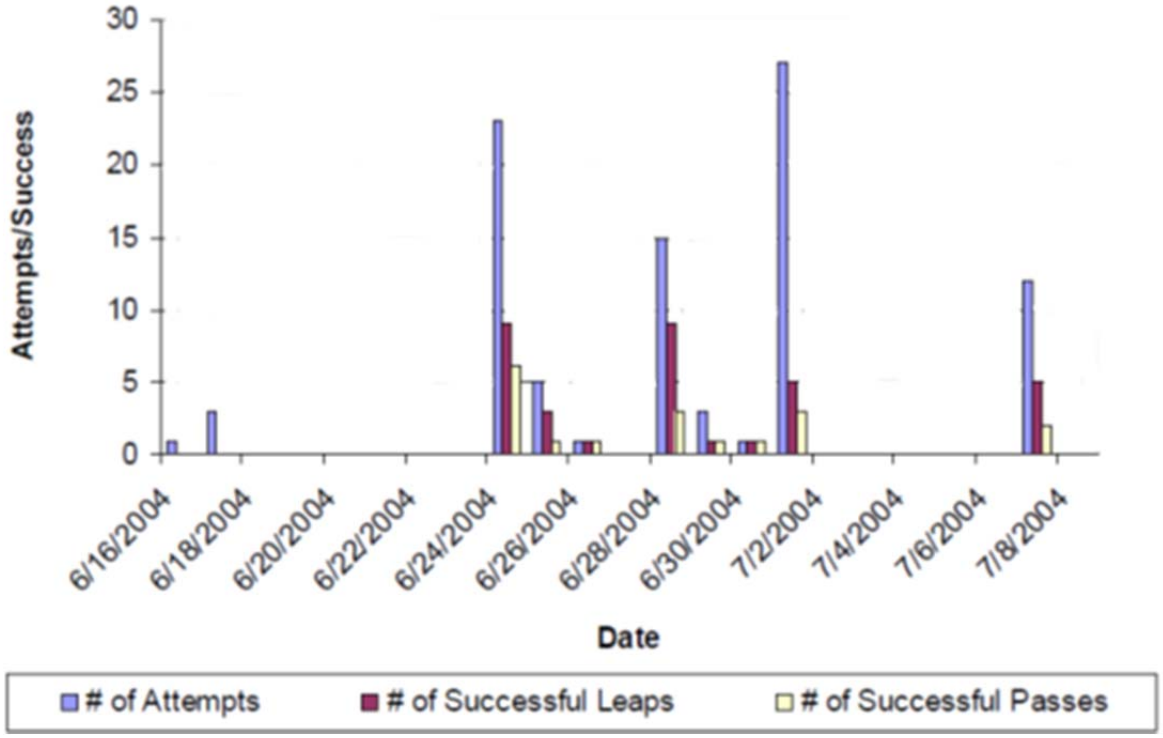

Figure 5.11: Summary of fish leaping attempts from June 16th to July 8th, 2004 (after Blank, 2008).

The geometry and flow characteristic have a great effect on the position where the fish enter the culvert. Figure 5.12 shows the flow characteristic downstream of the culvert for low and high flow. The presence of skew at this domain has an effect on the distribution of the flow. Blank (2008) divides the culvert entrance horizontally into 4 equal regions and determine the number of fish that enter the culvert from each region. Among the 89 attempts to enter the culvert from the downstream, 40 attempts were from region 4 in the outer part of the curve and 8 attempts were done from region 2 where the velocity at the culvert exit is high comparing to the other region. The lack of the available data in this area makes it difficult to include the effect of flow and geometry on the number of attempt at the entrance of the culvert in this model. However, the positions of the fish that enter the culvert can be calculated according to the statistics given by Blank (2008).

a. Flow rate 3.4 m^3/s b. Flow rate 0.8 m^3/s

Figure 5.12: Outlet region of culvert 1, looking upstream (after Blank, 2008)

5.1.6 Calculation of the actual fish energy

The model is applied to the data given in the 1st of July 2004. In this day, there were 27 leaping attempts to enter the culvert as shown in figure 5.13 and table 5.3. Among these attempts, 8 attempts were in the first region, 3 in the second region, 5 in the third region, and 9 in the fourth region. Additionally, two attempts have unknown locations.

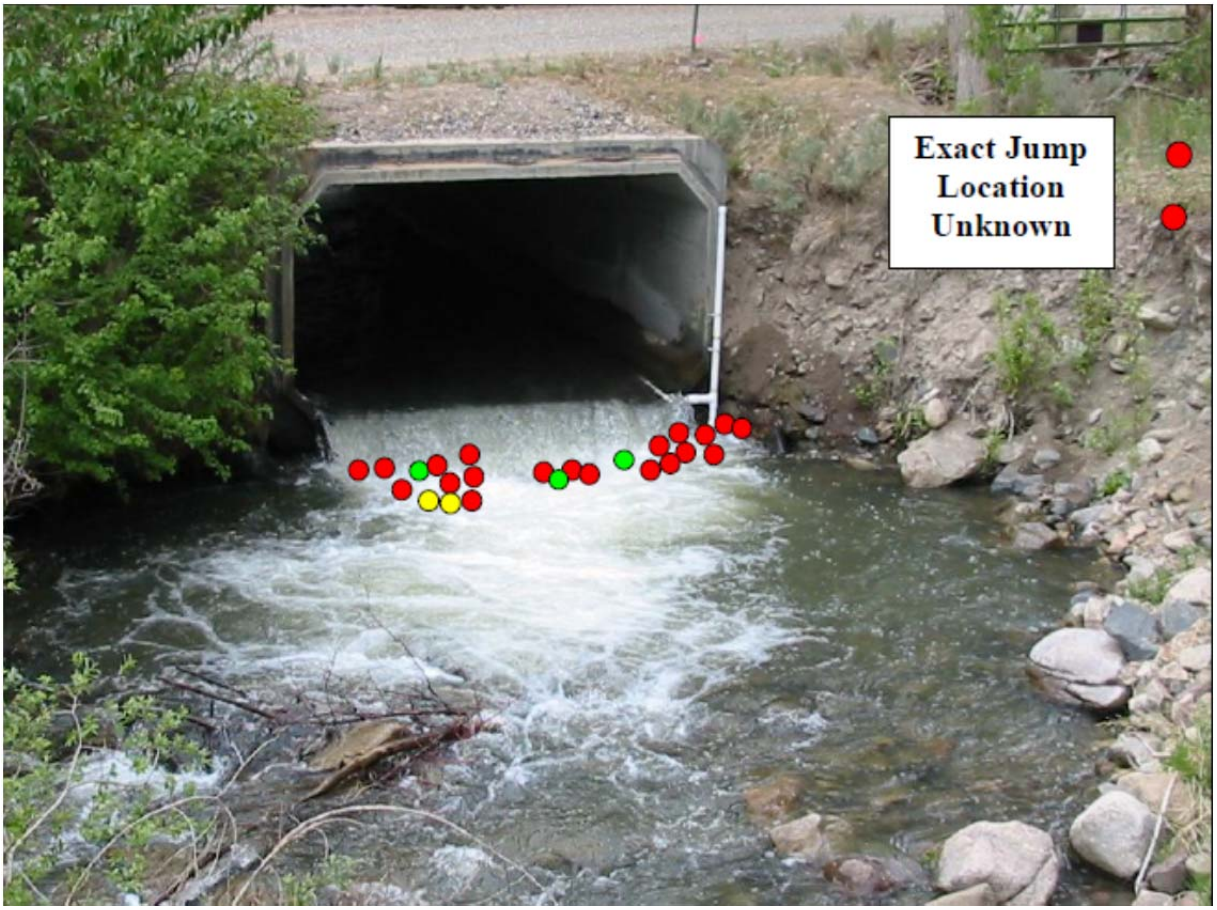

- The red circles represent unsuccessful leaps into culvert;
- The yellow circles represent successful leaps into but not successful passage through culvert;
- The green circles represent successful leaps into, and passage through culvert.

Figure 5.13: Leaping observation at culvert in the 1st of July 2004 (after Blank, 2008).

Table 5.3: Leaping attempts in 1st of July 2004

Region	**1**	**2**	**3**	**4**
Attempts	8	3	5	9
Leapt into	3	0	2	0
Pass the culvert	1	0	2	0

In order to adjust the actual fish energy, the model was run first for the fish in region 1. Among 8 attempts to leap into the culvert from this region, only 3 attempts succeed to enter the culvert with probability of each attempt to leap into the culvert equal to 0.375. The model allowed 10000 fish to leap randomly from all the points in region 1 into the culvert and the fish actual energy is calculated using equation (4.24) where the minimum and maximum fatigue times were adjusted according to the

probability of the fish to leap into and pass the culvert (see figure 5.14.a). The range of fatigue times were adjusted to be from 1 to 7.3 seconds. Using these values, the percentage of fish that could successfully pass the culvert is calculated and found to be 12.238 %. This value is approximately equal to the observed ratio between the fish succeeded to pass the culvert and the total number of attempts from this region (12.5 %). Using the same method, the range of fatigue times were adjusted for fish in region 3 to vary from 1 to 8.5 seconds (see figure 5.14.b). This value adjusted the percentage of fish that could successfully pass the culvert from this region to be 39.96% while the observed ratio was 40%.

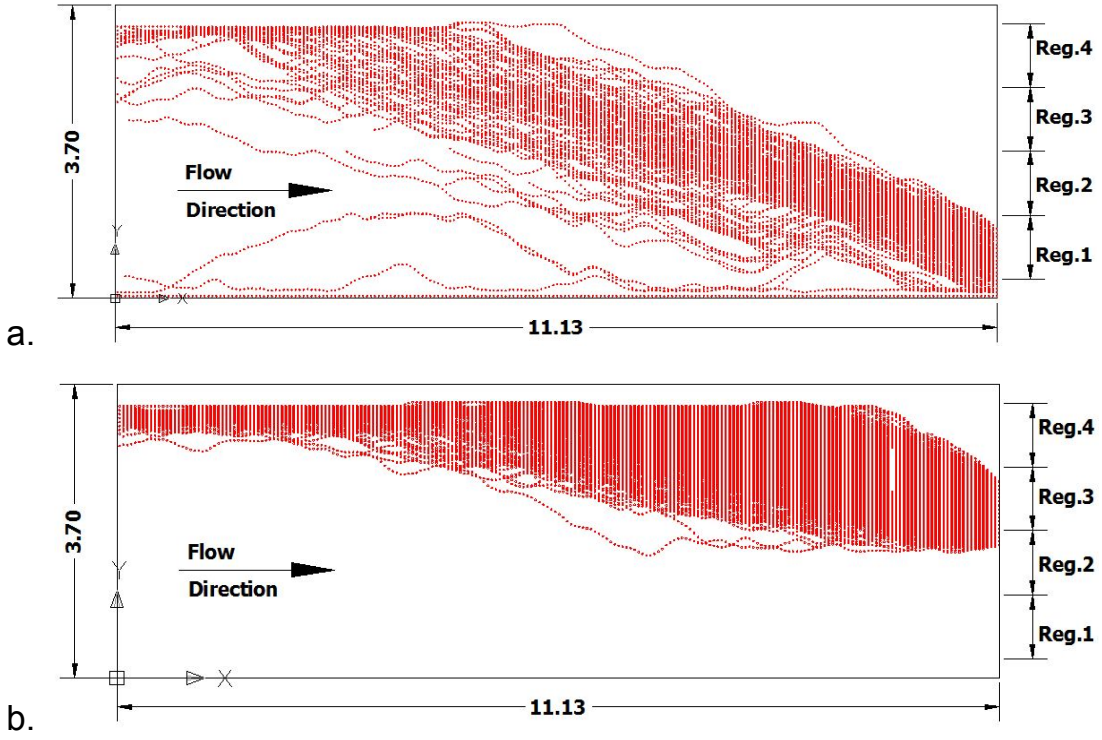

Figure 5.14: Sample of the fish movement results in the model for region 1 and 3.

Based on the previous part, the model was run for 10000 fish. The fish enter the culvert randomly from the downstream side with the distribution equal to the ratio between the number of fish which tried to enter the culvert from each region to the total number of the fish in this day. According to table 5.3 the distribution will be 8/25, 3/25, 5/25, and 9/25 for region 1, 2, 3 and 4 respectively. Additionally, the probability of each attempt to leap into the culvert was varied according to the position where the fish enter the culvert (3/8, 0.0/3, 2/5, and 0.0/9 for region 1, 2, 3 and 4 respectively). The fatigue time was adjusted according to the probability of passage so that the minimum time was 1.0 second and the maximum was 8.1 seconds. With these values, the passage probability was estimated as 12.07 %, while the observed passage probability was 12.0 %. A sample of the fish movement results is indicated in figure 5.15. The density of the lines in this figure is an indicator for the probability of the fish

to enter the culvert from each region. The figure shows also that some lines are stopped before the fish reach to the end of the culverts. This indicates that some fish exhausted before exiting from the culvert and their consumed energy becomes more than the fish actual energy.

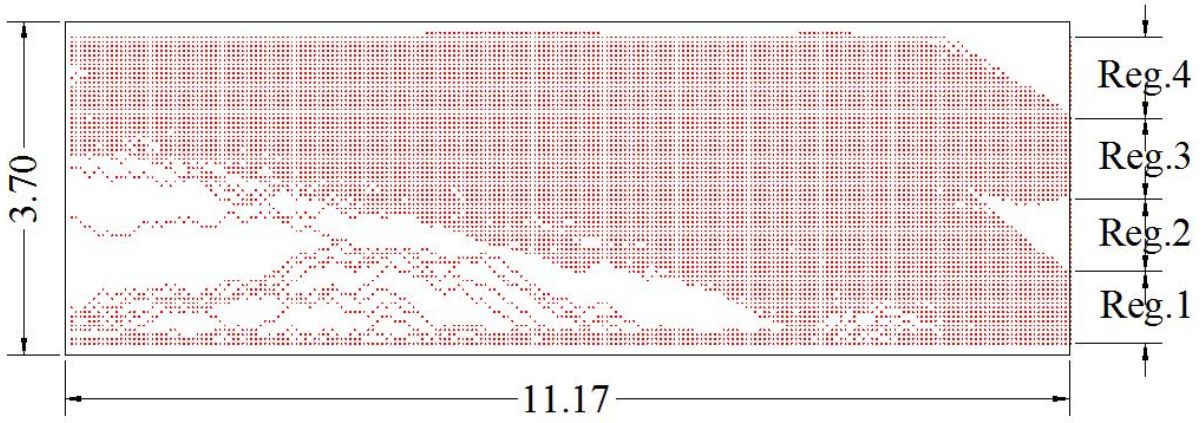

Figure 5.15: Sample of the fish movement results in the model.

The model is applied to the data given in 24th of June 2004 (table 5.4) with the same fatigue time range (1 to 8.1 seconds) and gives probability of passage equal to 24.6 % while the measured passage probability was 26.1 %. While these results are promising, more applications are required in order to validate and enhance the model results.

Table 5.4: Leaping attempts in 24th of June 2004

Region	**1**	**2**	**3**	**4**
Attempts	5	2	1	15
Leapt into	1	0	0	8
Pass the culvert	1	0	0	5

The results show that the ability of fish to leap into the culvert is one of the major reasons for decreasing the percentage of fish passage not only by the ability of fish to jump into the culvert but also by the energy consumed during the fish attempts to enter the culvert. More specific studies need to be done to adjust the probability of fish attempts to leap into the culvert.

5.1.7 Summary

The numerical method for predicting fish movement through a culvert of Blank (2008) was modified and tested with real data measurements. The method is based on the concept of energy expenditure with random movement and turbulence effect.

Based on this model, the energy expenditure is calculated for the measured and predicted path. Results of the simulation were compared to field studies of tracked fish. The model was applied to different flow distributions and provided good agreement with the observed fish movement paths. This study gives an interesting meso-scale investigation and approach to understand organism behavior that could influence culvert design. Although the simulation shows a good agreement with the measured data, more simulations for culverts with different slopes, cross-sections, and lengths as well as flow conditions are a good suggestion for future work to test its robustness and sensitivity. Based on this result, a new method for calculating the actual fish anaerobic energy is proposed and applied to the data given in the field study. Due to the lack of field measurement I could not investigate this method with some other culverts or fish species.

5.2 Case 2: Numerical simulation of flow and upstream fish movement through a single pool fishway

In the previous part, I studied a culvert as an example of a fish passage with almost uniform main flow directions. In that type, the upstream direction was easy to recognize by the fish and the fish was able to minimize its energy by travelling against the lowest flow direction. The use of culvert is limited by a maximum slope that can be accommodated with the design. When the required slope exceeds the practical limits of the culvert design approaches, a fishway may provide the right solution. Several types of fishway are developed including vertical slot, Denil fishways, pool-and-weir fishways. A pool-and-weir fishway consists of a number of pools arranged in a stepped pattern separated by weirs, each of which is slightly higher than the one immediately downstream (figure 5.16). In case of low flow conditions, the main flow direction is always near the wall and the bed while the circulating flow covers most of the pool tank. Additionally, the flow near the surface is reversed due to the back water effect. On the other hand for high flow condition, the main flow direction is near the water surface while the remaining part of the pool is covered by weak and circulated flow. The flows inside this fishway are mainly non-uniform and the fish has to follow the maximum velocity direction. In this part, the fish route inside the pool-and-weir fishway will be simulated using the model described in the part 4.1.3.

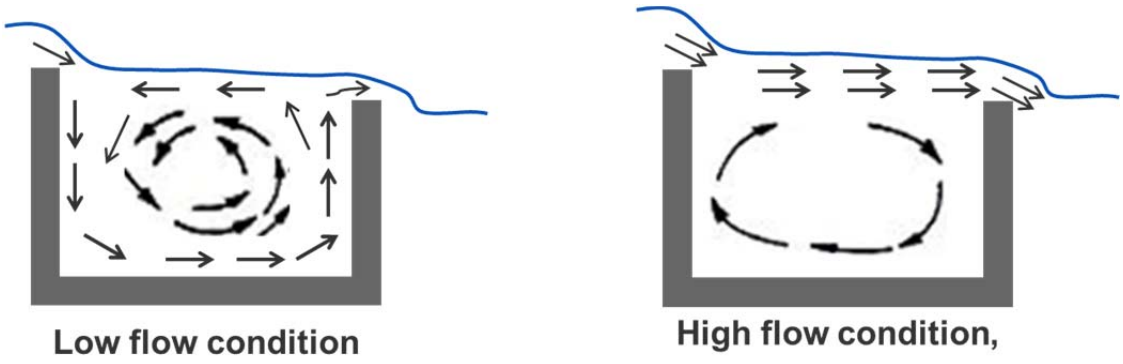

Figure 5.16: Flow stream inside pool-and-weir fishway.

5.2.1 Experimental data

Hayashida, et al., (2001) have conducted experiments for the flow and fish movement inside a pool-and-weir fishway. The experiment was done in a water channel that is 60 cm wide and consisting of two weirs, each 20 cm thick, and one pool, where L represents the pool length, H, the pool water depth, and the shape of the weir can be changed (figure 5.17). The head between the weirs and overflow water depth was fixed to 10 cm throughout the series of the experiments. The pool width was 60 cm and the thickness of the weir was 20 cm. The swimming behaviors of Japanese

Daces were studied by changing the scale of the pool and the shape of the weir. Eight different cases were set out by changing the pool length (L) to 50, 100 and 200 cm and the upstream and downstream weir height (H) to 30/20, 60/50 and 90/80 cm.

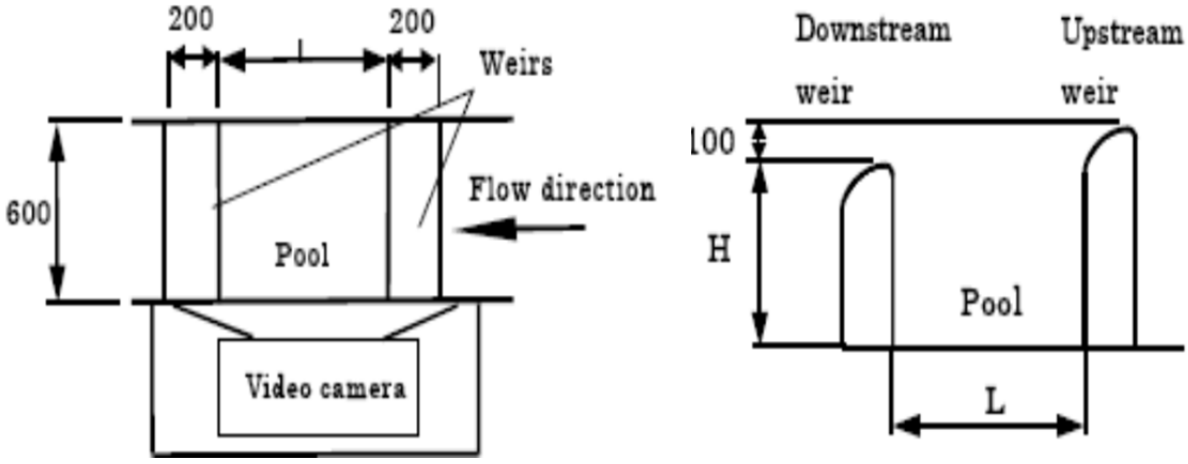

Figure 5.17: A plan view and longitudinal cross-section view of the pool and weir (Hayashida, et al., 2001).

Hayashida also measured the swimming motions of fish using an infrared observation room and observation window on the side of the water channel. A mesh was applied to the observation window at an interval of 10 cm. He measured the flow velocity at the central section of the water channel with a 5 to 10 cm mesh using a three-dimensional flow meter. Figure 5.18 shows a picture extracted from Hayashida's experimental work for case 2 (L=100 cm, H= 30/20 cm).

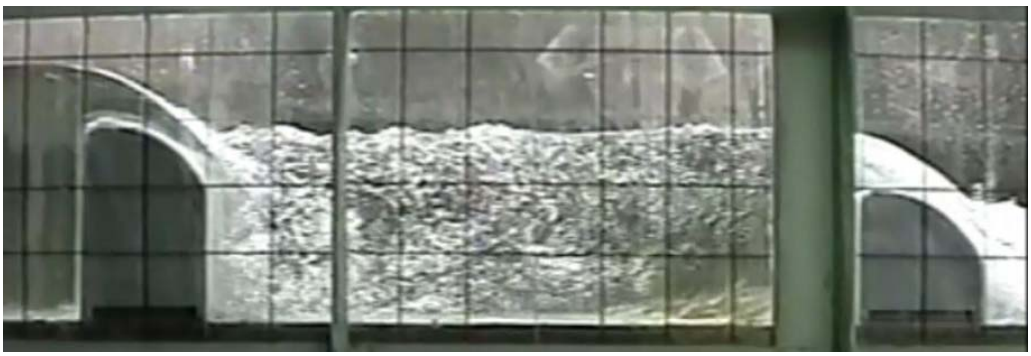

Figure 5.18: A photo for case 2 (L=100 cm, H= 30/20 cm) taken from Hayashida's experimental work.

Fifteen Japanese daces (Leuciscus hakonensis) were used for 4 hours in each case and the fish movement was extracted. The fish length varied from 6.0 – 18.0 cm with an average length of 12.44 cm.

5.2.2 Model calibration

The model was calibrated using the data for case-8 provided by Hayashida, et al., (2001). The numerical model was set up based on the experimental conditions. As shown in figure 5.19, the measured water elevation was used as an initial condition and the water elevations at the upstream and downstream boundary conditions were specified as 100.0 cm and 80.13 cm, respectively. All the simulations were two dimensions and the RNG turbulence model was used. A uniform 1.0 cm × 1.0 cm rectangular grid is used to mesh the domain. A third order upstream advection scheme was used to solve the momentum equations and the GMRES iterative solver to solve Poisson's equation for pressure. In order to calculate the shear stress at the channel bed, the standard wall-function with the roughness function is applied (Wilcox, 2000). Another parameter which could be useful in the model calibration is the turbulent mixing length parameter (TLEN). This parameter is used in the RNG turbulence model to compute the minimum values for the turbulent kinetic energy (k_{min}) and dissipation (ε_{min}). The default value of TLEN is computed as 0.07, which is based on the maximum value of the mixing length in fully-developed turbulent flow. However, this is a simple estimate and does not include geometry effects or the actual flow field scales. In this study the parameter TLEN is used to adjust the model during the calibrations.

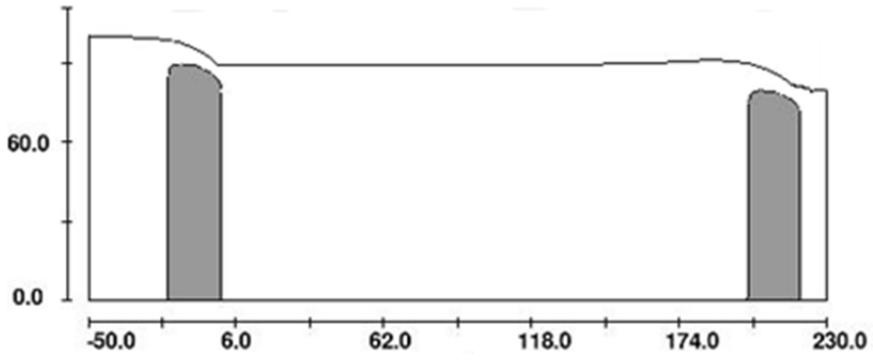

Figure 5.19: Model setup.

In figure 5.20, the simulated results were compared with the measurements of mean velocity in the domain. A good agreement between them has been achieved. In general, the velocity directions were non-uniform, and a large area was occupied by low velocities. It can be seen that, in the experiment as well as in the numerical model, the main flow was located in the domain near the wall and bed. The middle flow area is characterized by a circulated weak flow. On the other hand, the flow near the water surface is reversed due to the backwater effect. Figure 5.21 shows a comparison between the simulated maximum velocity paths and observations. The numerical model simulated the water surface elevation and the maximum velocity path with a good accuracy, while very small difference can be seen in the domain near the water

surface, where the flow takes place in the reversed direction. The reason of this difference may be due to the less number of measurements near the water surface in the experiment. Figure 5.22 represents the calculated and the measured maximum velocities near the bed. A good agreement between calculation and measurement has been also obtained.

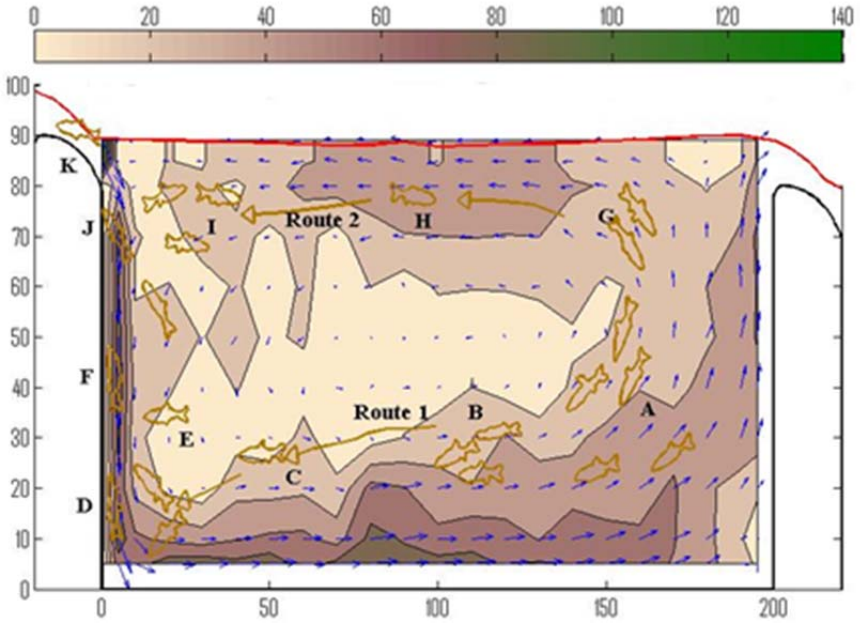

a. Measured velocity distribution and swimming behavior (after Hayashida et al., 2001)

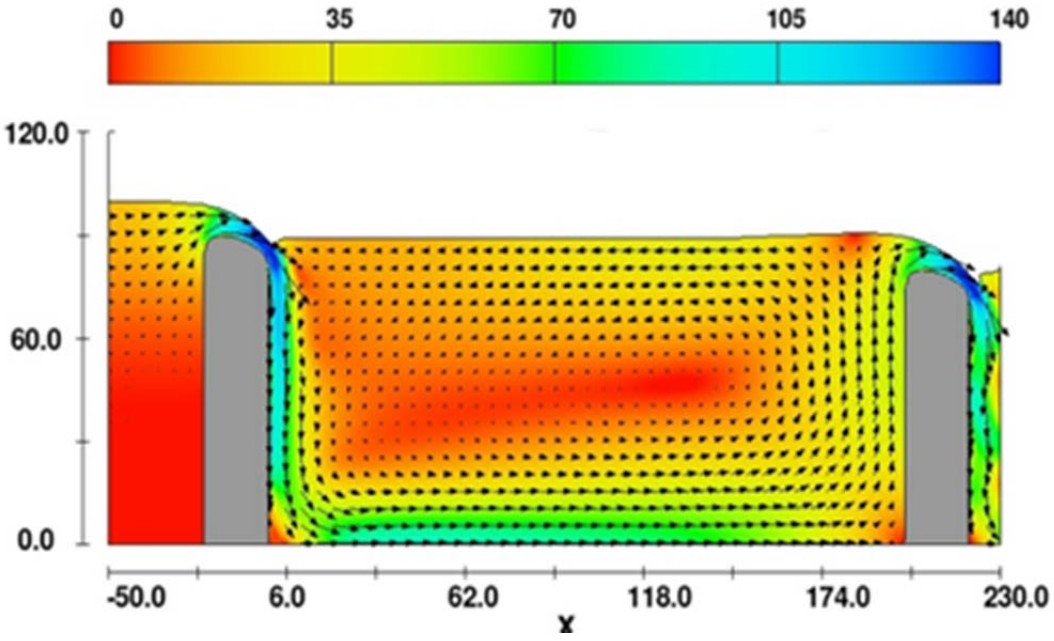

b. Simulated velocity distribution

Figure 5.20: Mean flow pattern inside the pool tank.

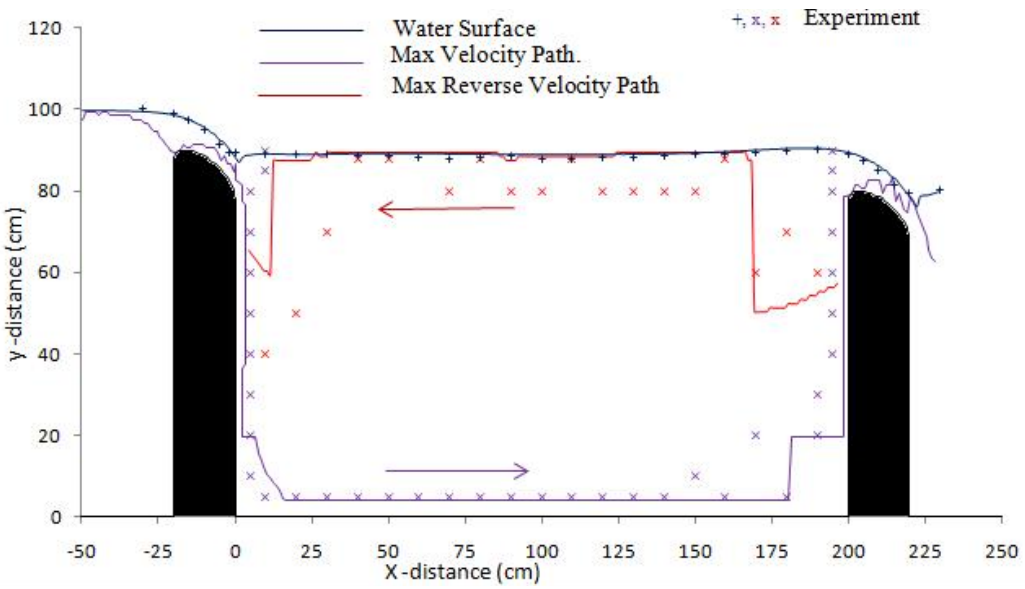

Figure 5.21: Maximum velocity paths inside the pool tank

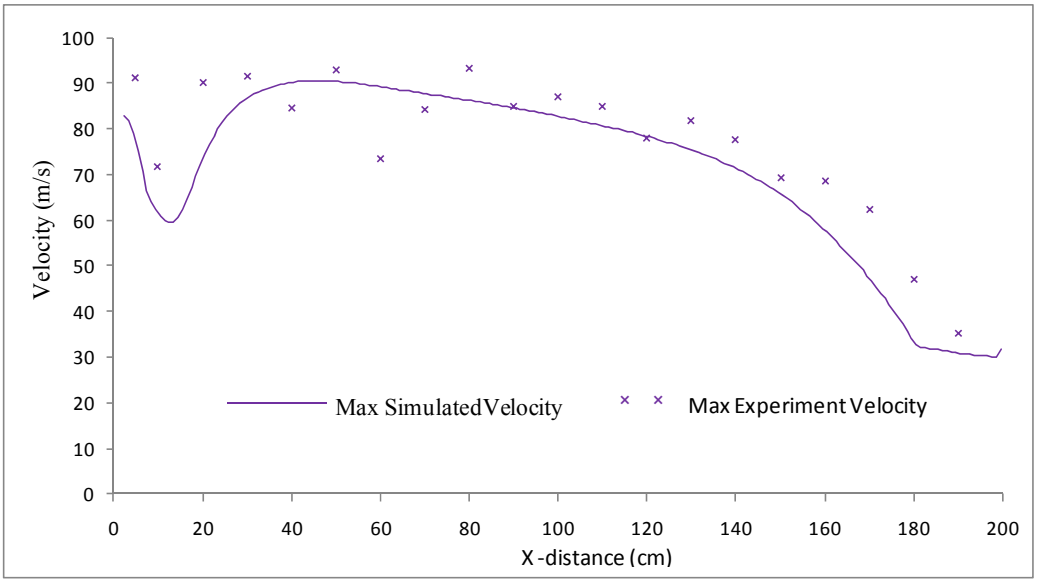

Figure 5.22: Maximum velocity near the bed.

Hayashida (2001) noticed that the fish stayed in the domain, where the velocity was slow and the current direction was constant. Most of the fish followed route 1 as indicated in figure 5.20.a. It was also noticed that the fish tried to avoid the circulated flow inside the middle section of the pool, where the direction of flow was not clear.

5.2.3 Model application

Hayashida et al., (2001) studied the swimming behavior of Japanese daces by changing the pool scale. Eight experiments were studied and the climbing frequency (the number of times that fish climb up the upstream weir) for each case was shown in figure 5.23. Finally, The eight experiments were classified to three levels according to

the climbing frequency where **Level 1** represents the highest climbing frequency; **Level 2**, a lesser climbing frequency; while **Level 3** is for the least climbing frequency. In order to understand the fish movement inside the pool tank, the effect of changing the pool scale were studied using FLOW-3D program for the flow simulation and combined with the observed and simulated fish movement.

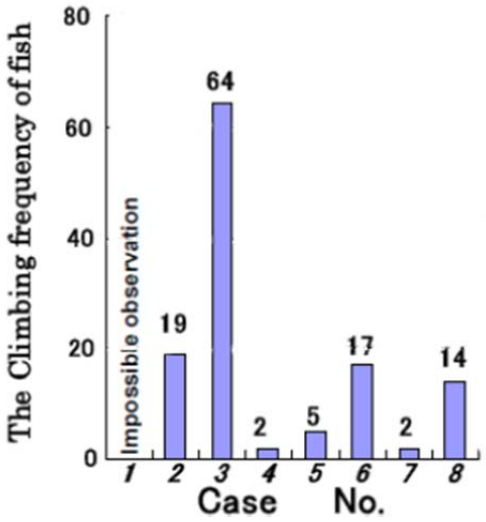

Figure 5.23: Climbing frequency of each case (after Hayashida et al., 2001).

5.2.3.1 Level 1

Figure 5.24.a shows the simulated velocity distribution for case 3 as an indicator for Level 1 (the highest climbing frequency). In this case, the pool length (L) was 200 cm and the weir height (H) was 30 cm for the upstream weir and 20 cm for the downstream weir. The calculated results show that in this case the flow has almost the same characteristic direction as flow directions for other cases. However, the circulation can be seen only in the upper part of the pool. This circulation vanishes in the middle of the tank and the flow becomes almost uniform and relatively slow. Flow pattern in case 3 could be ideal for fish as the flow was almost uniform with small velocity. The fish moved toward the upstream weir in the neighborhood of the surface where the path was short. In order to model the fish movement, the model was run for 100 times and the generated fish path was combined to give the area covered by the red color points in figure 5.24.b. The gray fish represent the fish path as indicated by Hashida (2001). It is clear from the figure that the simulated movements (red points) covered the measured fish path (the gray fish). The only difference in this case is that all the fish in the simulation go directly to the upstream and no circulation appeared in the fish movement. According to the high flow velocity over the upstream weir, few fish were pushed to reverse its direction and swim against the reversed flow near the surface. This situation is not included in the model as most of the fish passed the pool

tank directly from the first time.

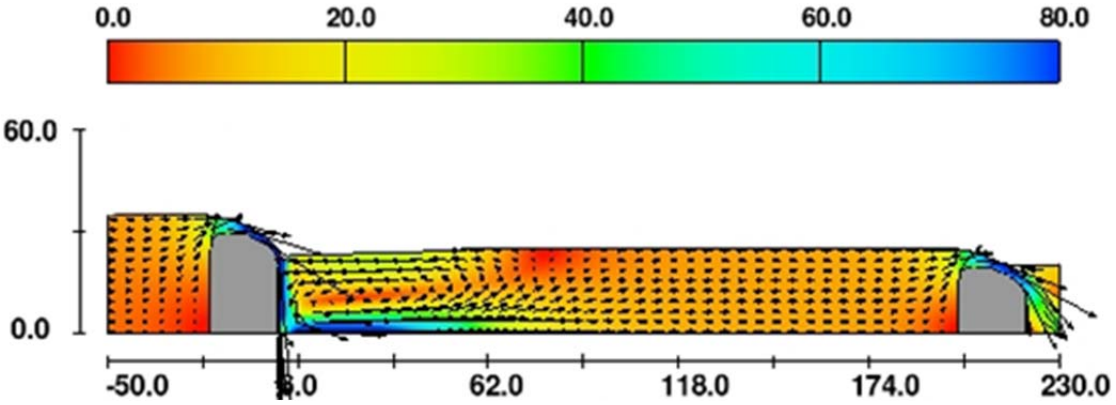

a. Simulated velocity distribution

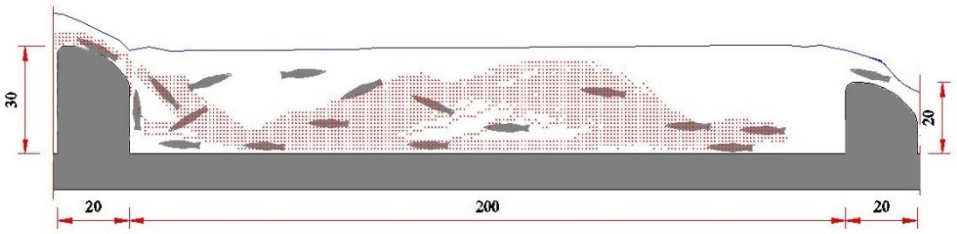

b. 100 fish movement paths

Figure 5.24: simulated flow pattern and fish movement inside the pool tank for case 3 Level 1.

5.2.3.2 Level 2

Level 2 represents a lesser climbing frequency and it includes three experiments; case 2 (The pool length (L) is 100 cm and the weir height (H) is 30 cm for the upstream weir and 20 cm for the downstream weir), case 6 (The pool length (L) is 50 cm and the weir height (H) is 90 cm for the upstream weir and 80 cm for the downstream weir) and case 8 (The pool length (L) is 200 cm and the weir height (H) is 90 cm for the upstream weir and 80 cm for the downstream weir). In this type, fish move in the range of the bottom layer to the middle layer where the velocity is slow and the current direction is constant. Figures 5.25.a, 5.26.a, and 5.20.b show the results for flow for case 2, case 6 and case 8, respectively.

Figure 5.25.a shows the velocity distribution inside the pool for case 2. In the upstream part, the flow is non-uniform and the main flow was located in the domain near the wall and bed. Small circulation can be seen around the center of the upstream part. This circulation is vanished in the middle of the pool and the flow starts moving

directly to the downstream weir. In the downstream part, the flow is separated from the bed leaving another circulation zone near the bed.

Figure 5.26.a shows the velocity distribution inside the tank for case 6. In this case the tank is deep and short. The main flow direction is beside the wall and bed. The flow near the bed is distributed in a wider range than the other cases. This decreases the maximum velocity near the bed and allows the fish to save its energy by swimming against the low flow. The flow in case 8 was previously described in section 5.2.3.

Figures 5.25.b, 5.26.b, and 5.27 show the results for the generated 100 fish paths for case 2, case 6 and case 8, respectively. It is clear from the figures that the water flow patterns are non-uniform. Since the fish are not familiar with the pool tank, they try to move against the maximum velocity flow direction in order to recognize the upstream direction. At the same time, the fish try to minimize the energy by traveling against the low flow near the recognized direction away from the circulated zone in the middle of the tank. Figure 5.25.b shows the generated path for case2. The fish enter the pool from the downstream and swim in the vicinity of the main flow direction. The simulated path mimics the measured fish path. The only difference is that, as mentioned in case 3, a few fish leave the main flow direction and swim back against the reversed flow near the surface.

Results of case 6 can be seen in figure 5.26.b. The fish enter the pool from the downstream and swim down until they reach the bottom of the tank. Furthermore, the fish move in the range of the bottom layer to the middle layer where the velocity is slow and the current direction is constant. Finally, the fish swim up against gravity and flow direction to the top of the weir where they exit the flow. Few fish swim back near the surface against the reversed flow.

Figure 5.27 shows the results of case 8. Like the previous two cases, the fish move in the vicinity of the flow direction near the wall and bed where the velocity is moderate and the flow direction is constant. Due to the large dimensions of the pool, compared to the previous cases, the area in vicinity of the main flow direction is large. Accordingly, fish which select to swim in the farthest point of the main flow direction within this area, will move against the reversed flow direction near the surface.

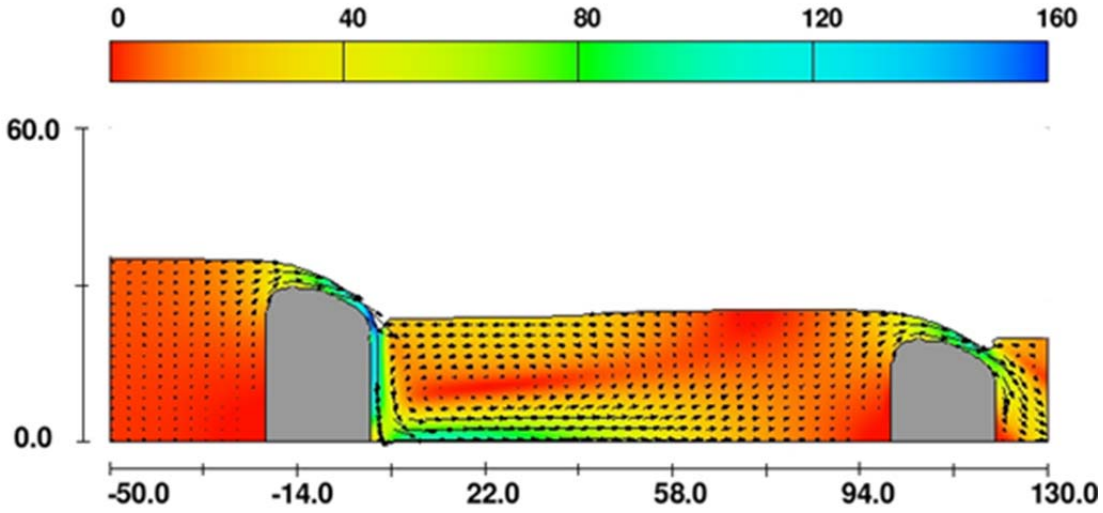

a. Simulated velocity distribution

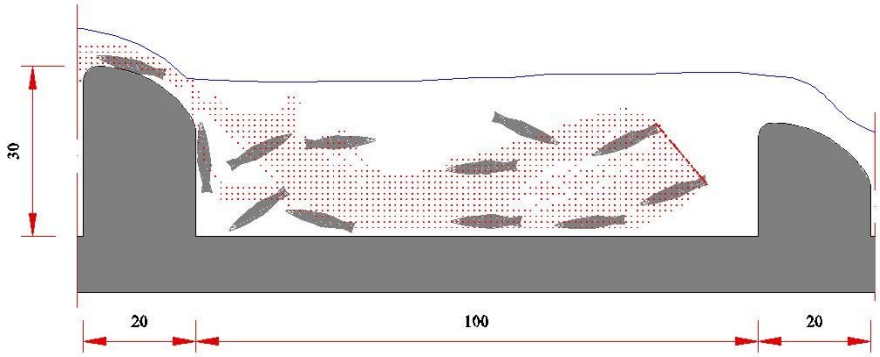

b. 100 fish movement paths

Figure 5.25: Simulated flow pattern and fish movement inside the pool tank for case 2 –Level 2.

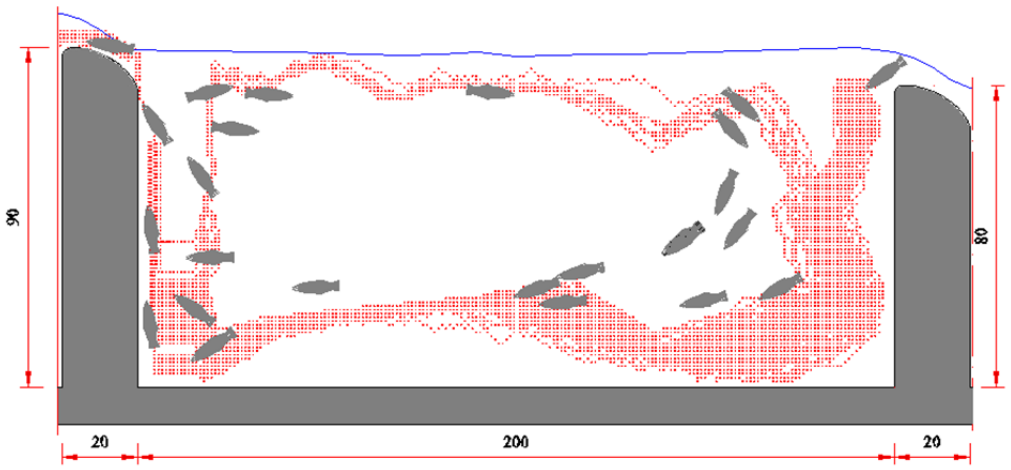

Figure 5.27: Simulated 100 fish movements inside the pool tank for case 8 –Level 2.

5.2.3.3 Level 3

Level 3 presents the least climbing frequency case and it includes three experiments; case 4 (The pool length (L) is 100 cm and the weir height (H) is 60 cm for the upstream weir and 50 cm for the downstream weir), case 5 (The pool length (L) is 200 cm and the weir height (H) is 60 cm for the upstream weir and 50 cm for the downstream weir) and case 7 (The pool length (L) is 100 cm and the weir height (H) is 90 cm for the upstream weir and 80 cm for the downstream weir). In this type, the fish move in the bottom layer where the velocity is very high and the current direction is constant. Figures 5.28, 5.29, and 5.30 show the results for the flow and the generated 100 fish paths for case 4, case 5 and case 7, respectively. It is clear from the figures that the water flow patterns were non-uniform. The main flow concentrates in the narrow area near the wall and bed while a large circulated flow in the middle area can be seen. As a result, the fish exert high energy in order to swim against the high flow. Finally, most of the fish could not pass the fishway.

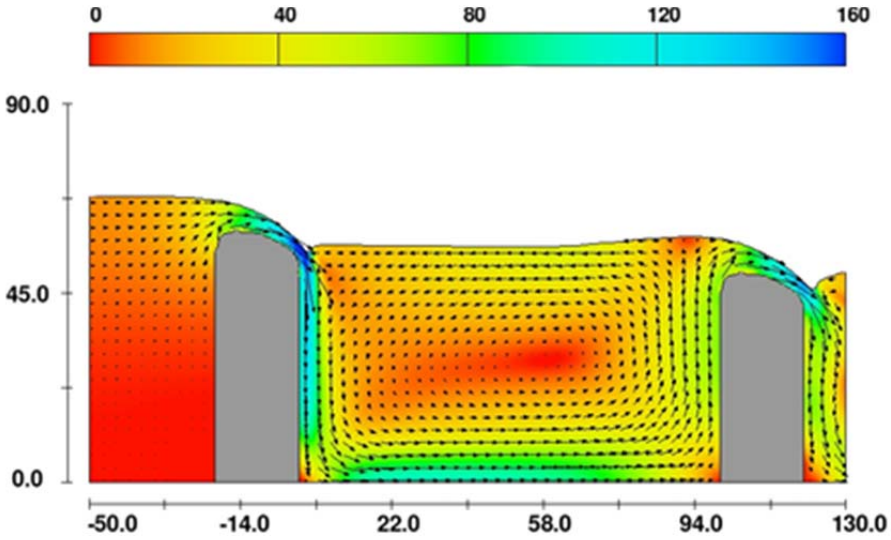

a. Simulated velocity distribution

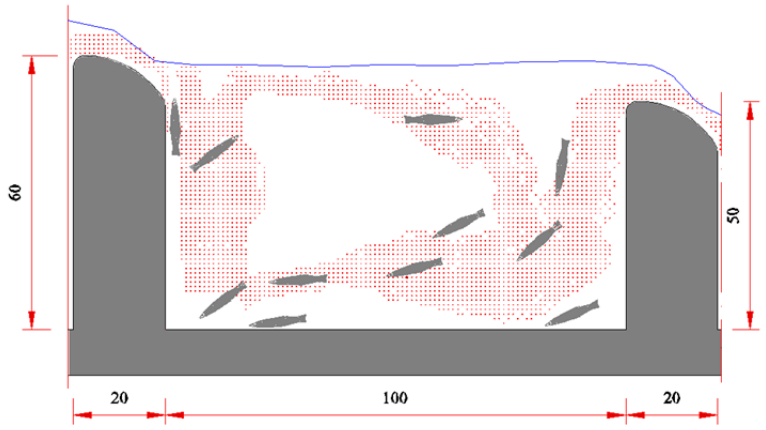

b. 100 fish movements paths

Figure 5.28: Simulated flow pattern and fish movement inside the pool tank for case 4 –Level 3.

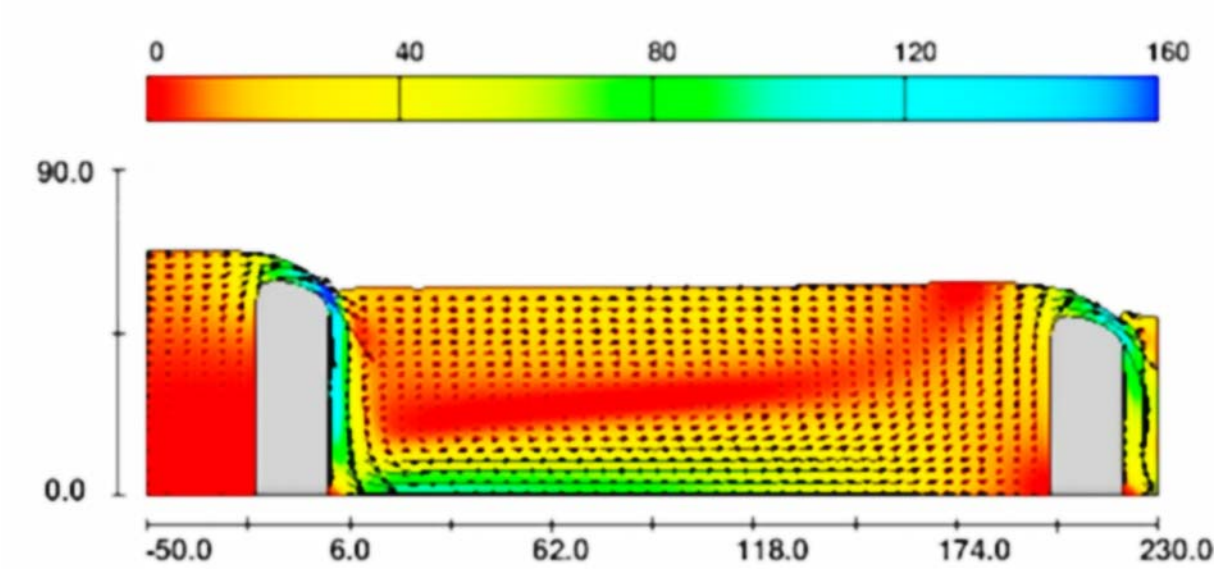

a. Simulated velocity distribution

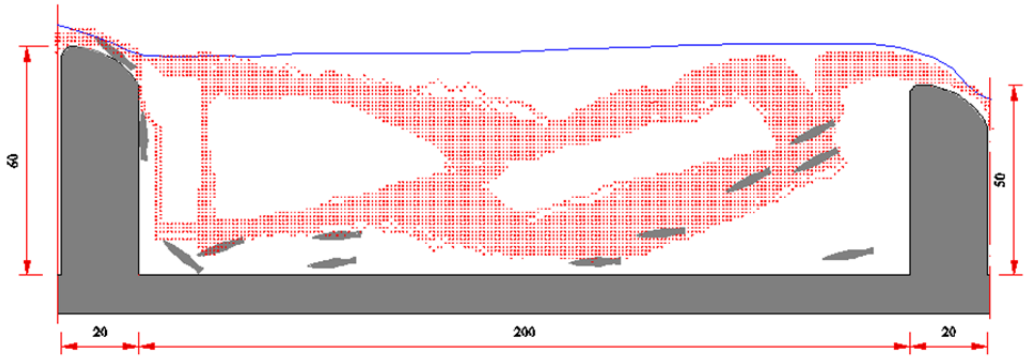

b. 100 fish movements paths

Figure 5.29: Simulated flow pattern and fish movement inside the pool tank for case 5 –Level 3.

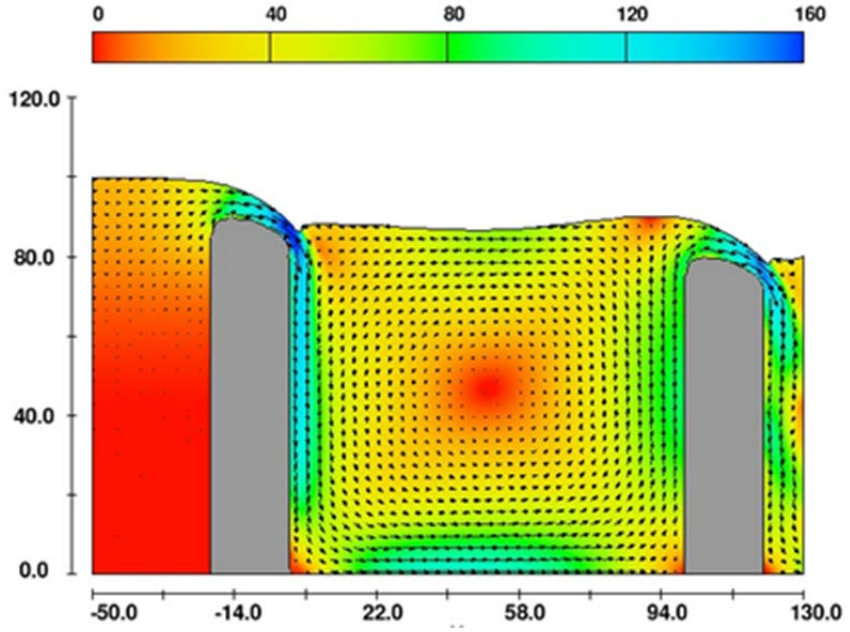

a. Simulated velocity distribution

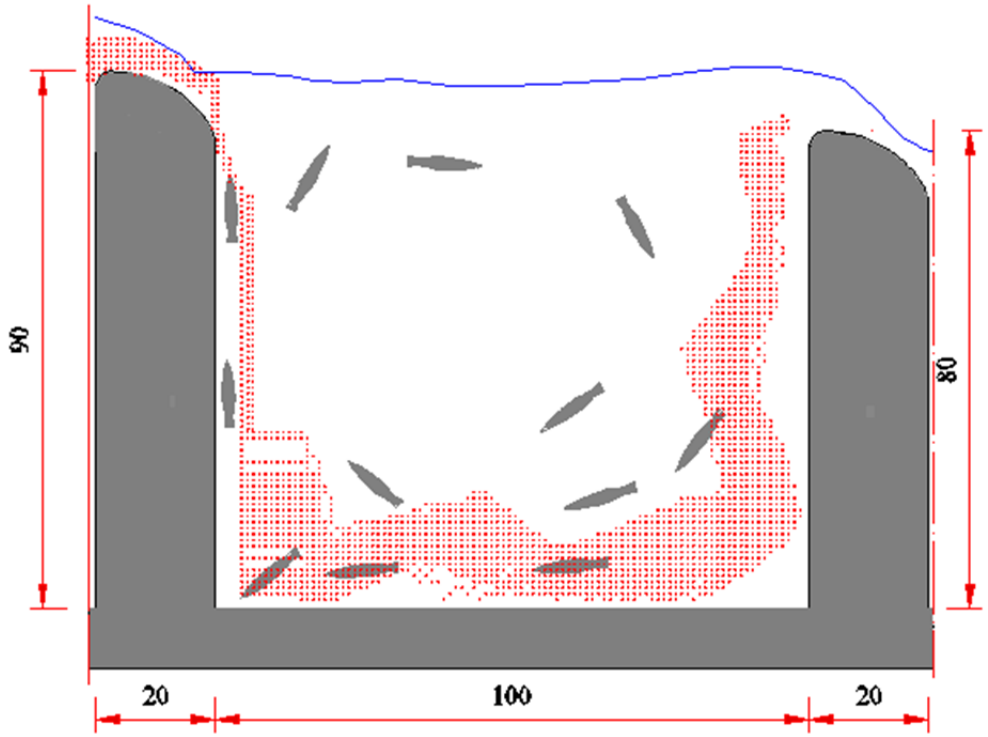

b. 100 fish movements paths

Figure 5.30: Simulated flow pattern and fish movement inside the pool tank for case 7 –Level 3.

5.2.4 Summary

The model has provided good results of flow pattern and fish movement compared to the experimental data provided by Hayashida (2001). The simulated results showed that the flow inside the pool was highly non-uniform and a large area was occupied by a low water current. The dimensions of the pool had a great effect on the distribution of flow in the pool. When the pool length is long and the weir height is small, the flow is almost uniform. These flow conditions could be perfect for Japanese daces which showed the most climbing frequency. By increasing the pool depth the flow, non-uniformity becomes more intensive and accordingly, the climbing frequency could be reduced. By decreasing the pool length, the strong circulation of the flow could cause very bad condition for fish climbing.

5.3 Case 3: Numerical simulation of flow and upstream fish movement through a multiple pool fishway

5.3.1 Experimental data

Atsushi *et al.*, (2008) and Atsushi (2009) studied the relationship between the flow structure and the swimming behavior of Leuciscus hakonensis in multiple pool-and-weir type fishway by changing several parameters. These included the pool length, the number of pools and the height difference of two successive weirs. For each of these experiments, the discharge is varied from 0.021 to 0.2 $m^3/s/m$'. Figure 5.31 shows a typical geometry shape of the experiments. Three types of experiments were done: Experiments of type A consist of a three pool tanks (N=3) with a length (L) of 80 cm, downstream weir height (H) of 40 cm, the thickness of each weir (D) was 20 cm, and the difference in height between two successive weirs (DY) was 10 cm. In type B experiments, only the difference in height between two successive weirs (DY) was changed to become 20 cm. On the other hand, experiments of type C consist of six pools (N=6), each is 30 cm in length, 40 cm weir height, and 10 cm deference in weir height. Table 5.5 summarizes the specification of each type. Four cases of experiments were done for each of these types. Table 5.6 summarizes the flow and the water head over the weir for these 4 cases.

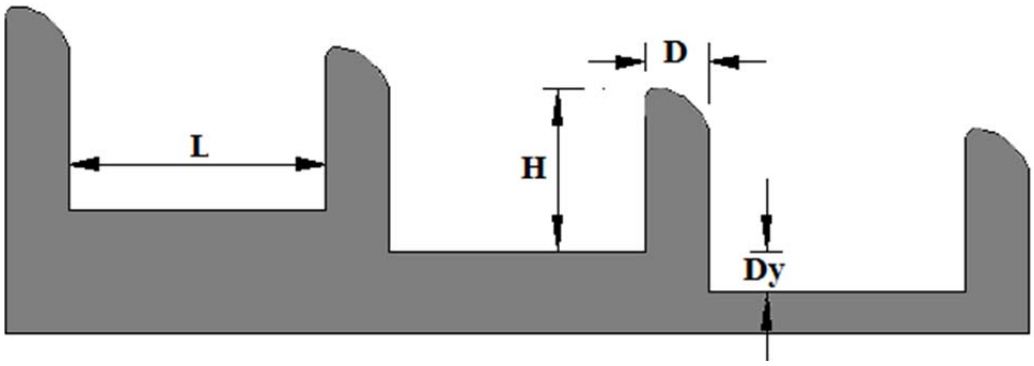

Figure 5.31: typical shape of the hydraulic model.

Table 5.5: The specifications of the hydraulic model (after Atsushi, 2009).

	Slope	N	H(cm)	Dy(cm)	D(cm)	L(cm)
Type A	1/10	3	40	10	20	80
Type B	1/5	3	40	20	20	80
Type C	1/5	6	40	10	20	30

Table 5.6: Discharge conditions (after Atsushi, 2009)

	Weir Overflow depth Δh (m)	Flow unit width q (m^3/s/m)
Case 1	0.05	0.021
Case 2	0.10	0.064
Case 3	0.15	0.127
Case 4	0.20	0.200

Similar to what Hayashida *et al.* used (2001), Atsushi (2009) also used Japanese daces (Leuciscus hakonensis) to examine the fishway. The fish length varied from 9.0 – 12.0 cm and its weight varied from 10 – 20 g. It was also mentioned that the maximum burst speed was 10 times the fish length (0.9 – 1.2 m/s). The fish movement was extracted using digital video camera and combined with the water velocity in order to determine the relationship between hydraulic conditions and fish movement.

5.3.2 Model calibration

The model was calibrated using the data obtained from Type A-experiment provided by Atsushi (2009). As shown in Figure 5.32, the measured water elevation was used as an initial condition and the water elevations at the upstream and downstream boundary conditions were specified as 84.52 cm and 44.00 cm, respectively. The RNG turbulence model was used and all the simulations were two dimensions. A uniform 1.0 cm rectangular grid was used in x and z directions to mesh the domain.

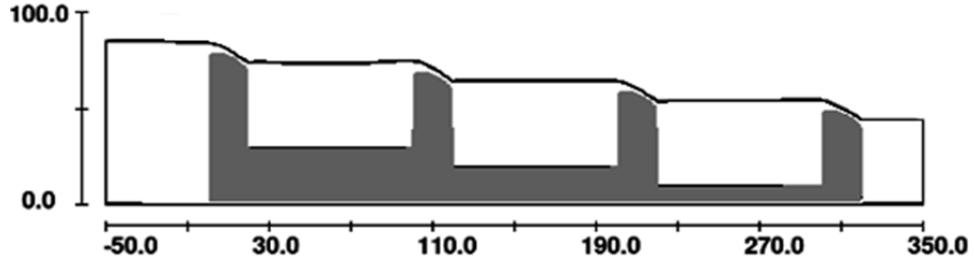

Figure 5.32: Model set up.

In Figure 5.33, the simulated results were compared with the measurements of mean velocity in the domain. In general, the velocity directions were non-uniform, and a large area was occupied by low velocities. It can be seen that, in the experiment as well as in the numerical model, the main flow was located in the domain near the wall and bed. The middle flow area was characterized by a circulated weak flow. On the other hand, the flow near the water surface was reversed due to the backwater effect. The measured velocity over the weir is smaller than the simulated one for the three weirs. Figure 5.34 shows a comparison between the measured and simulated maximum velocity near the walls and the beds. The numerical model could simulate the water surface elevation while some difference can be seen in the maximum velocity path. The measured velocity in the middle pool is smaller than that in the first and the third one. Even in the experiment itself, the velocity in the middle pool is smaller than the velocity in the other two pools. One of causes is that the inflow to the first pool comes from the upstream channel of hydrostatic state while the inflow to the middle pool comes from the first pool of turbulence state. Another difference is that the measured velocity over the weir is smaller than the simulated one. One reason for that is that in the experimental work, the given velocity over the weir is the horizontal component only and the vertical component could not be measured.

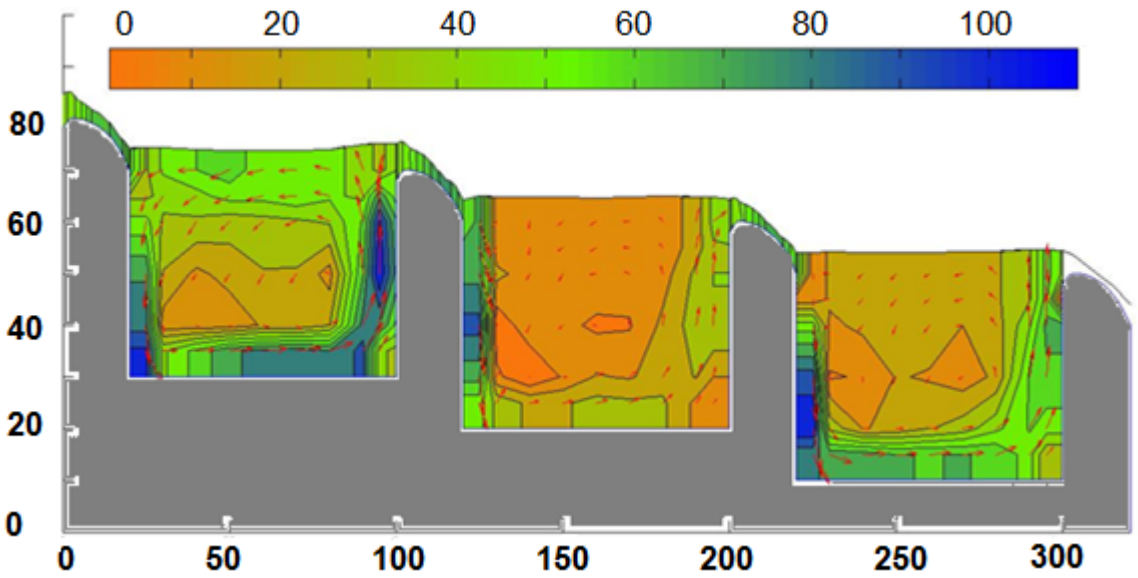

a. Measured velocity distribution and swimming behavior (after Atsushi, 2009)

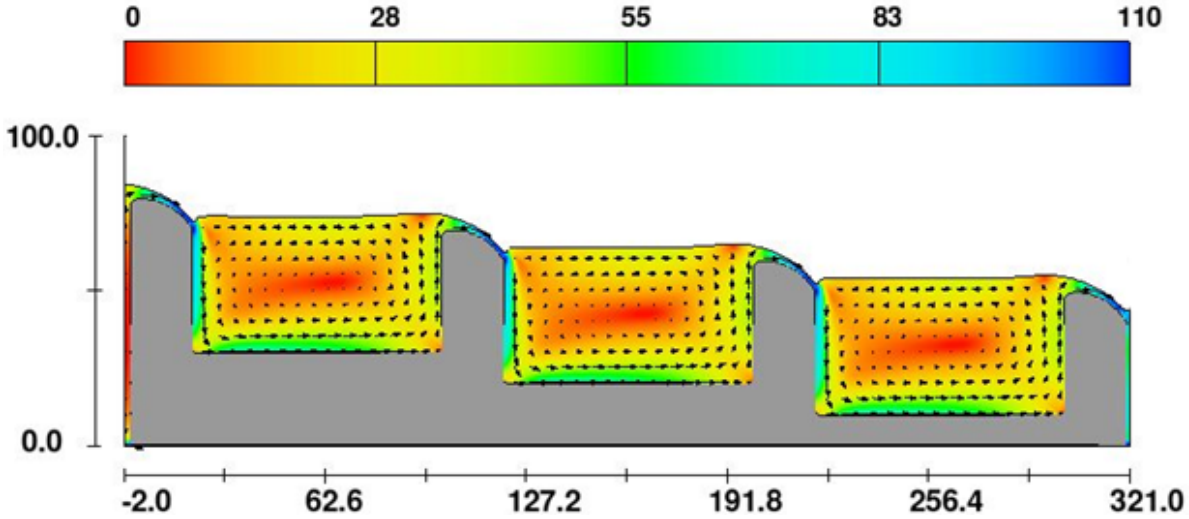

b. Simulated velocity distribution

Figure 5.33: Mean flow pattern inside the pool tank.

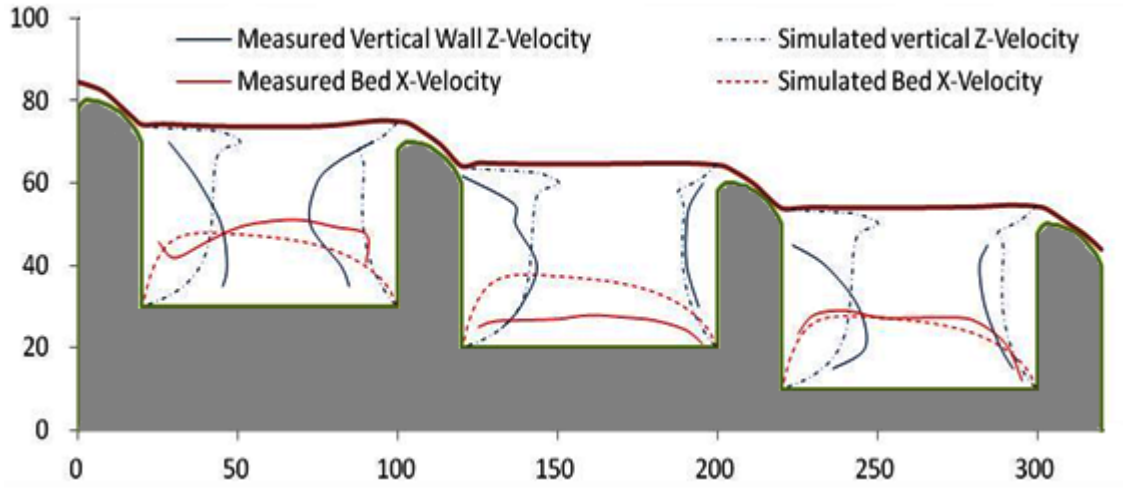

Figure 5.34: Comparison between measured and simulated maximum velocity near the bed and the walls.

5.3.3 Model application

The effects of pool dimensions and number of pools on the flow and fish movement were studied in the laboratory by Atsushi et al., (2008) and Atsushi (2009).

5.3.3.1 Type-A experiments

To study the effect of changing the flow on the velocity distribution and fish movements, the model was setup according to Type - A experiments. The flow as well as the water depth varied from one experiment to the other as indicated in table 5.6. Figure 5.35 represents the fish movement in the low flow conditions (0.021 $m^3/s/m$), while the velocity distribution of this case is previously represented in figure 5.33. The fish follow the flow direction and move in the neighborhood of the bed and walls. The simulation is in a good agreement with the measured fish path. The only difference can be seen in the middle pool where the simulated velocity is higher than the measured velocity.

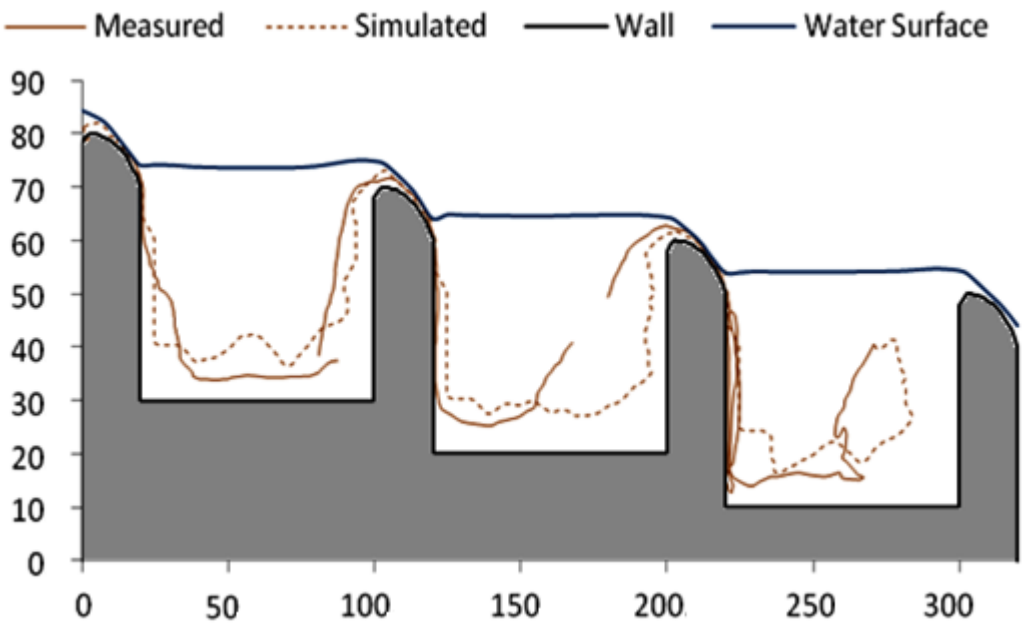

Figure 5.35: simulated and observed fish movement inside the pool tank for Type-A Experiment 1 ($\Delta H = 0.05$ m, $q=0.021$ $m^3/s/m$.)

By increasing the flow to 0.064 $m^3/s/m$, the flow is redistributed over higher distance from the bed and the wall as can be seen in figure 5.32.a. Additionally, the maximum velocity inside the pool as well as over the weir becomes higher. In this case, the fish move in the middle of the bottom layer where the velocity is constant and the direction of flow is clear. Figure 5.36.b shows a comparison between the measured and simulated fish path. In this case, the measured path cuts the circulation zone in the middle of the pool especially in the middle and the most downstream pools. The maximum difference between the simulation and measured path can be seen in the middle pool. The fish may use this area as a resting zone. The position as well as the period of the rest zone are not included in this study and needs more details to understand.

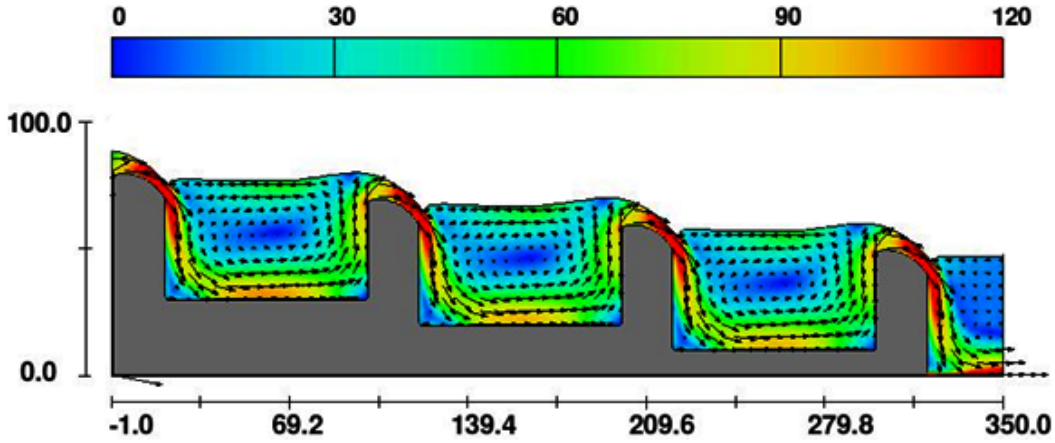

a. Simulated velocity distribution

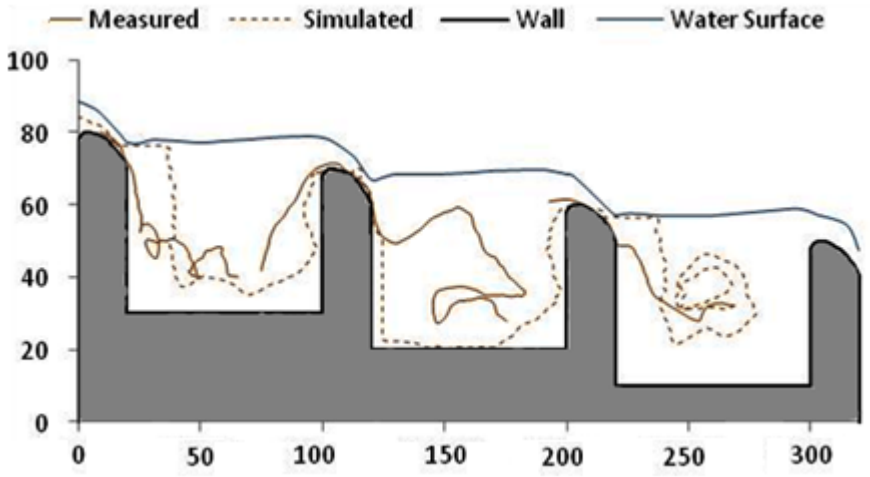

b. fish movement path

Figure 5.36: Simulated flow pattern and fish movement inside the pool tank for Type-A Experiment 2(ΔH = 0.10 m, q= 0.064 $m^3/s/m$).

Further increase of the flow to 0.2 $m^3/s/m$ has a great effect on the distribution of velocity inside the pool. Figure 5.37.a shows the simulated velocity distribution for case 4. In this case, the main flow direction moves up near the surface while the big circulation zone inside the pool is vanished and replaced with three small circulating zones around the main flow. The fish move in the neighborhood of the main flow where the velocity is constant and the direction is clear (figure 5.37.b). The fish exit this flow domain to the circulation zone during the resting time.

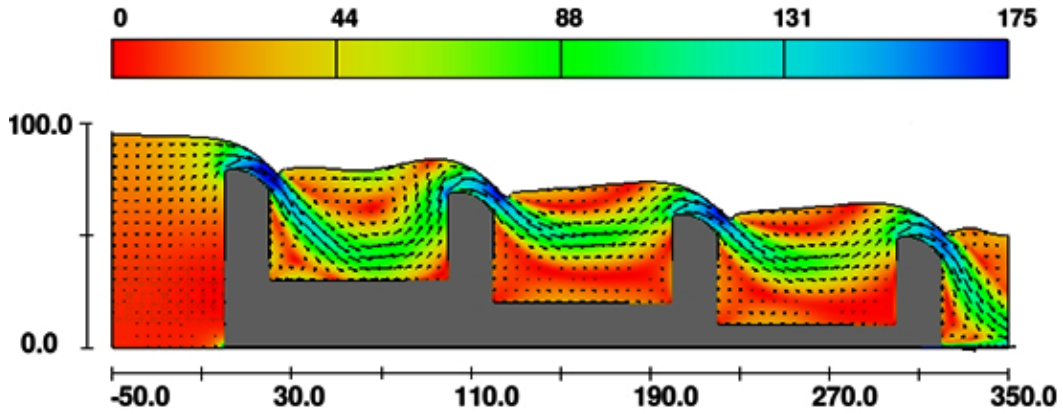

a. Simulated velocity distribution

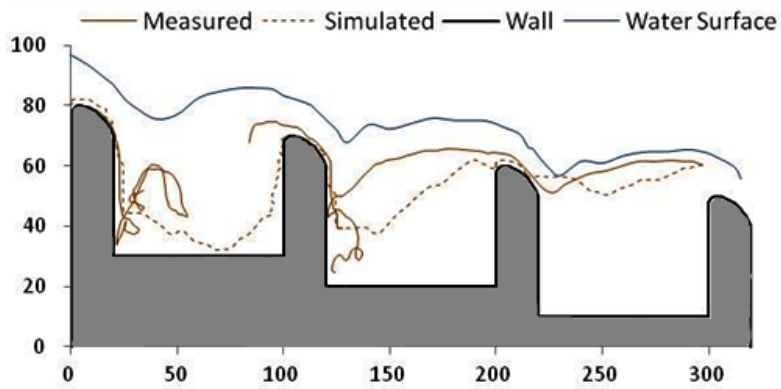

b. fish movement path

Figure 5.37: Simulated flow pattern and fish movement inside the pool tank for Type-A Experiment 4 (ΔH = 0.20 m, q= 0.20 m3/s/m').

5.3.3.2 Type-B experiments

According to the geographical features condition, there is a condition where the people had to build a fishway steeper than the standard condition. One way to do that is to change the step height between the pools. To study the effect of changing the pool step height, the model was set up according to Type B experiments where the difference in height between two successive weirs (DY) was changed to become 20 cm. The flows as well as the water depths are varied from one experiment to the other as indicated in table 5.6. Figure 5.38 represents the mean velocity distribution and fish movement in case1 as a representative to the low flow conditions (0.021 m^3/s/m). It can be seen that the velocity takes the same shape as in Type- A with main flow near the walls and bed, while a circulation covers a large area in the middle of the pool tank. The velocity is higher in comparison to Type-A experiment case 1. In the most downstream pool, the measured data show that the fish move against the high flow

near the boundary. In the middle pool as well as the most upstream pool, it seems that the fish use the bottom of the circulating zone as a rest area.

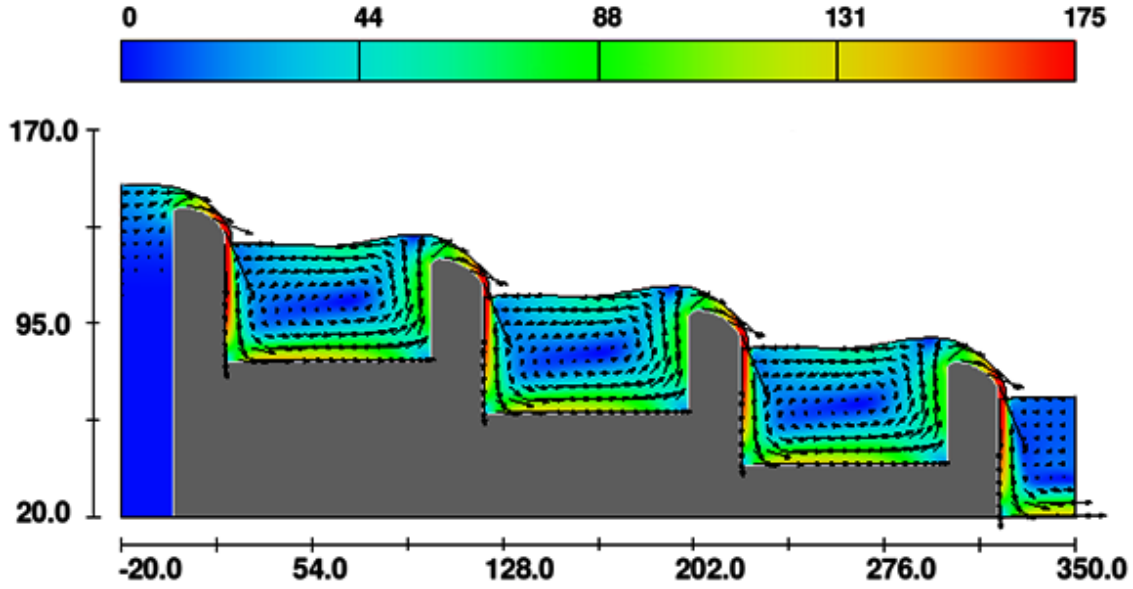

a. Simulated velocity distribution

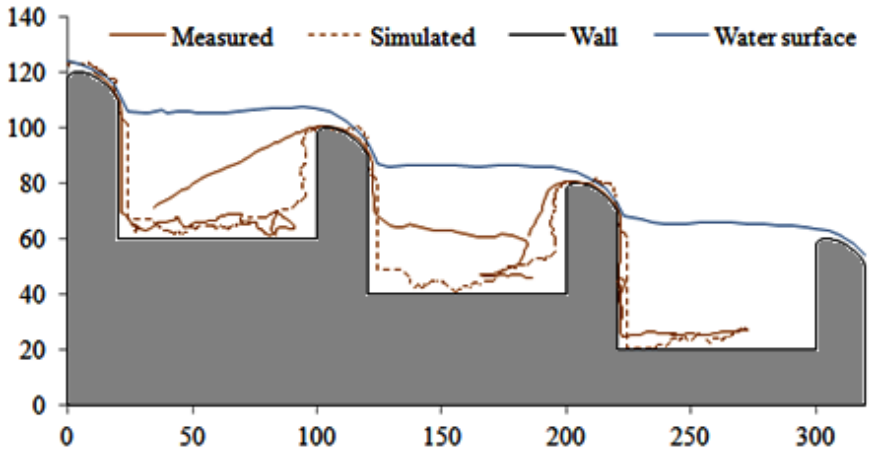

b. fish movement path

Figure 5.38: Simulated flow pattern and fish movement inside the pool tank for Type-B Experiment 1 (ΔH = 0.05 m, q= 0.021 $m^3/s/m'$).

In case of high flow (case 4, q =0.2 m3/s/m'), the flow is distributed over a wide distance. While the circulation zone decreases compared to Type-A experiment 4. Figure 5.39 shows the results of the mean velocity fish movement inside the pool tank for this case. Due to the high flow, after passing each pool, the fish need some rest and go directly to the area beside the wall where velocity as well as the circulation turbulence is small.

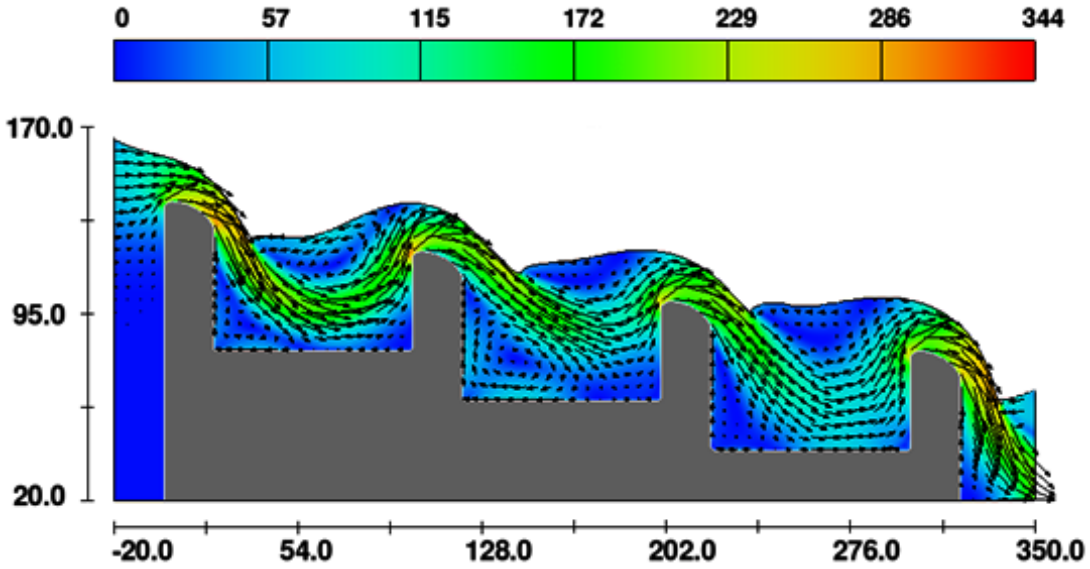

a. Simulated velocity distribution

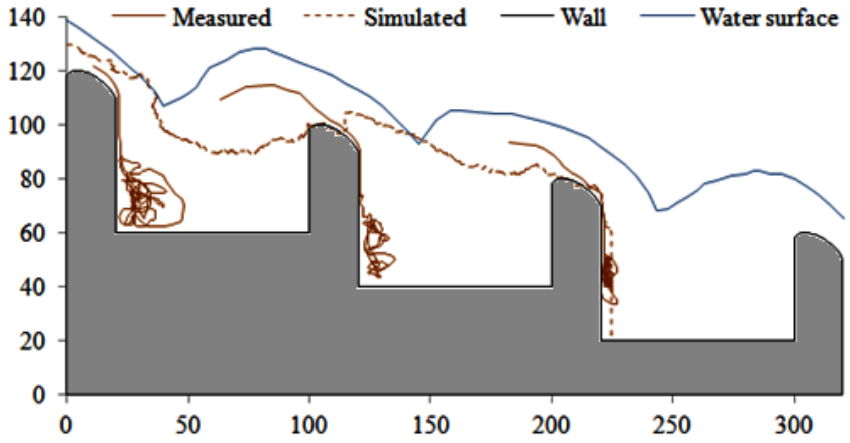

b. Fish movement path

Figure 5.39: Simulated flow pattern and fish movement inside the pool tank for Type-B Experiment 4 (ΔH = 0.20 m, q= 0.2 $m^3/s/m$).

5.3.3.3 Type-C experiments

Another way to increase the slope of the fishway is to make it with short pools in flowing direction. In this part, the model is set up according to experiments of Type-C which consist of six pools (N=6) each 30 cm in length, 40 cm of weir height, and 10 cm difference in weir height. The flows as well as the water depths are varied from one experiment to the other as indicated in table 5.6. Figure 5.40 represents the mean velocity distribution and fish movement in case1 as a representative to the low flow conditions (0.021 $m^3/s/m$).

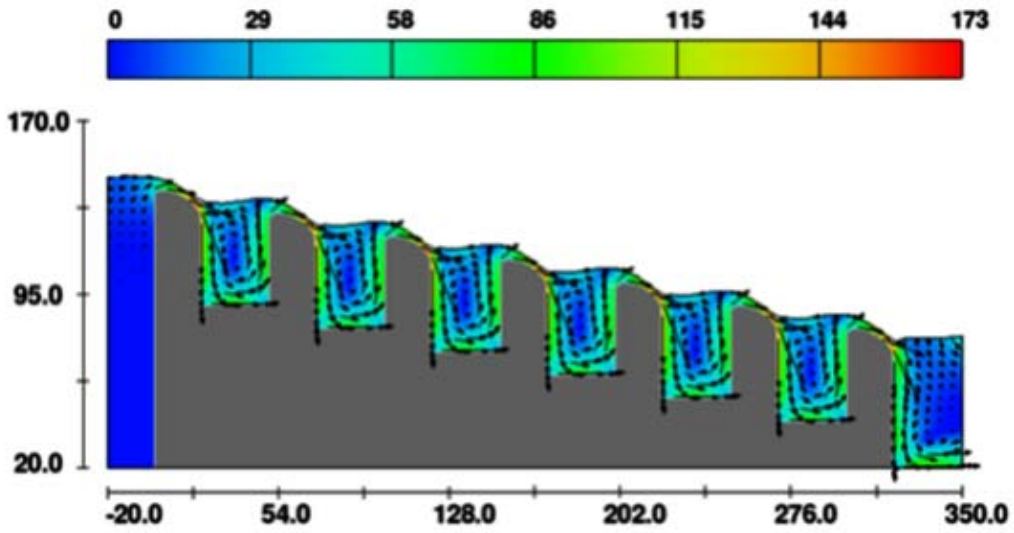

a. Simulated velocity distribution

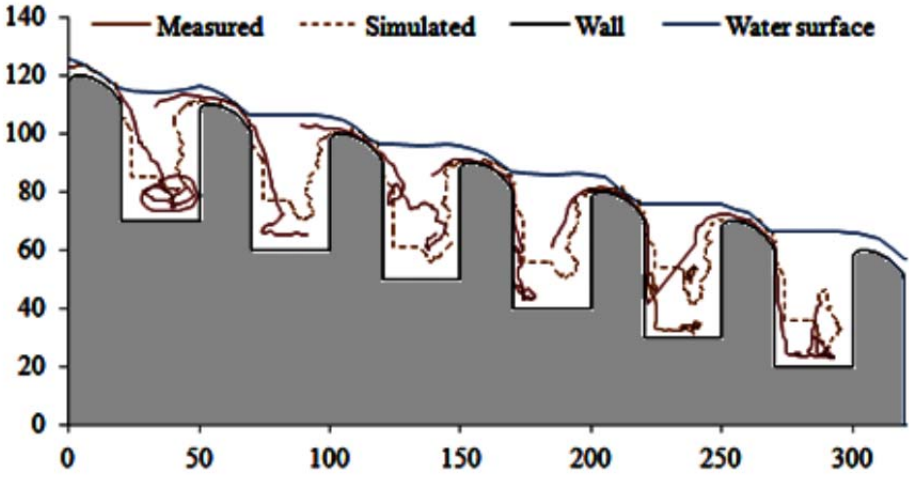

b. Fish movement path

Figure 5.40: Simulated flow pattern and fish movement inside the pool tank for Type-C Experiment 1 ($\Delta H = 0.05$ m, $q = 0.021$ $m^3/s/m$.)

5.3.4 Summary

The flow characteristic upstream of the fishway has a great effect on the distribution of velocity inside the fishway. In Low flow condition, the main flow was located in the domain near the wall and bed. The middle flow area is characterized by a circulated weak flow. On the other hand, the flow near the water surface is reversed due to the backwater effect. By increasing the flow, the main flow direction move gradually from the bottom near the bed to the top of the pool near the water surface. Accordingly, the velocity distributions as well as the position of the circulated weak flow are changed. The fish move against the main flow direction and use the

circulating zones as a rest zones. The numbers as well as the period of the resting areas are increased by increasing the flow.

Increasing the slope of the pool either by decreasing the pool length or increasing the steps between the pools increases the velocity inside the pool and decreases the passage of these pools. The model works well specially for the low flow conditions while it failed to simulate the cases where the resting areas are required. Additional features could be added to the model to enhance the results. One of these features is the need to include the fish energy in the model presented here. This is a challenge because the fish velocity is not constant and the energy is switched between the aerobic and anaerobic velocity according to the fish velocity. Another problem is that no data are available on the amount of energy the fish can retain by taking a rest for some time.

6. Conclusions and suggestions for further research

6.1 Main conclusions

The purpose of the present work was to follow the individual fish movements through passage in order to find some rules which help to evaluate and design the fish passage. I believe that the best way to design structures in which the fish move as individual rather than population, is to combine the individual based model with some statistical data which describe the variation between individuals. Parallel to the individual based model, there is a need to extract and analyze the fish movement from the field and experimental work.

Hence, an image processing-based approach was introduced and validated using several dataset. The methods of motion vector-based motion estimation and frame difference-based motion estimation are investigated towards their usability to track swimming fish for the purpose of automatic path capturing. The motion vector technique is found to be of limited performance. The frame difference technique is improved by performing background estimation and subtraction using morphological filtering, resulting in accurate fish tracking in a realistic dataset captured at lab. I furthermore add color filtering for fish identification in a multiple fish tracking scenario and demonstrate the principal capability to track and identify different fish.

Applying this technique to the fishway (dataset 3 in chapter 3), I found the fish velocity inside the fishway is varied from point to point starting from very small velocity at the resting zone to more than 10.0 fish length per second over the weir. This indicates that the fish uses a combination of aerobic and anaerobic energy when passing through the fishway. Although I achieve good results in tracking fish in realistic scenarios, I consider this chapter as a foundation for more elaborate methods that could result in more accurate and robust tracking by incorporating suitable post-processing techniques (outlier removal and adaptive smoothing). This is mainly motivated by the fact, that I have been able to acquire higher quality data later.

Further, the numerical method for predicting fish movement through a culvert of Blank (2008) was modified and tested with real data measurements. The method compare between the actual fish energy and the energy consumed inside the culvert. In This method, the fish movement depends on a low energy concept and random movements. The effects of turbulence and fish memory were also taken into account.

Based on this model, the energy expenditure was calculated for the measured and predicted path. Results of the simulation are compared to field studies of tracked fish. The model was applied to different flow distributions and provided good

agreement with the observed fish movement paths. This study gives an interesting meso-scale investigation and approach to understand organism behavior that could influence culvert design. Although the simulation shows a good agreement with the measured data, more culvert of different slope, cross-section, and lengths as well as flow conditions are a good suggestion for future work for both experimentalists and theoreticians to test its robustness and sensitivity.

Based on this result, a new method for culvert passage design is proposed and applied to the data given in the field study. Due to the lack of field measurement I could not investigate this method with some other culverts or fish species.

When the flow direction changes point by point e.g. in a pool-and-weir fishway, the fish recognizes the direction of the fishway based on high water flow. At the same time, the fish tries to minimize the energy expenditure by travelling against the lower velocities. The model has been developed for this case. It provided good results of flow pattern and fish movement compared to the experimental data provided by Hayashida (2001) and Atsushi (2009). The simulated results showed that the flow inside the pool was highly non-uniform and a large area was occupied by a low velocity current. The flow characteristic upstream of the fishway has a great effect on the distribution of velocity inside the fishway. In low flow condition, the main flow was located in the domain near the wall and bed. The middle flow area was characterized by a circulated weak flow. On the other hand, the flow near the water surface was reversed due to the backwater effect. By increasing the flow, the main flow direction moved gradually from the bottom near the bed to the top of the pool near the water surface. Accordingly, the velocity distributions as well as the position of the circulated weak flow were changed. The dimensions of the pool could have a great effect on the distribution of flow in the pool. When the pool length is long and the weir height is small, the flow is almost uniform. These flow conditions could be perfect for Japanese daces which showed the most climbing frequency. By increasing the pool depth, the flow non-uniformity becomes more intensive and accordingly, a climbing frequency could be reduced. By decreasing the pool length, the strong circulation of the flow could cause very bad conditions for fish climbing.

On the other hand, increasing the slope of the pool either by decreasing the pool length or increasing the steps between the pools increases the velocity inside the pool and decreases the successful passage of these pools.

The fish move against the main flow direction and use the circulating zones as rest zones. The numbers as well as the period of the resting areas increase by increasing the flow. The model works well specially for the low flow conditions while it failed to simulate the cases where resting areas are required. Additional features

could be added to the model to enhance the results. One of these features is the need to include the fish energy in the model presented here. This is a challenge because the fish velocity is not constant and the energy is switched between the aerobic and anaerobic velocity according to the fish velocity. Another problem is that no data are available about the amount of energy the fish can retain by taking a rest for some time.

6.2 Suggestions for further research

The research that has been undertaken for this thesis has highlighted a number of topics on which further research would be beneficial.

The first one is the fish swimming abilities in crossing velocity barrier where there are no or limited data for different fish species. The research should investigate swimming behavior of various species and life stages. More accurate swimming abilities and behavior information will significantly improve the predictive capacity of barrier assessments, the design of impassable barriers, and the design of new crossings and retrofit structures.

A second topic for a future research is to combine the fish swimming behavior with the advanced characterizations of velocity and turbulence through a variety of hydraulic structures at a large range of flows. another interesting topic is to study the characteristic of the resting area including the hydraulic conditions, the rest period, the amount of the fish retained energy, and how fish combines aerobic and anaerobic energy.

The last interesting topic is the fish ability to leap into the culvert for varies species. The research should embrace factors affecting the probability of succeed leaping, the number of trials the fish can make, the rest period between trials, and the retained energy the fish can gain during the rest period.

7. References

ADF&G; ADOT&PF (2001): Memorandum of agreement between Alaska Department of Fish and Game (ADF&G) and Alaska Department of Transportation and Public Facilities (ADOT&PF) for the design, permitting, and construction of culverts for fish passage.

Anderson, R.O.; Neumann, R.M. (1996): Length weight and associated structural indices, Pages 447 - 482 in B.R. Murphy and D. W. Willlis, editors, Fisheries techniques, 2nd edition. American Fisheries Society, Bethesda, Maryland

Andrew, F.J.; Geen, G.H. (1960): Sockeye and Pink Salmon production in relation to proposed dams in the Fraser river system, IPSFC Bull. XI. New Westminster, B.C.

Atsushi, N. (2009): Studies on design of pool-and-weir type fishway focusing flow structure in the fishway, Institute for Rural Engineering Report No. 49 (In japan).

Atsushi, N.; Masahiro, G.;Hiroyasu, K. (2008): The flow pattern of the Pool-and-Weir-Fishway in the pool and the swimming behavior of Leuciscus Hakonensis, Japanese Journal of Hydraulic Engineering, Vol. 52 (In japan).

Bagur, D. (2009): Where the fish are: An Angler's Guide to Fish Behavior, ISBN: 978-0-07-159292-5

Bainbridge, R. (1960): Speed and stamina in three fish, Journal of Experimental Biology, Vol. 37, 129-153.

Bay, H.; Ess, A.; Tuytelaars, T.; Van Gool, L. (2004): SURF: Speeded Up Robust Features, Computer Vision and Image Understanding (CVIU), Vol. 110, No. 3, pp. 346-359

Baumgartner, L.; Bettanin, M.; McPherson, J.; Jones, M.; Zampatti, B.; Beyer, K. (2010): Assessment of an infrared fish counter (Vaki Riverwatcher) to quantify fish migrations in the Murray-Darling Basin, Industry & Investment NSW Fisheries Final Report Series, No. 116, ISSN 1837-2112

Beach, M.H. (1978): The use of infra-red light and closed circuit TV to validate records from automatic fish counters, Journal of Fish Biology, Vol. 13, 639-644.

Beamish, F.W.H. (1978): Swimming capacity, In Fish Physiology, Vol. VII (ed. Hoar, W.S.; Randall, D.J.), 101–187, New York: Academic Press.

Behlke, C.E.; Kane, D.L.; Mclean, R.F.; Travis, M.D. (1991): Fundamentals of culvert design for passage of weak swimming fish, Report FHWA-AK-RD-90-10. Fairbanks, AK.

Bell, M.C. (1991): Fisheries handbook of engineering requirements and biological criteria, Fish Passage Development and Evaluation Program. U.S. Army Corps of Engineers, North Pacific Division Portland, OR.

Blake, R. W. (2004): Fish functional design and swimming performance, Journal of fish biology, Vol. 65, 1193–1222.

Blank, M. D. (2008): Advanced studies of fish passage through culverts: 1-d and 3-d hydraulic modeling of velocity, fish energy expenditure, and a new barrier assessment method, Ph.D. thesis, Montana State University.

Blank, M.D; Cahoon, J.E; Burford, D.; McMahon, T.; Stein, O. (2006): Studies of fish passage through culverts in Montana, Proceedings of the 2005 International Conference on Ecology and Transportation, Eds. Irwin C.L., Garrett P., McDermott K.P. Center for Transportation and the Environment, North Carolina State University, Raleigh, NC: pp. 647-661.

Blaxter, J.H.S. (1969): Swimming speeds of fish, FAO Fish, Rep. 62, Proc. FAO conference on fish behavior in relation to fishing techniques and tactics, Bergen.

Brehmera, P.; Do Chi, T.; Mouillotb D. (2006): Amphidromous fish school migration revealed by combining fixed sonar monitoring (horizontal beaming) with fishing data, Journal of Experimental Marine Biology and Ecology, Vol. 334, Issue 1, 139-150.

Brown, K. (2006): Evidence of spawning by green sturgeon, Acipenser medirostris, in the upper Sacramento River, California, J. Environmental Biology Fish, DOI 10.1007/s10641-006-9085-5.

Burwen, D.L.; Bosch, D.E.; Fleischman, S.J. (1995): Evaluation of hydroacoustic assessment techniques for chinook salmon on the Kenai River using split-beam sonar. Anchorage, Alaska Department of Fish and Game, Division of Sports Fish.

Cahoon, J.E.; McMahon, T.; Solcz, A.; Blank, M.; Stein, O. (2007): Fish passage in Montana culverts, phase II – passage goals, FHWA/MT-07-010/8181.

California department of transportation (2007): Fish passage design for road crossings, An Engineering Document Providing Fish Passage Design Guidance for Caltrans Projects.

Campenhausen, C.; Riess, I.; Weissert, R. (1981): Detection of stationary objects by the blind cave fish Anoptichthys jordani (Characidae), J. Comp. Physiol. A Neuroethol Sens Neural Behav Physiol, Vol.143, 369 –374.

Castro-Santos, T. (2005): Optimal swim speeds for traversing velocity barriers: an analysis of volitional high speed swimming behavior of migratory fishes, J. of experimental Biology, Vol. 208, 421-432.

Castro-Santos, T.; Haro, A. (2008): Fish Guidance and Passage at Barriers, Chapter 4 In "Fish Locomotion: An Etho-Ecological Approach. (P. Domenici and R. W. Blake, Ed.), Science Publishers, Enfield, NH.

Castro-Santos, T. (2012): Self contact.

Chagnaud, B. P.; Bleckmann, H.; Hofmann M. H. (2007): Kármán vortex street detection by the lateral line, J. Comparative Physiology, Vol. 193, 753-763

Clark, M.E.; Rose, K.A. (1997): Individual-based model of stream-resident rainbow trout and brook char: model description, corroboration, and effects of sympatry and spawning season duration, Ecol. Model, Vol. 94, 157-175.

Coffman, J.S. (2005): Evaluation of a predictive model for upstream fish passage through culverts, Master's thesis, James Madison University, Harrisonburg, VA.

Cookingham, M.N.; Ruetz Iii, C.R. (2008): Evaluating passive integrated transponder tags for tracking movements of round gobies, Ecology of Freshwater Fish, Vol. 17, 303–311.

Coombs, S. (1999): Signal detection theory, lateral-line excitation patterns and prey capture behaviour of mottled sculpin, Anim. Behav., Vol. 58, 421–430.

Denton, E.J.; Gray, J.A. (1988): Mechanical factors in the excitation of the lateral line of fishes, Atema, J., Fay, R.R., Popper, A.N., Tavolga, W.N. (Eds.), Sensory Biology of Aquatic Animals. Springer, New York, NY, 595–617.

Dijkgraaf, S. (1963): The functioning and significance of the lateral-line organs, Biological Reviews, Vol. 38(1), 51-105.

Dumont, U. (2012): The new DWA design manual on upstream fish passes, 9th International Symposium on Ecohydraulics.

Egli, D.P.; Babcock, R.C. (2004): Ultrasonic tracking reveals multiple behavioural modes of snapper (Pagrus auratus) in a temperate no-take marine reserve, ICES Journal of Marine Science, Vol. 61 (7), 1137-1143.

Enders, E.C.; Herrmann, J. (2003): Energy costs of spontaneous activity in horse mackerel quantified by a computerised imaging analysis, Arch. Fish. Mar. Res. Vol. 50, 205-219.

Everest, F.H.; Sedell, J.R.; Armantrout, N.B.; Nickerson, T.E.; Keller, S.M.; Johnson, J.M.; Parante, W.D.; Haugen, G.N. (1985): "Salmonids." Management of Wildlife and Fish Habitats in Forests of Western Oregon and Washington - Part 1, Brown E.R., ed., U.S.D.A. Forest Service, 199-230.

Webb, J. F.; Fay, R.; Popper, A. N (2008): Fish Bioacoustics, Springer, e-ISBN: 978-0-387-73029-5

Federal Highway Administration (2007): Design for fish passage at roadway-stream crossings, Synthesis Report, Publication No. FHWA-HIF-07-033.

FishXing (2006): FishXing version 3 user manual and reference, USDA Forest Service, Six Rivers National Forest. Eureka, CA.

Fitch, G.M. (1995): Nonanadromous fish passage in Highway culverts, Charlottesville, VA: Virginia Department of transportation; VTRC 96-R6. 530 Edgemont Road, Charlottesville, VA 229903-0817.

Flow Science, Inc. (2008): FLOW-3D User's Manual. Flow Science, Inc.

Forest Practices Advisory Committee on Salmon in Watersheds (2001): Section A: Fish Passage Restoration.

Goodwin, R.A.; Nestler, J.M.; Anderson, J.J.; Weber, L.J.; Loucks, D.P. (2006): Forecasting 3D fish movement behavior using a Eulerian-Lagrangian-agent method, Ecol. Model, Vol. 192, 197–223.

Goulet, J.; Engelmann, J.; Chagnaud, B. P.; Franosch, J. P.; Suttner, M.D.; Van Hemmen, J.L. (2008): Object localization through the lateral line system of fish: theory and experiment, J. Comp Physiol., Vol.194, 1–17

Gowans, A.R.D.; Armstrong, J.D.; Priede, I.G. (1999): Movements of adult Atlantic salmon in relation to a hydroelectric dam and fish ladder, Journal of Fish Biology, vol.54, 713–726.

Gresswell, R.E. (1988): Status and management of interior stocks of cutthroat trout, American Fisheries Society Symposium 4.

Grimm,V. (2008): Individual-Based Models, In: Jørgensen, S.E., Fath, B.D. (Eds.), Ecological Models, Vol. [3] of Encyclopedia of Ecology, vols. 5. Elsevier, Oxford, pp. 1959–1968.

Grimm,V. (1999): Ten years of individual-based modelling in ecology: what have we learned and what could we learn in the future?, Ecological Modelling, Vol. 115, 129–148

Guiny, E.M. (2001): Hydraulic and biological aspects of fish passes for dams, PhD thesis, University of Glasgow.

Haag, W.R.; Warren, M.L. (1998): Role of ecological factors and reproductive strategies in structuring freshwater mussel communities, Can. J. Fish. Aquat. Sci., Vol. 55, 297-306.

Haefner, J.W.; Bowen, M.D. (2002): Physical-based model of fish movement in fish extraction facilities, Ecological Model., Vol.152, 227–245.

Haselbauer, M. A. (2008): Geräuscharme Fischaufstiegsgerinne Experimentelle und numerische Analyse des Fischpasses vom Typ periodische Schütze, Dissertation, Fakultät für Bauingenieur- und Vermessungswesen, Technische Universität München.

Hassan, E.S. (1989): Hydrodynamic imaging of the surroundings by the lateral line of the blind cave fish Anoptichthys jordani, In the Mechanosensory Lateral Line: Neurobiology and Evolution (ed. S. Coombs, P. Gorner and H. Munz), p. 217-228. New York: Springer-Verlag.

Hayashida, k.; Honda, T.; Kayaba, Y.; Shimatani, Y. (2001): Flow Pattern of Pool-and-Weir Fishways inside the Pool and the Swimming Behaviors of Japanese Daces in the Fishways, Fish TREC-2001

Heape, W. (1931): Emigration, Migration and Nomadism, Heffer, Cambridge.

Hirt, C.W.; Nichols, B.D. (1981): Volume of Fluid (VOF) Method for the Dynamics of Free Boundaries, J. Computational Physics, Vol. 39, 201-225.

Hoar, W.S.; Randall, D.J. (1978): Fish physiology, vol. VII: locomotion. Academic Press, New York.

Hockersmith, E.E.; Muir, W.D.; Smith, S.G.; Sandford, B.P.; Perry, R.W.; Adams, N.S.; Rondorf, D.W. (2003): Comparison of migration rate and survival between radio-tagged and PIT-tagged migrant yearling chinook salmon in the Snake and Columbia rivers, North American Journal of Fisheries Management, Vol. 23, 404-413.

Hubert, W.A. (1985): Passive capture techniques, in Fisheries Techniques (Johnson, D.L. & Lampton, S.S., eds.), Maryland: American Fisheries Society.

Huth, A.; and Wissel, C. (1994): The simulation of fish schools in comparison with experimental data, Ecol. Model., Vol. 75, 135–145.

Jackson, S., (2006): Protecting and Enhancing River and Stream Continuity, Proceedings, 11th Triennial National Wildlife & Fisheries, Extension Specialists Conference.

Jenq-Neng, H. (2009): Multimedia Networking: from Theory to Practice, Cambridge: Cambridge University Press.

Kalmijn, A. J. (1989): Functional evolution of lateral line and inner ear sensory systems, in the Mechanosensory lateral line neurobiology and evolution (ed. Coombs, S.; Görner, P.; Münz, H.), Springer-Verlag, New York, NY, 187–215.

Kane, D.L.; Behlke, C.E.; Gieck, R.E.; McLean, R.F. (2000): Juvenile fish passage through culverts in Alaska: a field study, report FHWA-AK-RD-00-03. Fairbanks, AK.

Kane, A.S.; Salierno, J.D.; Gipson, G.T.; Molteno, T.; Hunter, C. (2004): A video-based movement analysis system to quantify behavioral stress responses of fish, Water Research, Vol. 38, 3993–4001.

Katopodis, C. (1992): Introduction to fishway design, working document, Freshwater Institute, Central and Arctic Region, Department of Fisheries and Oceans

Katopodis, C. (1993): Fish Passage at Culvert Highway Crossings. Presentation notes from Highways and Environment, Charlottetown, May 17-19

Katopodis, C. (2005): Developing a toolkit for fish passage, ecological flow management and fish habitat works, IAHR J. Hydraulic Research, Vol. 43(5), 451-467.

Khan, L.A. (2006): A three-dimensional computational fluid dynamics (CFD) model analysis of free surface hydrodynamics and fish passage energetics in a vertical-slot fishway, North American Journal of Fisheries Management, Vol. 26, 255-267.

Kondratieff, M. C.; Myrick, C. A. (2006): How high can Brook Trout Jump? A laboratory evaluation of Brook Trout jumping performance, Transactions of the American Fisheries Society, Vol. 135(2), 361-370.

Kisia, S.M.; Onyango, D.W. (2007): Fish Respiration and Environment, Edited by Kapoor, B.G., Science Publishers 2007, ISBN: 978-1-4398-4254-6, DOI: 10.1201/b11000-2

Kruse, C.G.; Hubert, W.A. (1997): Proposed Standard Weight (Ws) Equations for Interior Cutthroat Trout, North American Journal of Fisheries Management, Vol. 17(3).

Langill, D.A.; Zamora, P.J. (2002): An audit of small culvert installations in Nova Scotia: habitat loss and habitat fragmentation, Canadian Technical Report of Fisheries and Aquatic Science 2422, 34p.

Larinier, M. (2001): Environmental issues, dams and fish migration. In Marmulla, G. (ed.), FAO Fisheries Technical Paper 419, Dams, Fish and Fisheries opportunities, Challenges and Conflict Resolution. FAO, Rome, 45-89.

Lauritzen, D.V. (2002): Preferences, Behaviors and Biomechanics of Pacific Salmon Jumping at Waterfalls and Fish Ladders, Dissertation, University of California, Los Angeles, California.

Liao, J.C. (2002): Swimming in needle fish (belonidae): anguilliform locomotion with fins, Journal of Experimental Biology, Vol. 205(18), 2875-2884.

Liao, J.C. (2007): A review of fish swimming mechanics and behaviour in altered flows, Philosophical Transactions of the Royal Society, Biological Sciences, Vol. 362 (1487), 1973-1993.

Lowe, D.G. (2004): Distinctive Image Features from Scale-Invariant Key points, International Journal of Computer Vision, Vol. 60 (2), 91-110.

Lucas, M.C.; Baras, E. (2001): Migration of freshwater fishes, Blackwell Science Ltd., Malden, MA

Mackenzie, B.R.; Miller, T.J.; Leggett, W.C. (1994): Evidence for a dome-shaped relationship between turbulence, and larval fish ingestion rates, Limnol. Oceanogr., Vol. 39, 1790-1799.

Maine Department of Transportation (2004): Fish passage policy and design guide, 2nd Edition.

Makrakis, S.; Castro-Santos, T.; Makrakis, M.C.; Wagner, R.L.; Adames, M.S. (2012): Culverts in paved roads as suitable passages for Neotropical fish species, Neotrop. ichthyol. [Online], ISSN 1679-6225, Vol.10 (4), 763-770.

Minnesota department of transportation (2000): Drainage Manual, Issued by office of Bridge and structures, Transmittal letter no. 00-01.

Manikandan, M.; Vijayakumar, P.; Ramadass, N. (2006): Motion estimation method for video compression - an Overview, International Conference on Wireless and Optical Communications Networks, Bangalore, IEEE.

Matas, J.; Chum, O.; Martin, U.; Pajdla, T. (2002): Robust wide baseline stereo from maximally stable extremal regions, Proc. of the British Machine Vision Conference, Vol. 1, 384-393.

McArthur, T. (2011): A model study of the hydraulics related to fish passage through embedded culverts, Master Thesis, Department of Civil and Geological Engineering University of Saskatchewan, Saskatoon, Canada

McFarlane, W.J.; McDonald, D.G. (2002), Relating Intramuscular Fuel Use to Endurance in Juvenile Rainbow Trout, Physiological and Biochemical Zoology, Vol. 75(3), 250–259.

Morita, K.; Yamamoto, S. (2002): Effects of habitat fragmentation by damming on the persistence of stream-dwelling charr populations, Conservation Biology, Vol. 16, 1318-1323.

Maselko, J.M.; Wertheimer, A.C.; Thedinga, J.F. (2003): Selection and application of a Mark-and-Recapture Technique for estimating Pink Salamon Escapements, NOAA Technical Memorandum NMFS- AFSC-137.

Mayama, H. (1987): Ascending behavior of juvenile masu salmon (Oncorhyncus masou) in experimental fishway, Scientific Report of the Hokkaido Salmon Hatchery, 41: 137-153.

Müller, U.K.; Smit, J.; Stamhuis, E.J.; Videler, J.J. (2001): How the body contributes to the wake in undulatory fish swimming: Flow fields of a swimming eel (Anguilla anguilla), Journal of Experimental Biology, Vol. 204, 2751-2762.

Murphy, B.R.; Brown, M. L.; Springer, T.A. (1990), Evaluation of the relative weight (Wr) index, with new applications to walleye, North American Journal of Fisheries Management , Vol. 10, 85–97.

Nestler, J.M.; Goodwin, R.A.; Cole, T.; Degan, D.; Dennerline, D. (2002): Simulating movement patterns of blueback herring in a stratified southern impoundment, Trans. Am. Fish. Soc., Vol. 131, 55-69.

Nikora, V.I.; Aberle, J.; Biggs, B.J.; Jowett, I.G.; Sykes, J. (2003): Effects of fish size, time to fatigue and turbulence on swimming performance: a case study of Galaxias maculatus, Journal of Fish Biology, Vol. 63(6), 1365-1382.

Norton, S.F.; Eppley, Z. A; SidelJ, B. D. (2000): Allometric Scaling of Maximal Enzyme Activities in the Axial Musculature of Striped Bass, Morone saxatilis (Walbaum), Physiological and Biochemical Zoology, Vol. 73(6), 819-828.

Northcote, T.G. (1997): Potamodromy in Sahnonidae Living and Moving in the Fast Lane, North American Journal of Fisheries Management, Vol. 17(4), 1029-1045.

Olla, B. L.; Davis, M. W. (1990): Effects of physical factors on the vertical distribution of larval walleye pollock Theragra chalcogramma under controlled laboratory conditions, Mar. Ecol. Prog. Ser., Vol. 63, 105-112.

Otsu, N. (1979): A threshold selection method from gray-level histograms, IEEE Transactions on Systems, Man and Cybernetics, 62-66.

Poff, N.L.; Hart, D.D. (2002): How dams vary and why it matters for the emerging science of dam removal, Bioscience, Vol. 52, 659-668.

Pavlov, D.S.; Lupandin, A.I.; Skorobogatov, M.A. (1994): Influence of flow turbulence on critical flow velocity for gudgeon (Gobio gobio), Doklady Biological Sciences, Vol. 336, 215-217.

Pearson, M.P.; Spriet, L.L.; Stevens, E.D. (1990): Effect of sprint training on swim performance and white muscle metabolism during exercise and recovery in rainbow trout, J. Exp. Biol., Vol.149, 45–60.

Pearson, W.; Richmond, M.; Johnson, G.; Sargeant, S.; Mueller, R.; Cullinan, V.; Deng, Z.; Dibrani, B.; Guensch, G.; May, C.; O'Rourke, L.; Sobocinski, K.; Tritico, H. (2005): Protocols for evaluation of upstream passage of juvenile salmonids, Publication Number WA-RD 614.1, Battelle Memorial Institute, Pacific Northwest Division.

Pearson, W.; Southard , S.; May, C.; Skalski , J.; Townsend, R.L.; Horner-Devine, A.; Thurman, D.; Hotchkiss, R.; Morrison, R.; Richmond, M.; Deng, D. (2006): Research on the upstream passage of juvenile salmon through culverts: Retrofit baffles, Washington State Department of Transportation (WSDOT), Agreement No. GCA2677, PNWD-3672.

Pinkiewicz, T. (2012): Computational techniques for automated tracking and analysis of fish movement in controlled aquatic environments, PhD thesis, University of Tasmania.

Powers, P.D.; Orsborn, J.F.; Bumstead, T.W.; Klinger-Kingsley, S.; Mih, W.C. (1985): Fishways: an assessment of their development and design, Bonneville Power Administration, DOE/BP-36523-4, Portland, Oregon.

Prentice, E.F.; Flagg, T.A.; McCutcheon, C.S.; Brastow, D.F.; Cross, D.C. (1990): Equipment, methods, and an automated data-entry station for PIT tagging, in Fish-marking techniques (eds. Parker, N.C.; Giorgi, A.E.; Hedinger, R.C.; Jester, D.B.; Prince, E.D.; Winans, G.A.), American Fisheries Society, Symposium 7, Bethesda, Maryland, 335–340.

Rajput, S. (2003): The effects of low-water bridges on movement, community structure and abundance of fishes in streams of the Ouachita Mountains, Master's thesis, Arkansas Tech University, Russellville, Arkansas.

Railsback, S. (1999): Reducing uncertainties in instream flow studies, Fisheries, Vol. 24 (4), 24-26.

Reid, D.P. (2011): Modelling the hydrodynamics of swimming fish, from individuals to infinite schools, PhD thesis, University of Groningen, ISBN: 978-90-367-5123-0

Rodriguez, T.; Agudo, J.P.; Mosquera, L.P.; Gonzale, E.P. (2006): Evaluating vertical-slot fishway designs in terms of fish swimming capabilities, ecological engineering, Vol. 27, 37-48.

Rouse W. (2007): Marine biology research experiment: Population dynamics of barnacles in the intertidal zone, http://marine-life.suite101.com/ article.cfm/ marine_biology_research_experiment.

Russ, J.C. (1995): The Image Processing Handbook, CRC Press, Boca Raton, FL.

Schlieper, C. (1972): Research methods in marine biology, University of Washington Press, Seattle.

Schoby, G.P.; Curet, T. (2007), Seasonal Migrations of Bull Trout, Westslope Cutthroat Trout, and Rainbow Trout in the Upper Salmon River Basin, Idaho Department of Fish and Game. 56 pages.

Sicilian, J. (1990): A "Favor" based moving obstacle treatment for FLOW-3D, Flow Science, Inc. Internal publication (FSI-90-00-TN24).

Smith, D.L.; Brannon, E.L.; Odeh, M. (2005): Response of juvenile Rainbow Trout to turbulence produced by prismatoidal shapes, Transactions of the American Fisheries Society, Vol. 134, 741-753.

Solcz, A. (2007): Assessment of culvert passage of Yellowstone cutthroat trout in a Yellowstone River tributary using a passive integrated transponder system, Master's thesis, Montana State University, Bozeman, MT.

Solomon, C.; Breckon, T. (2011): Fundamentals of Digital Image Processing, John Wiley & Sons.

Spampinato, C.; Chen-Burger, H.; Nadarajan, G.; Fisher, R.; (2008): Detecting tracking and counting fish in low quality unconstrained underwater videos, VISAPP (2), 514-519.

Stöcker, S. (1999): Models for tuna school formation, Math. Biosci., Vol. 156, 157-190.

Stuart, T.A. (1962): The leaping behaviour of salmon and trout at falls and obstructions, Freshwater and Salmon Fisheries Research 28, Dept. Agriculture and Fisheries For Scotland, Pitlochry, Scotland.

Suzanne, L.M.; Gove, N.E. (2004): The feasibility of estimating migrating salmon passage rates in turbid rivers using dual frequency identification sonar (Didson), Anchorage, Alaska Department of Fish and Game, Division of Commercial Fisheries.

Tarrade, L.; Texier, A.; David, L.; Larinier, M. (2008): Topologies and measurements of turbulent flow in vertical slot fishways. Hydrobiologia, Vol. 609(1), 177-188.

Therrien, J.; Bourgeois, G. (2000): Fish passage at small hydro sites, Report by Genivar Consulting Group for CANMET Energy Technology Centre, Ottawa, 114 p.

Tiffan, K.F.; Rondorf, D.W. (2004): A review of hydroacoustic studies for estimation of salmonid downriver migration past hydroelectric facilities on the Columbia and Snake Rivers in the 1980's, Reviews in Fisheries Science 1, 27-56.

Tytell, E. D.; Lauder, G.V. (2004): The hydrodynamics of eel swimming, I. Wake structure, Journal of Experimental Biology, Vol. 207, 1825–1841.

U.S. Department of Energy (1991): Environmental mitigation at hydroelectric projects, Vol. I, Current Practices for Instream Flow Needs, Dissolved Oxygen, and Fish Passage, DOE/ID-10360 (Idaho Falls, ID: U.S. Department of Energy).

U.S. Government Printing Office (1995): Fish passage technologies: Protection at hydropower facilities, OTA-ENV-641 (Washington, DC).

Videler, J.J. (1993): Fish swimming, Chapman and Hall, London, GB.

Videler, J.; Weihs, D. (1982): Energetic advantages of burst-and-coast swimming of fish at high speeds, Journal of Experimental Biology, Vol. 97,169-178.

Warburton, K.; Lazarus, J. (1991): Tendency-distance models of social cohesion in animal groups. J. Theor. Biol., Vol. 150, 473-488.

Wardle, C.S.; Videler, J.J.; Altringham, J. D. (1995): Tuning in to fish swimming waves body form, swimming mode and muscle function, Journal of Experimental Biology, Vol. 198, 1629-1636.

Warren, M.L.; Pardew, M.G. (1998): Road crossings as barriers to small-stream fish movement, Transactions of the American Fisheries Society, Vol. 127, 637-644.

Washington Department of Fish and Wildlife (2003): Design of Road Culverts for Fish Passage, WDFW Publications, 112p.

Webb, P.W. (1971): The Swimming Energetics of Trout: II. Oxygen Consumption and Swimming Efficiency, Journal of Experimental Biology, Vol. 55(2), 521-540.

Webb, P. W., (1975): Hydrodynamics and energetics of fish propulsion, Fisheries Research Board of Canada, Bulletin 190, 1-159.

Weissert, R.; Von-Campenhausen, C. (1981): Discrimination between stationary objects by the blind cave fish Anoptichthys jordani (Characidae), J. Comp. Physiol., Vol. 143 (3), 375-381.

Wibe, A.E.; Nordtug, T.; Jensen, B.M. (2001): Effects of bis(tributyltin)oxide on antipredator behavior in threespine stickleback Gasterosteus aculeatus L., Chemosphere, Vol. 4(3), 475-81.

Wichmann, B.A.; Hill, I.D. (1982): Algorithm AS 183: An efficient and portable psuedo-random number generator, J. Applied Statistics, Vol. 31, 188-190.

Wu, G.; Zeng, L. (2007): Video tracking method for three-dimensional measurement of a free-swimming fish, Science in China Series G: Physics Mechanics and Astronomy, Vol. 50 (6), 779-786.

Wu, S.; Rajaratnam, N.; Katopodis, C. (1999): Structure of Flow in Vertical Slot Fishway, J. Hydraul. Eng., Vol. 125(4), 351–360.

Xingqiao, L.; Jiao, G., Feng, J., Dean, Z. (2008): Using Matlab image processing to monitor the health of fish in Aquiculture, Proceedings of the 27th Chinese Control Conference.

Zydlewski, G.B.; Haro, A.; Whalen, K.G.; McCormick, S.D., (2001): Performance of stationary and portable passive transponder detection systems for monitoring of fish movements, Journal of Fish Biology Vol. 58 (5), 1471-1475.

Appendix 1: Data collected in a Culvert in Mulherin Creek

The Field observed data were collected at Mulherin Creek, a tributary to the Yellowstone River with the confluence near Gardiner, Montana, USA during the summer of 2004 as shown in figure A1. This tributary is characterized by the high gradient stream with an average of 11.6 % from the headwater to the mouth and 2 to 5 % in the study area. The stream has a variety of flow ranged from base flow around 0.28 cubic meters per second (m3/s) to a measured flow 3.1 m^3/sec recorded on June 6, 2004 (Blank et al., 2006 and Blank, 2008).

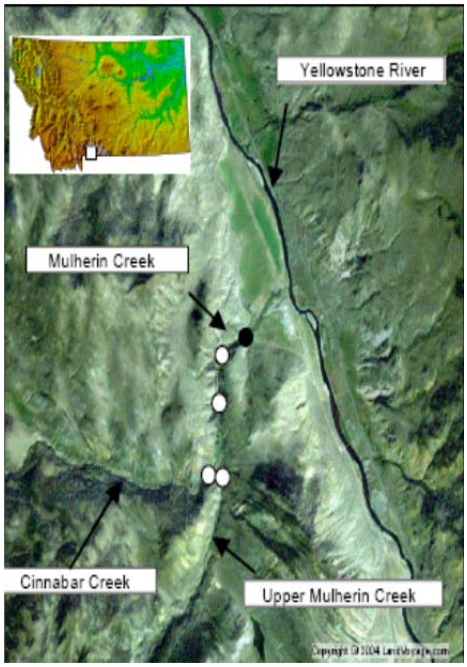

Figure A1: Location of the culvert (after Blank et al., 2006).

Several native species live in Mulherin Creek such as Yellowstone cutthroat trout, mountain whitefish (*Prosopium williamsoni*), white sucker (*Catostomus commersoni*) in addition to non-native species including rainbow trout and brown trout (Salmo trutta) (Blank, 2008). The study focused on Yellowstone cutthroat trout as a native species.

The mark recapture technique with fish traps was used to track the fish movements. The first trap was set up 200 m upstream of the confluence of the Yellowstone River and Mulherin Creek in order to capture the Yellowstone cutthroat trout that migrate from the Yellowstone River into Mulherin Creek to spawn. The trout was directed to the trap #1 opening using fences as indicated by Figure A2. The captured fish were first anesthetized. Then, the data related to the length, the weight and the species were recorded. Finally, Visual Implant (VI) alphanumeric tags were inserted in the periocular transparent tissue of the fish. Two additional traps were

placed upstream and downstream of the culvert. Trap #2 was placed 50 m downstream of the culvert to capture any fish that had migrated from the tagging trap, 1500 m downstream, towards culvert 1, while trap #3 was placed 25 m upstream of the culvert to capture the fish that had migrated through the culvert. If the captured fish were already tagged the tag number, the trap number, the date and time will be recorded. Otherwise, they will be tagged. The total number of the captured trout was 366 divided to 322 Yellowstone cutthroat trout, 23 rainbow trout, and 21 hybrids between Yellowstone cutthroat and rainbow trout.

Figure A2: Fences that direct fish to the opening of trap #1 (after Blank, 2008).

The studied culvert was a concrete box culvert with chamfered corners. The culvert had a slope of 1.1 percent, length of 11.13 m, width of 3.6 m and an outlet drop that averaged 0.49 m during the course of the study. The velocities were measured using an acoustic Doppler velocimeter (ADV) with a signal processor connected to a lap-top computer collected the 3-D velocity data sets (Figure A3). At the upstream as well as the downstream boundary of the culvert, the velocities were measured each 0.15 m to 0.3 m in the horizontal direction and 0.03 m to 0.06 m in the vertical direction (figure A4). Plan view velocity data sets were collected to provide the pattern of velocities in a horizontal plane parallel to the culvert bed. The culvert was divided to several cross-sections each 2.0 m. In each cross-section, the velocity was measured 0.06 m above the bed each 0.3 m as shown in Figure A5. The fish were observed

swimming at the height of 0.06 m from the bed.

Figure A3: Typical measurement of the upstream and Downstream Velocity (after Blank, 2008).

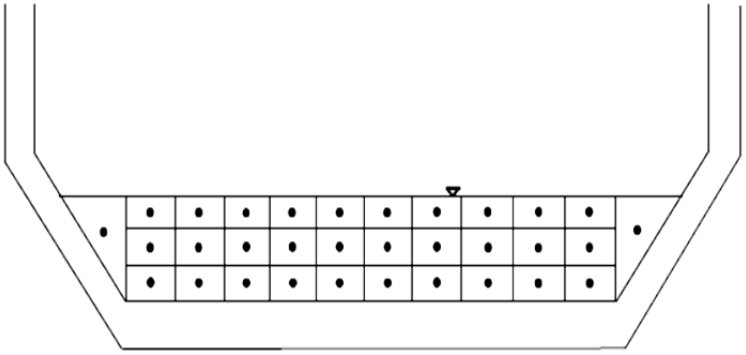

Figure A4: Typical inlet and outlet velocity sampling (after Blank, 2008).

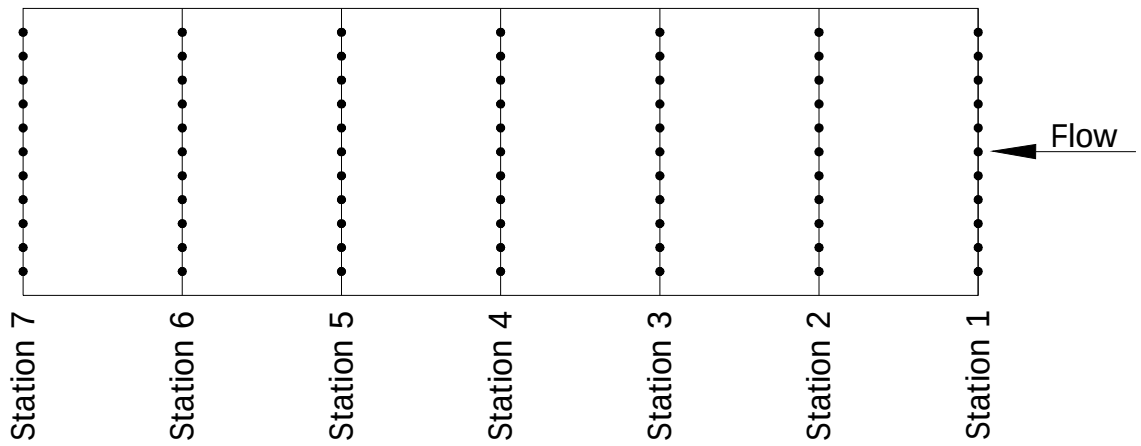

Figure A5: Location of velocity observations collected on a plane 0.06 m above the culvert bed (after Blank, 2008).

Based on the measured velocity, Blank (2008) presented the velocity contour lines at 0.06 m height from the bed. Figure A6 shows an example of this contour line. Due to the 40° degree channel Skew upstream of the culvert, the water was forced to the right side of the culvert which created a lower velocity region on the left side of the culvert.

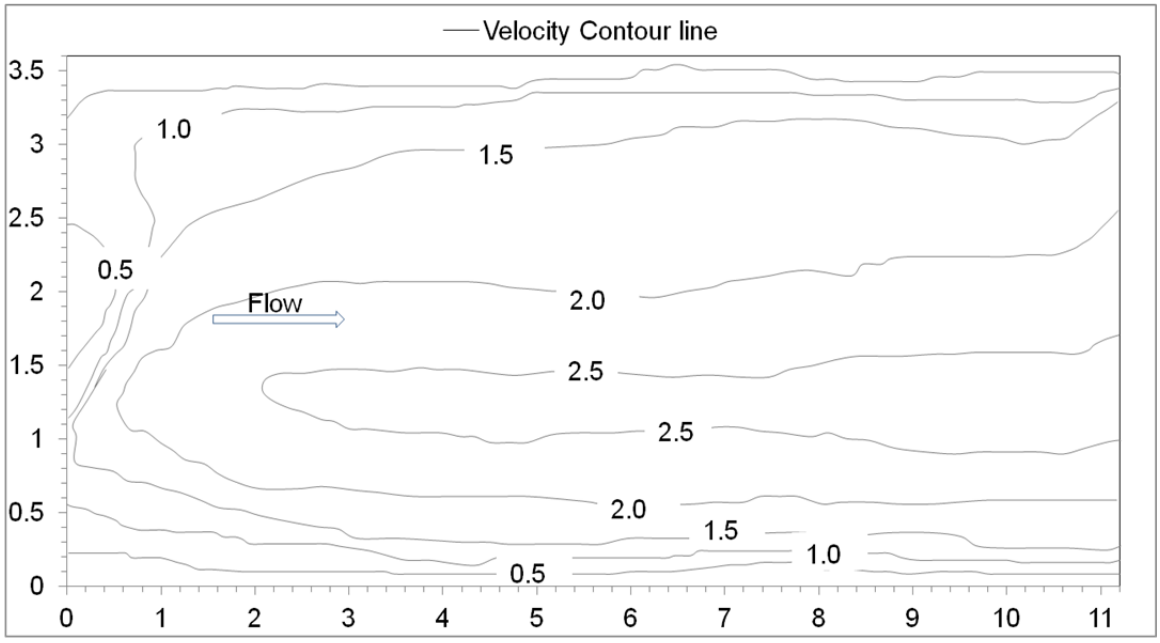

Figure A6: Velocity contour line inside the culvert on 1st July 2004 (observed data from Blank, 2008).

Publikationen:

Abdelaziz, S.; Bui, M. D.; Atsushi, N.; Rutschmann, P.: Numerical Simulation of Flow and Upstream Fish Movement inside a Pool-and-Weir Fishway. 35th IAHR World Congress, 2013 (accepted)

Abdelaziz, S.; Al-Nuaimi, A.; Chugh, P.; Bui, M. D.; Rutschmann, P.: Algorithms for tracking of fish path using image processing. Proc. of the 2nd IAHR European Congress, 27. – 29.6.2012, TU München. Eds.: Peter Rutschmann, Markus Grünzner, Stephan Hötzl. München: Eigenverlag, Lehrstuhl u. Versuchsanstalt f. Wasserbau u. Wasserwirtschaft d. TU München, 2012, Topic Ecohydraulics, Paper D10, 6 pages, USB-Stick; ISBN 978-3-943683-03-5

Abdelaziz, S.; Bui, M. D.; Hayashida, K.; Rutschmann, P.: Numerical Simulation of flow pattern inside a pool and weir fishway. – In: Water infinitely deformable but still limited. Proc. of the 2nd IAHR European Congress, 27. – 29.6.2012, TU München. Eds.: Peter Rutschmann, Markus Grünzner, Stephan Hötzl. München: Eigenverlag, Lehrstuhl u. Versuchsanstalt f. Wasserbau. Wasserwirtschaft d. TU München, 2012, Topic Ecohydraulics, Paper D11, 6 pages, USB- Stick; ISBN 978-3-943683-03-5

Abdelaziz, S.; Bui, M. D.; Hayashida, K.; Rutschmann, P.: Numerische Simulation der Aufstiegsbewegung von Fischen in einem Becken-Fischpass. . – In: Tagungsband Wasserbausymposium 2012, Wasser – Energie, Global denken – lokal handeln, Graz, 12. –15.9.2012. Hrsg.: Gerald Zenz. Graz, Österreich: Verlag der Technischen Universität Graz,2012, Thema B: Numerische Modellierung, Paper 59495, S 267 – 274. ISBN 978-3-85125-230-9.

Abdelaziz, S.; Jhanwar, R.; Bui, M. D., 2011: Rutschmann, P.: A numerical model for fish movement through culverts. Proc. of the 34th IAHR World Congress Brisbane, Australia: (IAHR), 2011, pp. 2736 – 2743, CD; ISBN 978-0-85825-868-6.